Innate Immune Surveillance in Ovarian and Pancreatic Cancer

A thesis submitted in fulfilment of the requirement for the Degree of Doctor of Philosophy

By Anuvinder Kaur

September 2017

Division of Biosciences
College of Health and Life Sciences
Brunel University London

Declaration

I hereby declare that the research presented in this thesis is my own work, except where other specified and has not been submitted for any other degree

Anuvinder Kaur

Acknowledgments

Firstly, I would like to express my sincere gratitude to my supervisor Dr Uday Kishore for his continuous support during my PhD and related research, for his patience, motivation and immense knowledge. I could not have imagined having a better advisor and mentor. I greatly benefited from his profound scientific insight, ability for solving seemingly challenging lab difficulties and to put complex ideas into simple terms.

Besides my supervisor, I would like to thank the rest of my PhD committee: Dr Ansar Pathan (my second supervisor), Dr Predrag Slijepcevic and Dr Sabrina Tosi for their insightful comments and encouragement, but also for the hard question which helped me to widen my research from various perspectives. I am thankful to Dr Ansar Pathan for his lab expertise and insights that greatly assisted this research.

Every result described in this thesis was accomplished with the help and support from my fellow lab-mates Sami Sultan, Suleman Riaz, Arshad Mehmood, Basudev Paudyal, Valarmathy Murugaiah and Praveen Mathews. Thank you being there to save the day when things got out of hand and stimulating discussions to do even better.

I would like to thank Dr Shiv K Singh for pancreatic cancer project and Dr Emmanouil Karteris for ovarian cancer project, for sharing their knowledge and providing expertise to make these projects successful.

My sincere thanks to Dr Anthony Tsolaki and Dr Beatrice Nal for their support.

I would also like to thank Helen Foster, Mathew Themis, Helen Blakes and Gerry Hatton, who facilitated this research by being the last-minute rescuers on a number of occasions. Without training and support provided by Helen Foster, it would not have been possible to conduct this research.

Finally, I would also like to acknowledge the immense impact and support that my family has given me, whose encouragement and support is beyond description. I am grateful to my friends, who supported me spiritually throughout the PhD.

Table of Contents

List of Figures

List of Tables

Table 1.1 List of Abbreviations

ADCC	antibody-dependent cellular cytotoxicity
AF	ascitic fluid
Afu	*Aspergillus fumigatus*
APS	Ammonium Persulfate
ATP	Adenosine 5'-triphosphate
BSA	Bovine serum albumin
CAPS	N-cyclohexyl-3-aminopropanesulfonic acid
ct	Cycle Threshold
cDNA	Complementary Deoxyribonucleic acid
CLR	C-type lectin receptors
CNT	Carbon nanotubes
CRD	carbohydrate recognition domain
CR1	Complement receptor 1
CTL	cytotoxic T lymphocytes
DAB	3,3'-diaminobenzidine
DAF	decay-accelerating factor
DAMP	damage-associated molecular patterns
DIABLO	direct inhibitor of apoptosis protein binding protein
DC	dendritic cells
Derp	*Dermatophagoides pteronyssinus*
DMEM	Dulbecco's Modified Eagle Medium
EDTA	Ethylenediaminetetraacetic acid
EGF	epidermal growth factor
EGFR	epidermal growth factor receptor
EMT	epithelial-to-mesenchymal transition
FADD	Fas-associated death domain protein
FCS	fetal calf serum
FHL-1	factor H like protein 1
FITC	Fluorescein Isothiocyanate
HMGB1	high-mobility group box 1
HRP	Horse radish Peroxidase
HSP	heat shock proteins
IAP	Inhibitor of apoptosis protein
IFN-γ	Interferon gamma
IGF1R	insulin-like growth factor 1 receptor
IKK	IκB kinases
IL	interleukin
LAL	Limulus amebocyte lysate
LB	Luria Broth
KIR2DL3	Killer-cell immunoglobulin-like receptor 2DL3
MAC	Membrane attack complex
MASP-2	MBL-associated serine protease-2
MBP	Mannose-binding protein
MBL	mannose-binding lectin
MCA	3'-methylcholan-threne
MCP	Membrane cofactor protein

MHC-I	major histocompatibility complex
MICA	MHC class-I-chain-related protein A
MISIIR	Mullerian inhibitory substance type II receptor
mRNA	Messenger Ribonucleic acid
mTOR	Mammalian target of rapamycin
mTORC1	Mammalian target of rapamycin complex 1
mTORC2	Mammalian target of rapamycin complex 2
MTT	3-[4,5-dimethylthiazol-2-yl]-2,5-diphenyltetrazolium bromide
mt	mutant
NITR	novel immune-type receptor
NK cells	Natural killer cells
NKG2D	Natural killer group 2D
NKGA	Natural killer group A
NKT Cells	natural killer T cells
NLRs	NOD-like receptors
OSE	Ovarian Surface Epithelium
PAMPs	pathogen associated molecular patterns
PARP	Poly (ADP-ribose) polymerase
PBS	Phosphate-buffered saline
PBST	Phosphate-buffered saline Tween
PDA	Pancreatic ductal adenocarcinoma
PI	Propidium Iodide
PRRs	pattern recognition receptors
PS	phosphatidylserine
qPCR	quantitative polymerase chain reaction
RAG	recombinase activating gene
RANKL	receptor activator nuclear factor-κB ligand
RAPTOR	regulatory-associated protein of mTOR
RM	Rainbow Marker
rfhSP-D	recombinant fragment of human SP-D
RICTOR	rapamycin-insensitive companion of mTOR
RLRs	RIG-I-like receptors
RNA	Ribonucleic acid
rRNA	Ribosomal Ribonucleic acid
SDS	Sodium dodecyl sulfate
shRNA	short hairpin RNA
smac	second mitochondria-derived activator of caspase
SP-D	Surfactant protein D
SRs	scavenger receptors
TAA	tumour associated antigens
TEMED	Tetramethylethylenediamine
TGF-β	Transforming growth factor-beta
TLR	Toll like receptors
TNF	Tumor necrosis factor
TNFR1	TNF type I receptor
TRAIL	TNF- related apoptosis inducing ligand
TRADD	Tumor necrosis factor receptor type 1-associated DEATH domain
UT	Untreated
wt	Wild-type
ZEB1	zinc finger E-box binding homeobox 1

Papers Published

1. **Kaur A**, Sultan S, Murugaiah V, Pathan A, Alhamlan F, Karteris E, Kishore U., Human C1q Induces Apoptosis in an Ovarian Cancer Cell Line via Tumor Necrosis Factor Pathway. **Frontiers in Immunology**. 2016;7: 599 (IF 6.4)

2. Pondman K, Paudyal B, Sim R, **Kaur A**, Kouser L, Tsolaki A, Jones LA, Salvador-Morales C, Khan HA, ten HB, Stenbeck G, Kishore U. Pulmonary surfactant protein SP-D opsonises carbon nanotubes and augments their phagocytosis and subsequent pro-inflammatory immune response. **Nanoscale**. 2017;9(3):1097-1109. (IF 7.8)

3. Pednekar L, Pathan A, Paudyal B, Tsolaki A, **Kaur A**, Abozaid S, Kouser L, Khan HA, Peerschke EI, Shamji MH, Stenbeck G, Ghebrehiwet B, Kishore U. Analysis of the Interaction between Globular Head Modules of Human C1q and Its Candidate Receptor gC1qR. **Frontiers in Immunology**. 2016;7:567 (IF 6.4)

4. Pednekar L, Pandit H, Paudyal B, **Kaur A**, Al-Mozaini M, Kouser L, Ghebrehiwet B, Mitchel DA, Madan T, Kishore U. Complement Protein C1q Interacts with DC-SIGN via Its Globular Domain and Thus May Interfere with HIV-1 Transmission. **Frontiers in Immunology**. 2016;7:600 (IF 6.4)

5. Kouser L, Madhukaran S, Shastri A, **Kaur A**, Ferluga J, Al-Mozaini M, Kishore U Emerging and Novel Functions of Complement Protein C1q. **Frontiers in Immunology**. 2015;6: 317 (IF 6.4)

6. Dodagatta-Marri E, Mitchell DA, Pandit H, Sonawane A, Murugaiah V, Thomas S, Nal B, Al-Mozaini AM, **Kaur A**, Madan T and Kishore U. Protein-protein interaction between surfactant protein SP-D and DC-SIGN via C-type lectin domain can suppress HIV-1 transfer. **Frontiers in Immunology**, 2017 Jul 31; 8:834. (IF 6.4)

Under Review

7. **Kaur A**, Riaz M S, Singh Shiv K., Kishore U Human Surfactant Protein D suppresses epithelial-to-mesenchymal transition in pancreatic cancer cells by downregulating TGF-β. Cancer Research

8**. Kaur A**, Riaz M S, Mathews P, Singh S. K., Kishore U Human Surfactant Protein D induces apoptosis in pancreatic cancer cell lines. Oncogene.

9. Kouser L, Paudyal B, **Kaur A**, Flahaut E, Abozaid S, Stover C, Sim RB and Kishore U. Human properdin opsonizes nanoparticles and triggers a potent pro-inflammatory response by macrophages. **Frontiers in Immunology, in revision**

10. Kandov E, **Kaur A**, Hosszu KK, Kishore U, Irrizary D, Peerschke E IB, Ghebrehiwet B. The dual roles of membrane and soluble forms of gC1qR and C1q in the breast cancer microenvironment. **Frontiers in immunology,** submitted.

In progress

11. **Kaur A** et al., Surfactant protein D exerts its anti-proliferative and anti-migratory effects on an ovarian cancer cell line via negative regulation of mTOR pathway. **Frontiers in Immunology.**

12 Ferluga J, **Kaur A**, RB Sim RB, Kishore U. Complement and Collectin receptors in innate and adaptive immune development and homeostasis. 2017. Immunological Reviews, in preparation.

13. **Kaur A**, Roberta Bulla, Uday Kishore. C1q as a double-edged sword in human cancer. **Frontiers in Immunology.**

Summary of the thesis

Activation of innate immune surveillance mechanisms during the development of cancer is well-documented. However, knowledge of how these innate immune proteins, when added exogenously, independent of tumour microenvironment, affect tumour cells is limited. In Chapter 3, the effects of human C1q and its individual globular domains (ghA, ghB and ghC) on an ovarian cancer cell line, SKOV3, have been examined. C1q and globular head modules induced apoptosis in approximately 55% of cells, which involved upregulation of TNF-α and Fas and activation of the caspase cascade. This occurred in parallel to the downregulation of mTOR, RICTOR and RAPTOR survival pathways, which are often over-expressed in the majority of the cancers. Thus, this study provided evidence for another complement-independent role of C1q. The second part of this thesis was to investigate the effect of Human Surfactant Protein-D (SP-D), which is known to modulate secretion of a range of cytokines and chemokines by effector immune cells, such as TNF-α and TGF-β, at mucosal surfaces during infection and inflammation. Our hypothesis was that SP-D can influence these soluble factors as a part of its putative role in the immune surveillance against pancreatic cancer, where the inflammatory tumour microenvironment contributes to the epithelial-to-mesenchymal transition (EMT) invasion and metastases. In this study, a recombinant fragment of human SP-D (rfhSP-D) inhibited TGF-β expression in a range of pancreatic cancer cell lines, thereby reducing their invasive potential by downregulating Smad2/3 expression that may have interrupted signal transduction negatively, which affected the transcription of key mesenchymal genes such as Vimentin, Zeb1 and Snail. Furthermore, prolonged treatment with rfhSP-D induced apoptosis in the pancreatic cancer cell lines via activation of the caspase cascade. Thus, this study added another layer to the well-known protective role of SP-D.

Chapter 1

Introduction

1.1 Immune surveillance in Cancer

The immune system is a highly effective host defense mechanism comprising layered protective subsystems, such as innate and adaptive immune systems, which launch an attack against altered self (apoptotic cells, transformed cells, virus-infected cells etc) and non-self (pathogens, grafts etc) by initiating inflammatory responses (Pio et al, 2014). Carcinogenesis is associated with frequent genetic and epigenetic alterations, which radically change phenotype of the cells by altering the morphology, structure of cell membrane components including the origin of tumour associated antigens, abnormal glycosylation (Hakomori, 2002) and an aberrant rise in the metabolism of membrane phospholipids (Glunde and Serkova 2006; Griffin and Kauppinen, 2007). Immune cells and proteins participate in an immune surveillance mechanism via its innate and adaptive wings to eliminate tumour cells. It can also make tumour cells quiescent, as evident from the presence of dormant tumours in the autopsy of patients deceased due to other reasons (Schreiber et al., 2011; Aguirre-Ghiso, 2007; Welch and Black, 2010). The immune surveillance comes into play when the normal cells undergoing transformation express distinctive pro-inflammatory factors or damage-associated molecular patterns (DAMPs), which act as danger signals recognised by the immune cells for eradication (Garg et al., 2013). The nature of the danger signals depends on various factors such as type of physical or chemical stress, chemistry of cell stress response, tumour cell type and the nature of the injury or cell death. DAMPs include chaperones (calreticulin and heat shock proteins; HSP70 and HSP90), extracellularly secreted factors (Adenosine 5'-triphosphate (ATP), high-mobility group box 1 (HMGB1) and uric acid) and cellular components produced during cell death (mitochondrial components and nucleic acid). Immune cells such as natural killer (NK) cells, dendritic cells (DCs) and T cells recognise the danger signals and participate in elimination process of newly transformed immunogenic tumour cells. However, rare tumour cells acquire mutations, which escapes the detection and elimination by the immune system, thus, continue to survive and proliferate until clinically detectable (Teng et al., 2008; Grivennikov et al., 2010). The escape tactics may include activation of regulatory T cells, varied antigen profile, shedding of tumour antigens to neutralise tumour specific antibodies, loss of major histocompatibility complex (MHC-I) expression, elevation of immunosuppressive

cytokines such as IL-10 or transforming growth factor-beta (TGF-β) and by downregulating the cell death receptors and caspases (Garg et al., 2013).

Tumour growth advances not only due to the acquired genetic mutations to overcome various defense mechanisms initiated by immunosurveillance, but also by altering the local microenvironment to a favourable niche for its survival, proliferation and migration (Barcellos-Hoff et al., 2013; Shankaran et al., 2001). Tumour cells colonised in the tissue enter an equilibrium phase, in which they survive either by generating new less immunogenic tumour variants, or by altering the mechanisms that activate immune defense (Shankaran et al., 2001). These findings led to the concept of dynamic process of 'immunoediting', which comprised three stages: (i) elimination via cancer immunosurveillance, followed by (ii) equilibrium, a phase of immune-mediated latency following the partial tumour elimination, and (iii) escape during which tumour overcomes the immunological limitations of the equilibrium phase and outgrows (Dunn et al., 2004; Dunn et al., 2002).

Various studies have shown the active role of innate and adaptive immune molecules in oncogenesis. However, the immuno-oncology field is constantly evolving due to heterogeneity associated with cancer cells, and hence, the activation of distinct immune mechanisms. Traditionally, the main focus of immuno-oncology research was based on the recognition and cytotoxic effects of immune cells. However, recent scientific advancements have shown that immune proteins can equally contribute to cancer treatment, which has been successfully translated into immunotherapies in a number of cases (Pandya et al., 2016).

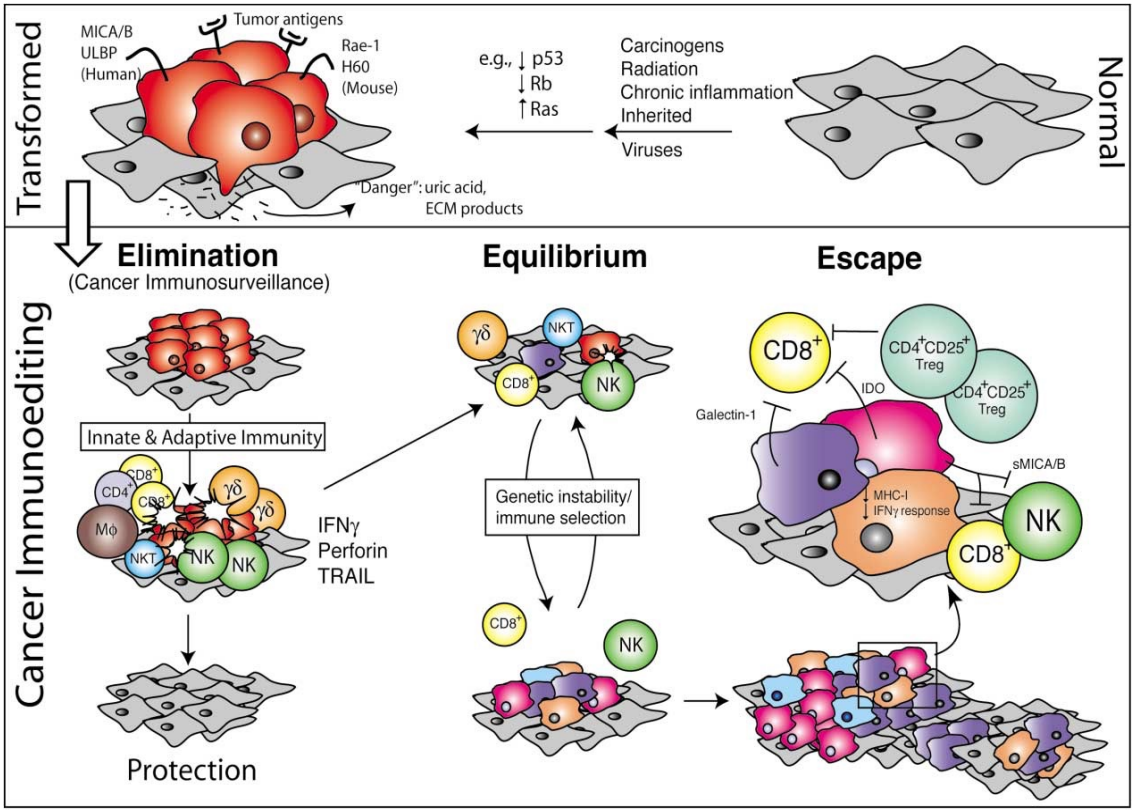

Figure 1.1 Cancer Immunoediting comprises three phases: elimination, equilibrium and escape. Normal cells undergo transformation in response to oncogenic stimuli and the process of tumorigenesis begins. During early stages of tumorigenesis, these transformed cells may express tumor associated markers and secrete danger signals. This initiates the immunoediting process, which begins with elimination phase by the combined action of innate and adaptive immunosurveillance network for the eradication of the developing tumor. In an unsuccessful event of elimination, the cancer cells enter the equilibrium phase, where they alter the immune responses and produce new tumor variants. These variants eventually overcome the immune responses and escape until it becomes clinically detectable (Figure 1.1 was taken from Dunn et al., 2004).

1.2 Innate Immunity

Innate immunity is the first line of defense against pathogens invading via epithelia, which is composed of epithelial cells held together by tight junctions in the form of skin and linings of the body's tubular structures such as gastrointestinal, respiratory and urogenital tracts (Murphy, 2012). Epithelial cells not only form a physical barrier but also secrete various protective anti-microbial glycoproteins (mucins), enzymes (lysozymes), and peptides (defensins, cathelicidins and histatins), which inhibit the microbial growth. The innate immune responses depend on a set of proteins and phagocytic cells such as neutrophils and macrophages, which recognise the conserved features of the pathogens, called pattern associated molecular patterns (PAMPs), or DAMPs, which are associated with host cells, via pattern recognition receptors (PRRs) to distinguish between self and non-self and promptly become activated to destroy them (Murphy, 2012). PRRs are divided into membrane bound PRRs (Toll like receptors; TLRs and C-type lectin receptors; CLRs), cytoplasmic PRRs (NOD-like receptors; NLRs and RIG-I-like receptors; RLRs) and soluble PRRs such as collectins, ficolins etc. PAMPs are highly conserved within different pathogens and can consist of protein, lipid, carbohydrate moieties or nucleic acid, that are recognised by TLRs. TLRs are a type of PRR, 13 of which have been identified so far, that are usually expressed on DC, macrophages, and NK cells (Lu et al., 2002; Reid, 1998; Haagsman, 1998; Crouch and Wright, 2001).

Over last two decades, various studies have demonstrated the role of major effector cells of innate immunity such as dendritic cells (DC), macrophages, basophils, eosinophils, natural killer (NK) cells, and mast cells and the cytokines and chemokines they produce, can influence the immunoediting process of elimination, equilibrium and escape during tumour development (Liu et al., 2012).

1.2.1 Innate immune surveillance in various cancers

The most powerful evidence for immune surveillance appeared when recombinase activating gene (RAG)-2 knockout mice model was developed. The knock-out mouse was incapable of somatically rearranging the lymphocyte antigen receptors, and thereby cannot produce peripheral natural killer T (NKT) cells, αβ T cells, γδ T cells or B cells. Thus, the model offered an insight into the effects of lymphocyte insufficiency on the development of tumour (Shinkai et al., 1992; Shankaran et al., 2001). RAG-2 knockout mice developed chemical carcinogen 3'-methylcholan-threne

(MCA) induced sarcomas quicker and more frequently, as compared to wild-type controls (Shankaran et al., 2001). NKT and γδ T cells were later found to play a key role in linking innate and adaptive immune responses, as evident from their interactions with $CD4^+$ and $CD8^+$ T lymphocytes (Dranoff, 2004). Subsequent studies showed that αβ and γδ T cell subsets played a critically distinct role against tumour development as mice lacking either αβ or γδ T cells were more prone to MCA-induced tumour development as compared to wild type mice (Girardi et al., 2003; Gao et al., 2003). Additional studies using chimeric mice with γδ T cells that could not produce IFN-γ were more prone to MCA-induced tumour suggesting, anti-tumour functions of IFN-γ (Gao et al., 2003).

The immune surveillance role of NK cells against cancer has been extensively studied. Mice depleted of NK and NKT using monoclonal antibody anti-NK1.1 were up to three times more prone to MCA-induced tumour as compared to the wild type mice (Smyth et al., 2001). The perforin produced by NK cells has been shown to protect mice from MCA induced sarcomas (van den Broek et al., 1996). Moreover, clinical evidence suggests that NK cells infiltrate in tumour tissues are associated with favourable prognosis in the cancer patients (Ishigami et al., 2000).

1.2.2 Immune surveillance mechanisms induced by Innate Immunity

During the innate immune response against non-major histocompatibility complex (MHC) or low MHC-I expressing tumour cells, NK cells are stimulated to initiate the primary immune response when its stimulatory cell surface receptor, Natural killer group 2D (NKG2D), binds to the tumour cell ligands including MHC class-I-chain-related protein A (MICA) (Bauer et al., 1999), MICB (Salih et al., 2003; Vetter et al., 2002) and UL-16 binding protein (Champsaur and Lanier, 2010) in human. The stimulated NK cells secrete IFN-γ, perforin and TNF-α, which induces apoptosis in the cancer cells (Schoenborn and Wilson, 2007; Liu and Zeng, 2012). The importance of IFN-γ has also been supported by the mice studies. IFN-γ prevents chemically induced tumour formation in vivo; in addition, tumours grow rapidly in mice lacking IFN-γ (Kaplan et al., 1998). TNF family ligands such as TNF, TNF- related apoptosis inducing ligand (TRAIL) and Fas are widely expressed on the NK cell surface. These can engage with their corresponding receptors such as TNF receptor, TRAIL receptor, or Fas, which are overexpressed in various tumours (Beutler and van Huffel, 1994; Gruss, 1996), leading to efficient induction of cell death by apoptosis (Nagata, 1997).

The C57BL/6 mice treated with TRAIL-neutralising antibodies, developed MCA-induced fibrosarcoma more rapidly than the wild-type control (Takeda et al., 2002).

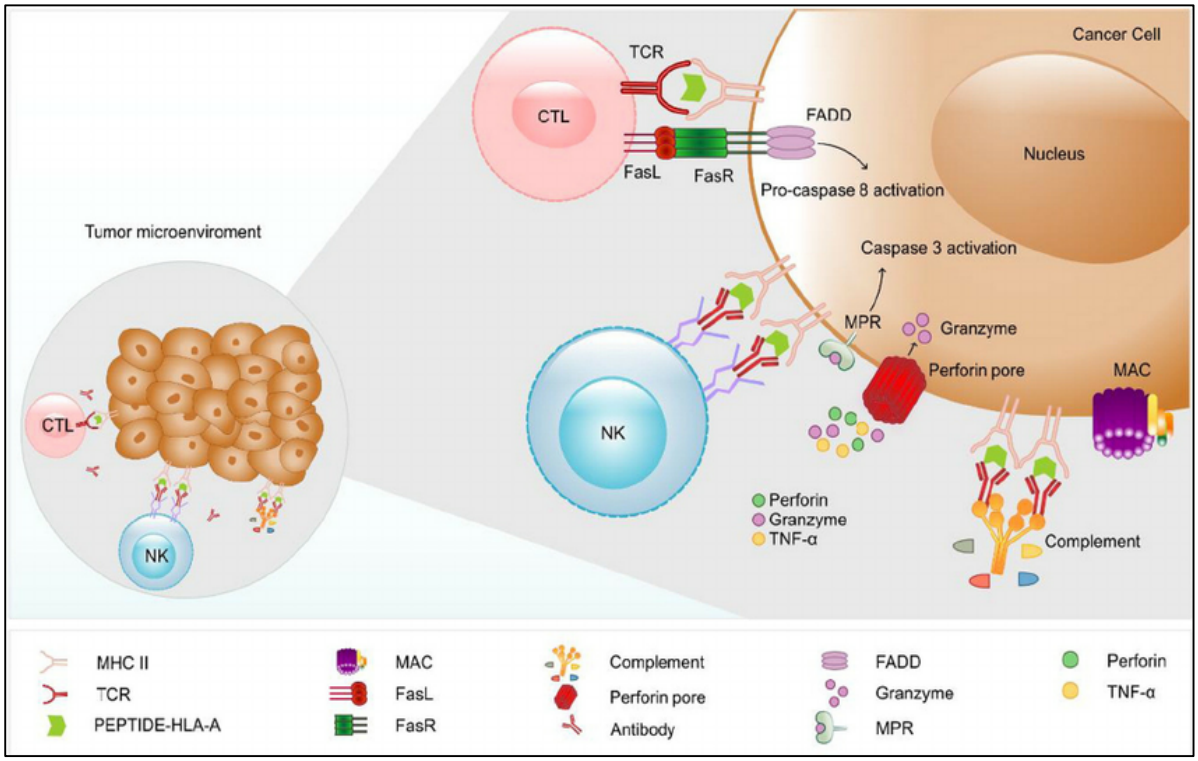

Figure 1.2 Immune response triggered by effector cells against cancer cells. Immune response may occur either via recognition of tumour associated antigens (TAA) either by cytotoxic T lymphocytes (CTL) or by specific antibodies, which opsonize the cancer cells for recognition by natural killer (NK) cells. CTL bind to TAA and causes cell death via FasL-FasR, whereas NK cells recognize the TAA associated antibody and release granules with perforin, granzyme, and TNF-α. Subsequently, caspase 3 is activated upon internalization of either granzyme via mannose-6-phosphate receptor (MPR) or perforin via perforin complex pores, which leads to apoptosis. These responses may lead to complement activation which culminates in membrane attack complex (MAC) and eventually the cell content leakage occurs. (Figure 1.2 was taken from Peres Lde et al., 2015).

Furthermore, stress signals secreted by the apoptotic tumour cells share similarities to the events triggered by microbial pathogens. These include danger signals recognised via PRRs such as TLRs, nucleotide-binding and oligomerisation domains, leucine-rich repeat containing NLRs and scavenger receptors (SRs). The phagocytic and antigen presenting cells can recognize both exogenous pathogens as well as endogenous modified molecules via these receptors (Murphy, 2012). The danger signals from apoptotic tumour cells which include lipid phosphatidylserine (PS) or calreticulin, activate the macrophages for recognition and elimination by phagocytosis (Gardai et al., 2006; Gardai et al., 2005). However, limitations to these danger signals

exit as they may initiate immune responses against the tumour locally as part of elimination phase. Several recent studies have shown that excessive inflammation may promote the tumour development (Dranoff, 2004). The macrophages in the tumour microenvironment are considered to promote chronic inflammation that provides an immune deficient environment favourable for tumour growth (Ostrand-Rosenberg, 2008).

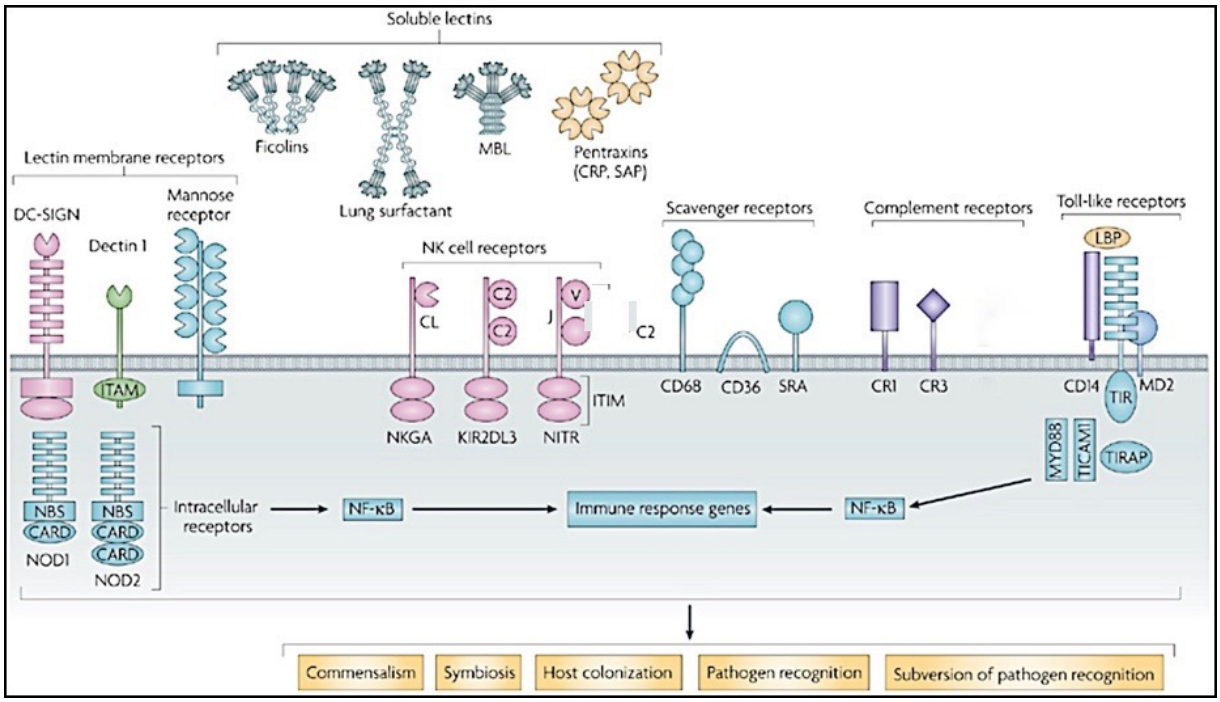

Figure 1.3 Various soluble and membrane bound pattern-recognition receptors (PRRs). These include soluble lectins such as collectins (MBL, surfactant proteins SP-A & SP-D), ficolins and pentraxins (C-reactive proteins and serum amyloid –P), integral membrane receptors (DC-SIGN, Dectin-1 and Mannose Receptor), natural killer (NK) cell receptors (NKGA, KIR2DL3 and NITR), scavenger receptors, complement receptors and Toll-like receptors (TLR). These receptors regulate the interactions with non-self cells that could lead to activation of various immune system mechanisms for their elimination (Figure 1.3 was taken from Vasta et al., 2009 with minor modification).

1.3 The Complement System

Complement system is an integral arm of the innate immune system, which is composed of more than 40 circulating or cell surface bound plasma proteins (Reid, 1986; Walport, 2001). These proteins participate in various processes such as mediators of adaptive immunity, microbial resistance, clearance of apoptotic cells, angiogenesis, regulation of coagulation system, synapse pruning, lipid metabolism and several immunological processes that substantially contribute to homeostasis (Ricklin et al., 2010). The complement system is activated depending on the ligand via classical, lectin or alternative pathway (Lu and Kishore, 2017).

The classical pathway is activated by C1q binding to IgM or IgG immune complexes or other activators such as apoptotic cells, necrotic cells etc, which initiates a cascade reaction of complement proteins that starts with activation of C1s and C1r. C1s, a serine protease cleaves C4 into C4b (binds to target surface) and C4a (diffuses away). Then, C2 binds to C4b and this complex is further cleaved by C1s into C2a and C2b, which remains bound to C4b, to generate a classical pathway C3 convertase (C4bC2b). In this complex, C2b (serine protease) cleaves C3 into C3b and C3a. C3b then binds to the target surface and joins C3 convertase to form C5 convertase, C4bC2bC3b. C5 is then cleaved into C5a (a potent anaphylatoxin like C3a) and C5b, which then assembles the components of C5b-9 (membrane attack complex, MAC), which may cause cell lysis. This process is known complement-dependent cytotoxicity (CDC), if the activating particle is a cell (Pangburn and Rawal, 2002) (Figure 1.4).

The lectin pathway is activated upon binding of mannose-binding lectin (MBL), which recognise and bind repetitive carbohydrate patterns such as mannose and N-acetyl-glucosamine on pathogens. The proteins then form a complex with MBL-associated serine protease-2 (MASP-2), which cleaves C4 and C2 to form C3 convertase C4bC2b, which is common to the activation of classical pathway Figure 1.4 (Pio et al., 2014).

The alternative pathway is initiated by hydrolysis of C3, which causes the cleavage of a thioester bond in C3 to form C3 (H_2O). This allows its binding to Factor B, which is cleaved by Factor D into Ba and Bb to form alternative pathway C3 convertase, C3 (H_2O)Bb. This complex then converts C3 into C3b and C3a. C3b is usually rapidly in activated, however, a few C3b molecules can bind complement

activating surfaces. This causes cascade reaction again as it then binds to Factor B, which can be cleaved by Factor D, forming C3 convertase (C3bBb). An amplification loop initiates as the Bb fragment on C3 convertase cleaves more C3, generating more C3b, capable of creating new C3 convertase and C5 convertase (Figure 1.4) (Pio et al., 2014).

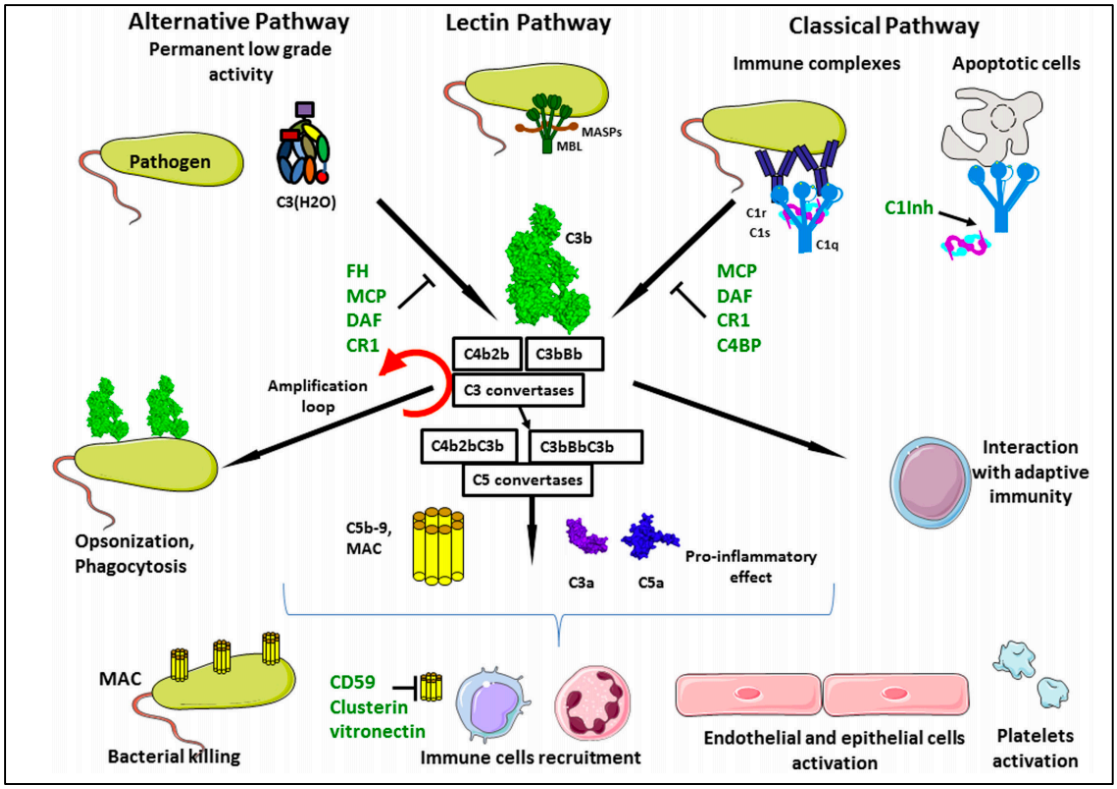

Figure 1.4 Three pathways of Complement system. The classical pathway is activated, when C1 complex binds to immune complexes leading to the formation of C4bC2b enzyme complex (C3 convertase) or brings about complement activation by binding to apoptotic cells. The lectin pathway is activated via either MBL or and MASP binding to a range of mannose groups on the bacterial cell surfaces, leading to the generation of C3 convertase. The alternative pathway is activated by hydrolysed C3 and factor B, which leads to formation of C3 convertase. All three pathways converge at C3 convertase. C3 convertase then forms C5 convertase enzyme, which subsequently forms MAC. Several factors including CR1, DAF, C4BP, MCP can inhibit the activity of C3 and C5 convertase. Proteins such as CD59, clusterin and vitronectin can block the assembly of the MAC complex. Complement activation subsequently leads to bacterial lysis by MAC complex and recruit immune cells, platelet activation and endothelial and epithelial cell activation. In addition, complement proteins opsonises the pathogens for phagocytosis. (Figure 1.4 was taken from Merle et al., 2015).

1.3.1 Complement mediated immune surveillance in various cancers

Although there is no direct and convincing evidence of effective complement mediated immune surveillance against cancer, it is assumed that the conventional role of complement system such as opsonisation of transformed cells and recognition by immune cells for elimination, may contribute to the inhibition of tumour growth. There is substantial evidence to suggest that tumorigenesis is accompanied by complement activation; however, it fails to completely eliminate the tumour cells.

Several studies have shown the presence of complement deposition in and around tumour cells, including the tumour microenvironment. These include C5 deposits and ability to generate C5a by lung cancer cell lines (Corrales et al., 2012), C3b presence in primary lung cancer cells (Niehans et al., 1996), elevated C3c and C4 in lung cancer patients (Gminski et al., 1992) and elevated C3a and soluble C5b-9 in the intraperitoneal ascitic fluid of ovarian cancer patients (Bjorge et al., 2005). Increased lectin pathway activation has been reported in colorectal cancer patients as compared to healthy subjects (Ytting et al., 2004). Increased complement haemolytic activity and C3 levels were found in serum samples from children with neuroblastoma (Carli et al., 1979). Elevated complement levels in digestive tract carcinoma patients (Maness and Orengo, 1977) and brain cancer (Matsutani et al., 1984) have also been reported. Furthermore, in vivo studies have also reported altered classical complement pathway activation in chronic lymphatic leukemic patients (Fust et al., 1987; Schlesinger et al., 1996), papillary thyroid carcinoma (Lucas et al., 1996), and follicular lymphoma and mucosa-related lymphoid tissue lymphoma (Bu et al., 2007). The alternative pathway activation was reported in lymphoblastoid cell lines (McConnell et al., 1978) and patients with multiple myeloma (Kraut and Sagone 1981). Additional associations between complement and tumorigenesis that have been reported include complement levels correlation with tumour size (Nishioka et al., 1976), survival correlation with activation of classical pathway of complement (Varga et al., 1995), and MASP-2 concentration in serum as an independent marker for poor prognosis (Ytting et al., 2005).

1.3.2 Complement Resistance Mechanisms in various tumors

Neoplastic transformation is associated with complement activation; however, cancer cells achieve resistance to complement attack by expressing membrane bound CD59, CD55 or soluble complement regulators (factor H, C1q) (Jurianz et al., 1999). For example, increased levels of CD59, a membrane attack complex (MAC) inhibitor, in prostate cancer (Jarvis et al., 1997); neuroblastoma (Chen et al., 2000) and melanoma (Coral et al., 2000) have been associated with resistance to complement mediated toxicity and increased metastatic capacity. Similarly, overexpression of CD55, a complement decay-accelerating factor (DAF), and its receptor CD97 in prostate cancer (Loberg et al., 2005) colorectal carcinoma (Durrant et al., 2003) and medullary thyroid carcinoma (Mustafa et al., 2004) has been reported. This is of significance as lack of CD55 in mice enhances the T cell response by hypersecretion of IFN-γ and interleukin (IL)-2 to active immunization as compared to wild type mice, suggesting the overexpression of CD55 supresses adaptive immune response (Liu et al., 2005).

Soluble complement proteins such as factor H or factor H like protein 1 (FHL-1) are overexpressed in bladder cancer (Cheng et al., 2005), lung adenocarcinomas (Cui et al., 2011) and ovarian carcinomas (Junnikkala et al., 2002). This can promote inactivation of C3b in H2 glioblastoma cells (Junnikkala et al., 2000), and regulate complement activation in melanoma cell line SK-MEL-93-2 (Ollert et al., 1995). In contrast, neutralisation of factor H using anti-factor H antibodies enhanced the CDC mediated killing of Burkitt's lymphoma cells (Corey et al., 1997; 2000). Moreover, when Factor H knockout A549 non-small cell lung cancer cell line, was injected into athymic mice (adaptive immune deficient with normal complement activity), xenografts formed by Factor H deficient mice were significantly smaller as compared to control mice. Immunohistochemistry analysis of the xenograft tumours Factor H deficient mice showed higher levels of C3 deposits, when compared with the control mice xenografts (Ajona et al., 2007). Other soluble complement regulatory proteins that protect cancer cells from complement mediated killing include Factor I, which cleaves C3b and C4b, and C4b-binding protein (C4BP) in non-small-cell lung cancer (Okroj et al., 2008) and C1 inhibitor (Bjorge et al., 2005). Additionally, complement resistance mechanisms may also include secretion of proteases, which cleave complement activating components (Ollert et al., 1990) and endocytosis or

vesiculation of MAC (Morgan, 1992; Moskovich and Fishelson, 2007) by cancer cells.

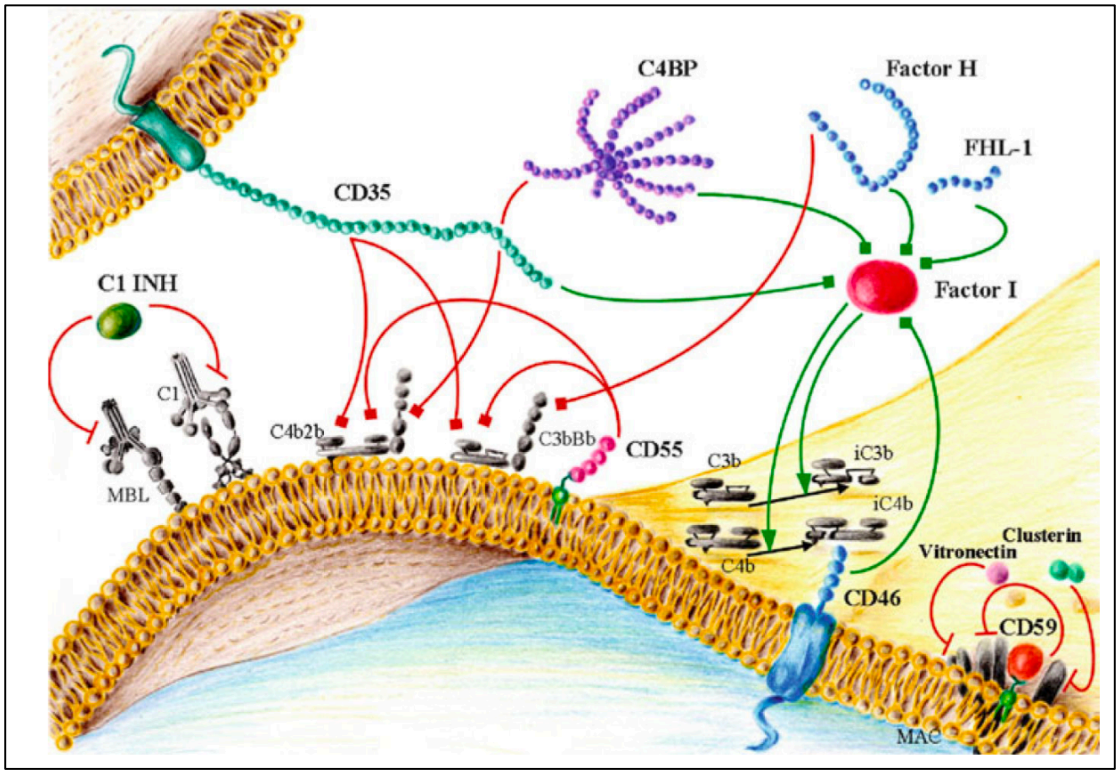

Figure 1.5 Main complement inhibitors including soluble proteins and membrane bound complement regulators. Red lines ending in a bar show the inhibitory effect such as Factor H and FHL-1 inhibit the activation of C3 and C4BP inhibits C4b2b. Red lines ending with a square show accelerated decay activity. Overexpression of complement regulator such as CD59 (MAC inhibitor), CD35 (complement receptor), and CD55 (C4b2b C3 and C3bBb C3 convertase inhibitor) and Green lines ending with square show cofactor activity, and the ones ending with arrowhead show protease activity such as inactivation C3b and C4b by serum factor I. Vitronectin and clusterin inhibit insertion of MAC into the membrane (Figure 1.5 was taken and modified from Pio et al., 2014).

1.3.3 C1q

C1q, an innate immune molecule, is the first subcomponent of the C1 complex that recognises the IgG-or IgM containing immune complexes and activates the complement classical pathway. It is the key molecule of classical pathway of complement. It can bind a wide variety of self and non-self ligands and regulates a range of homeostatic functions such as clearance of immune complexes, pathogens, necrotic and apoptotic cells (Kishore et al., 2004). In addition to Kupffer cells cells in the liver, C1q is also produced by macrophages, immature DCs and adherent monocytes (Lu and Kishore, 2017). Interestingly, C1q has also been found in the microenvironment of various tumour tissues, where it was unable to activate complement and promoted proliferation (Bulla et al., 2016), suggesting its complement-independent function.

Human C1q, 460 kDa, molecule comprises 18 polypeptide chains (6A, 6B and 6C). The A chain (223 residues), B chain (226 residues), and C chain (217) residues and each C1q chain has a short N-terminal region (3-9 residues), followed by a collagen like sequence of ~81 residues and a C-terminal globular (gC1q) region of ~135 residues. The inter-chain disulfide bridges link N-terminal regions of A and B chains yielding 6A-B dimer subunits and two C chains yielding 3C-C dimer subunits. The triple helical collagen region from A-B subunit and a C-C subunit forms a structural unit (ABC-CBA), joined by covalent and non-covalent bonds. These three subunits assemble together to form a full-length protein, held together with strong non-covalent bonds (Figure 1.6), (Kishore and Reid, 2000; Kishore et al., 2004).

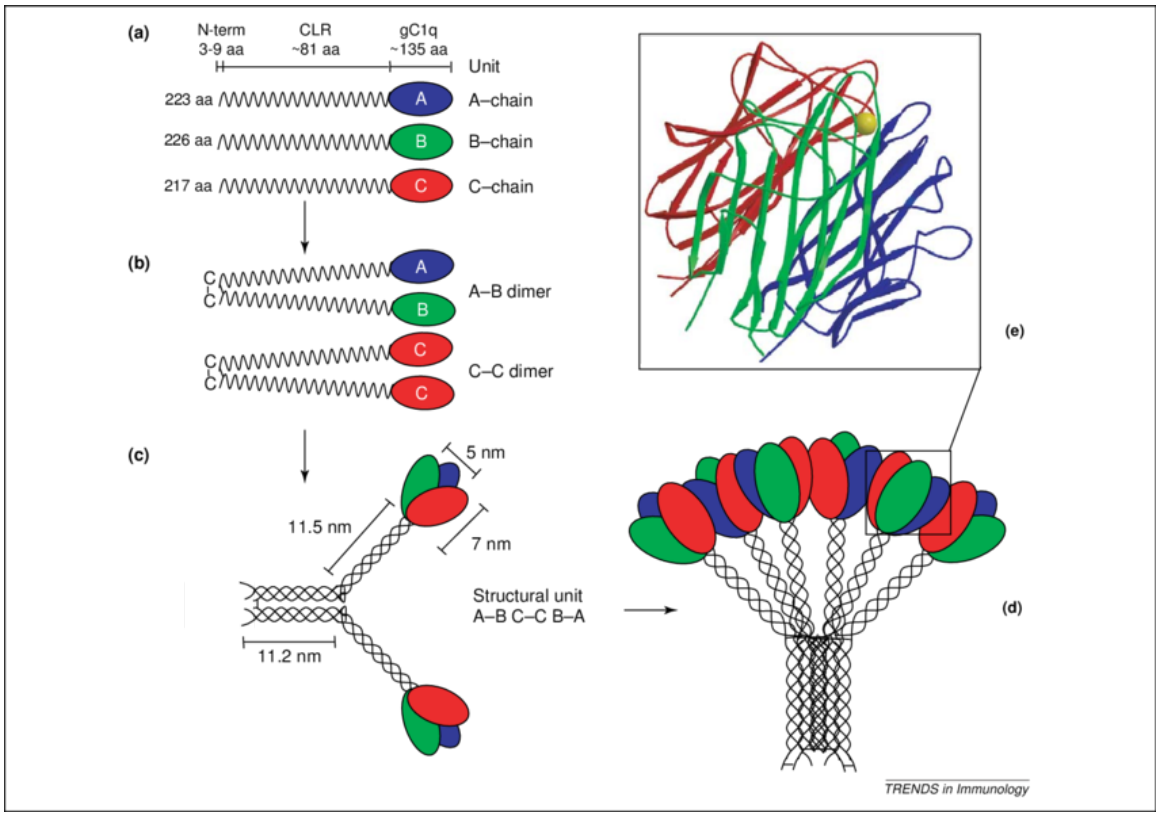

Figure 1.6 Schematic representation of structural assembly of C1q molecule. C1q (460Kda) comprises 18 polypeptide chains (6A, 6B, and 6C), encoded by three different genes (*C1QA, C1QB, and C1QC*). (a) Each chain comprises a short N-terminal region, followed by collagen region (CLR) of ~81 residues and a C-terminal globular region (gC1q domain) of ~135 residues. (b) The interchain disulfide bridges link N-terminal regions of A and B chains yielding 6A-B dimer subunits and two C chains yielding 3C-C dimer subunits. (c) The triple helical collagen region from A-B subunit and a C-C subunit forms a structural unit (ABC-CBA), joined by covalent and non-covalent bonds. (d) These three subunits assemble together to form a full-length protein, held together with strong non-covalent bonds. (e) The crystal structure of the gC1q domain of human C1q (Protein Data Bank code 1PK6, presented as a ribbon diagram of ghA in blue, ghB in green, ghC in red, with the calcium ion shown as a yellow ball), shows a compact, spherical, heterotrimeric assembly (50 Å diameter), held together predominantly by non-polar interactions, with non-crystallographic pseudo-threefold symmetry (Figure 1.6 was taken from Kishore et al., 2004).

1.3.3.1 Complement independent functions of C1q

Based on the presence of jellyroll topology of the gC1q domain (Shapiro and Scherer, 1998; Ghebrehiwet et al., 2003; Ghai et al., 2007), it became evident that C1q was possibly a prototypical molecule of the TNF family, hence, the C1q-TNF superfamily came to be recognised (Kishore et al., 2004). Thus, expansion of the C1q family has led to the identification of a range of immunomodulatory functions of C1q that are independent of its role in the complement activation (Kouser et al., 2015; Kishore et al., 2016). These include modulation of dendritic cell (DC) functions (van Kooten et al., 2008), neuronal synapse pruning (Stevens et al., 2007) and cancer development (Bulla et al., 2016). Indeed, C1q is also involved in cellular differentiation, pathology of pregnancy, immunologic tolerance and extensive cross-talk with extracellular matrix proteins (Kishore et al., 2016).

Several functional overlaps between C1q and the TNF family exist. This became even more evident, when it was established that C1q may regulate TNF-α in the ovarian cancer cell line SKOV3, leading to apoptosis of the target cells (Kaur et al., 2016; Chapter 3 of this thesis). In this context, a cytokine-like function of C1q has also been proposed recently (Ghebrehiwet et al., 2012). Interestingly, the recombinant fragments of the gC1q domain of human C1q A, B, and C chains (ghA, ghB and ghC) were also able to induce apoptosis in SKOV3 cells (Kaur et al., 2016; Chapter 3 of this thesis). Furthermore, C1q was also shown to induce apoptosis in the DU145 prostate cancer cells via activation of WOX1, a pro-apoptotic and a tumour suppressor protein, and disrupted cell adhesion (Hong et al., 2009).

The presence of C1q was shown in the stroma and vascular endothelium of various human malignant tumours, including adenocarcinoma of such as lung, colon, pancreas and breast, as well as melanoma (Bulla et al., 2016). The locally synthesised C1q has a tumorigenic role via promoting adhesion, evasion and proliferation without the activation of complement. *C1qa* deficient mice exhibited slower growth of tumour and prolonged survival as compared to wild type mice, when melanoma cancer cells (B16/F10) were injected intramuscularly. The tumour growth rate in C3- and C5-deficient mice was similar to wild type. Similarly, a significant difference was seen in tumour growth of C1qa deficient and wild type syngeneic mouse model of lung carcinoma (Bulla et al., 2016).

In conclusion, the role of C1q against cancer, thus appears to be dampened due to the expression of complement regulators such as CD55 (C4b2b C3 and C3bBb

C3 convertase inhibitor) and CD59 (MAC inhibitor), rendering the inefficient immune surveillance mechanism despite its presence in the tumour microenvironment; however, C1q regains its functions when added exogenously to the cancer cells (Bjorge et al., 2005, Kaur et al., 2016, Bulla et al., 2016, Hong et al., 2009).

1.4 Collectins

Collectins (collagen containing C-type lectins) are soluble pattern recognition molecules that bind to a wide range of carbohydrate on the cell surfaces of a range of pathogens including bacteria, fungi and viruses in a calcium dependent manner and bring about complement activation (in case of MBL) and phagocytosis. The collectins can recognise PAMPs and DAMPs (Lu et al., 2002; Reid, 1998; Haagsman, 1998; Crouch and Wright, 2001). Binding of collectins to microbes via lectin domains results in activation of multiple immunological processes that include agglutination/aggregation, enhanced phagocytosis and complement activation (Lu et al., 2002). Nine members of collectin family have been identified so far, including Mannan binding lectin (MBL) (Kawasaki et al., 1978), Surfactant protein A (SP-A) (White et al., 1985), Surfactant protein D (SP-D) (Persson et al., 1988), collectin liver 1 (CL-L1), which are the well characterised members of the collectin family (Lu et al., 1997; Ohtani et al., 1999). One of the aim of this thesis is to explore the effect of SP-D in immune surveillance against cancer.

1.4.1 Human Surfactant Protein D

Human SP-D plays a vital role in linking the innate and adaptive immunity to protect against infection, allergy and inflammation (Kishore et al., 2006). SP-D can act as a potent opsonin for viruses, bacteria and fungi, and bring about clearance mechanisms via aggregation/agglutination, enhanced phagocytosis, production of superoxide radicals, direct microbicidal effect, and macrophage activation (Kishore et al., 2005). In most instances, SP-D binds to carbohydrate on the pathogen surface via its CRD region, whilst the collagen region binds to its putative receptor (calreticulin/CD91 complex being one of them) on the surface of macrophages and other phagocytic cells and brings about effector functions (Gardai et al., 2005).

SP-D is a hydrophilic protein, that is a polymer made up of a single polypeptide chain (43 kDa) with a cysteine containing N-terminal region, region of collagen sequence containing repeated Gly-X-Y triplets, an α-helical coiled-coil neck

region and a C-type lectin domain or carbohydrate recognition domain (CRD). Three identical polypeptide chains of 43 kDa form an oligomer of 130 kDa subunit. Four homotrimeric subunits linked via their N-terminal regions form a tetrameric structure of 520 kDa (Kishore et al., 2006, Nayak et al., 2012) (Figure 1.7). Earlier findings indicated that SP-D was secreted by type II pneumocytes and Clara cells in the lungs. However recently its extrapulmonary presence in tissues such as trachea, brain, testis, heart, prostate, kidneys, and pancreas has also been reported (Madsen et al., 2000; Kishore et al., 2006; Nayak et al., 2012). Although its homeostatic role in lungs has been widely studied, its specific functions at extrapulmonary tissues are poorly understood (Kishore et al., 2006).

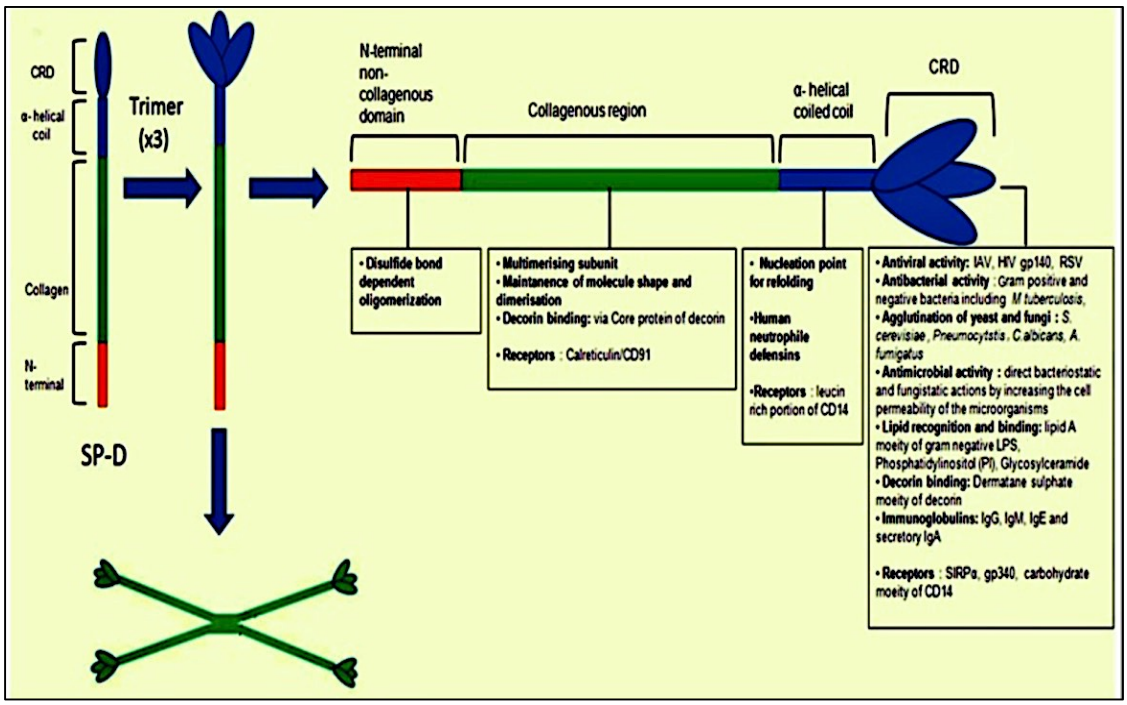

Figure 1.7 Schematic presentation of human Surfactant Protein D (SP-D) structure. The SP-D polypeptide monomer comprises cysteine rich N-terminal region (required for disulfide bonds for oligomers), collagen region containing repeated Gly-X-Y triplets, α-helical coiled-coil neck region and a C-type lectin domain or carbohydrate recognition domain (CRD). Human SP-D is composed of three single polypeptide chains of 43 kDa forming a trimer subunit of 130 kDa. Four of these oligomer subunits then assemble a tetrameric structure of SP-D, 520kDa. SP-D binds via CRDs to various ligands while the collagen region regulates the recruitment of immune cells for the clearance of pathogens, allergens and apoptotic/necrotic cells (Figure 1.7 was taken from Nayak et al., 2012).

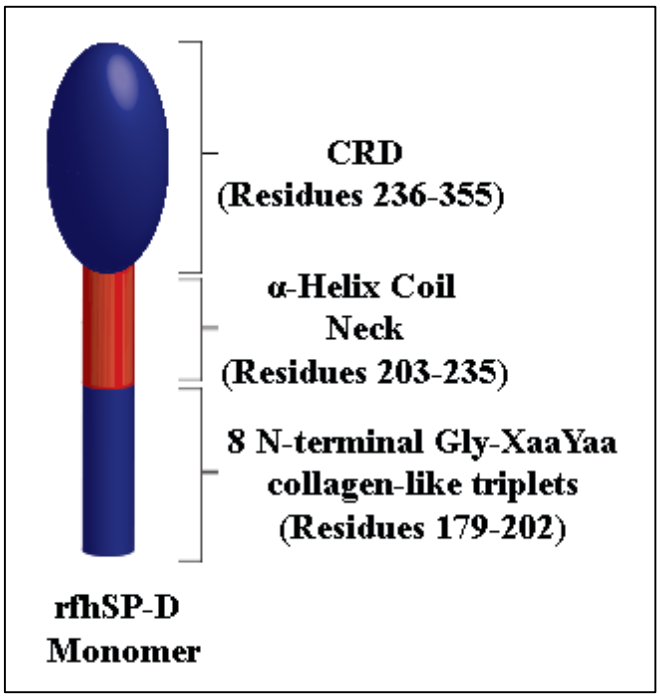

Figure 1.8 Schematic presentation of a recombinant fragment of human Surfactant Protein D (rfhSP-D) structure. The SP-D polypeptide monomer comprises 8 N-terminal Gly-XaaYaa collagen-like triplets (residues 179–202), Helical coiled-coil neck region (residues 203–235) and CRD region (residues 236–355) (Figure 1.8 was adapted from Kishore et al, 2006).

1.4.1.1 Immune surveillance by SP-D

Initially, SP-D and a recombinant fragment of human SP-D containing α-helical coiled-coil neck and CRD region (rfhSP-D) (Figure 1.8) were shown to bind the house mite extract (*Dermatophagoides pteronyssunus;* Derp), and allergens of *Aspergillus fumigatus (Afu)* derived from 3-week culture filtrate (3wcf) and glycoprotein allergens such as gp55 and gp45 in a calcium dependent manner, inhibit IgE binding to these allergens and thereby blocking the allergen triggered histamine release from basophils derived Derp and *Afu* sensitised patients (Wang et al., 1996; 1998; Madan et al., 1997). When exogenous rfhSP-D was administered therapeutically in a murine model of pulmonary hypersensitivity induced by *Afu* allergen/antigens, it lowered specific IgG and IgE levels, suppressed peripheral and pulmonary eosinophilia, and polarised Th2 to Th1 immune response in the spleen (Madan et al., 2001). These studies highlighted SP-D as a potent link between innate and adaptive immunity and a modulator of inflammation by virtue of its ability to control inflammatory response and helper T cell polarization (Nayak et al., 2012).

These initial studies were followed by observations that eosinophils derived from sensitized individuals were susceptible to apoptosis induction, oxidative burst and CD69 expression by rfhSP-D in vitro as compared to eosinophils derived from healthy and non-sensitised individuals. However, eosinophils derived from healthy donor primed with IL-5 turned out to be susceptible to rfhSP-D induced apoptosis. rfhSP-D binding to human eosinophils in calcium-dependent manner indicated the involvement of its carbohydrate recognition domain (Mahajan et al., 2008).

Using an eosinophilic cell line, AML14.3D10 (a model cell line for leukaemia), it was established, via proteomics analysis, that apoptosis induction by rfhSP-D involved upregulation of p53 (Figure 1.8). The treatment with SP-D and rfhSP-D induced cell cycle arrest via activation of G2/M checkpoints i.e. increased p21 levels and phosphorylation of cdc2, activated pro-apoptotic marker cleaved caspase 9 and downregulated pro-survival protein HMGA1 in the leukemic cell line AML14.3D10 (Mahajan et al., 2013; Mahajan et al., 2014).

Another crucial study by Pandit et al., (2016) revealed that rfhSP-D was able to induce apoptosis in activated human PBMCs, but not in resting, non-activated PBMCs. rfhSP-D treatment was found to restore homeostasis by regulating the expression of immunomodulatory receptors and cytokines and subsequent apoptosis induction in the activated lymphocytes. It caused significant downregulation of pro-inflammatory receptors such as CD69, TLR2, TLR4 and CD11c and thus, inhibited Th response. Levels of Th1 cytokines IFN-γ, TNF-α and IL-6 were downregulated, however, Th2 cytokines (IL-4 and IL-10) and TGF-β levels were not affected (Pandit et al., 2016). These studies, for the first time, raised the possibility that SP-D can have a function of immune surveillance against activated self and perhaps altered/transformed self.

Subsequently, involvement of SP-D in the control of cancer has recently been examined (Hasegawa et al., 2015). Human lung adenocarcinoma cells (A549 cell line), when exogenously treated with SP-D, showed suppressed epidermal growth factor (EGF) signalling by reducing the EGF binding to EGFR, which subsequently reduced the cell proliferation, invasion and migration of cancer cells. SP-D was found to directly bind to sEGFR in a calcium dependent manner, which involved interactions between carbohydrate recognition domains of SP-D and N-glycans of

EGFR (Hasegawa et al., 2015). Therefore, effect of SP-D on pancreatic cancer has been further evaluated in this study.

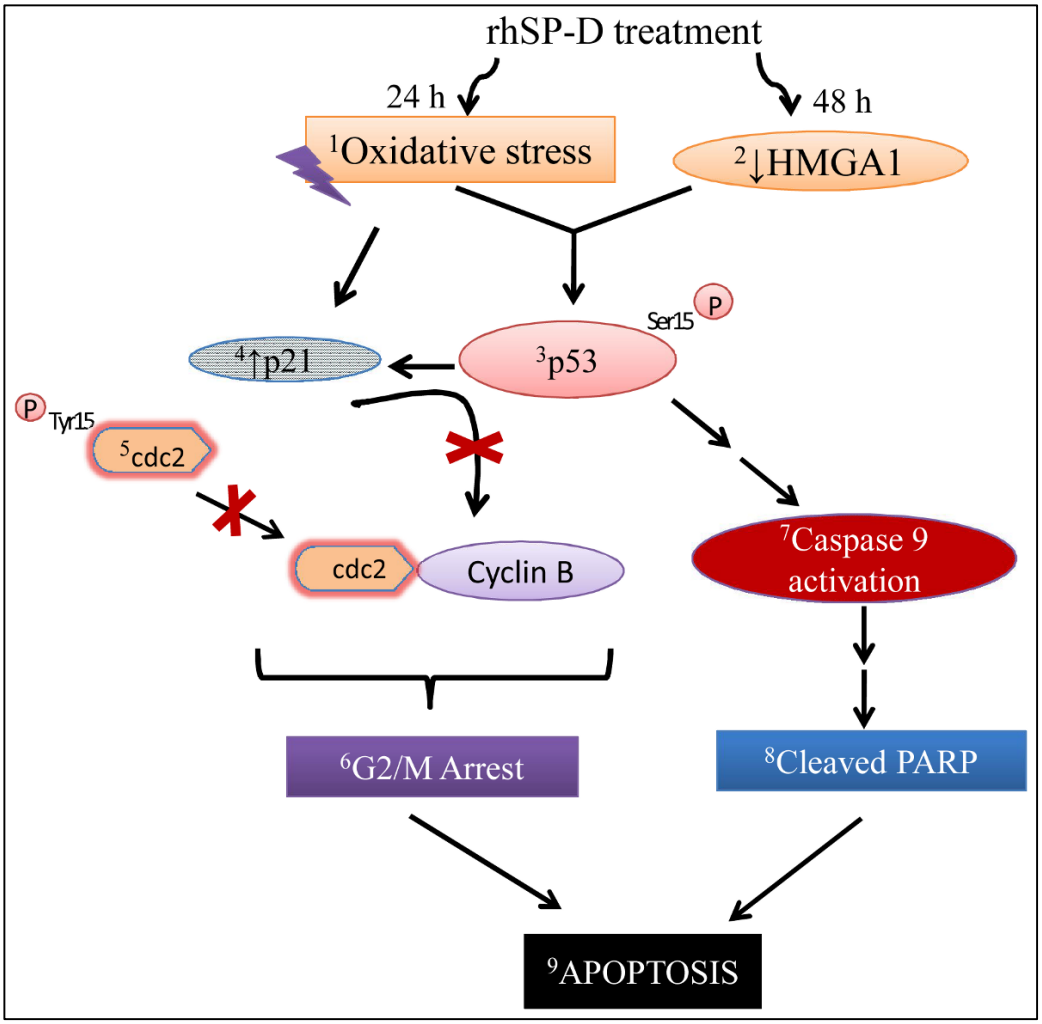

Figure 1.9 Mechanism involved in apoptosis induction by rfhSP-D in AML14.3D10 leukemic cell line. rfhSP-D treatment enhanced the oxidative stress and downregulated pro-survival marker, HMGA1, which causes phosphorylation of p53 and cdc2. p21, was upregulated and cdc2 phosphorylation causes inhibition of cdc2, leading to G2/M phase cell cycle arrest. p53 was upregulated, which caused activation of caspase 9, which further caused cleavage of Poly (ADP-ribose) polymerase (PARP), and subsequent apoptosis (Figure 1.8 was taken from Mahajan et al., 2013).

1.5 Main Aims of this Study

In order to investigate the effects of innate immune molecules on ovarian and pancreatic cancer, the following aims have been outlined:

1. To investigate the complement independent effects of exogenous C1q and recombinant forms of globular head modules (ghA, ghB and ghC) on an ovarian cancer cell line, SKOV3 in order to determine if C1q has pro-or anti-tumorigenic effect in ovarian cancer, which is presented in Chapter 3.
2. To assess a possible anti-tumorigenic role of rfhSP-D on invasive-mesenchymal phenotype in pancreatic cancer cell lines, which is presented in Chapter 4.
3. To examine a possible p53 independent pro-apoptotic role of rfhSP-D in pancreatic cancer cell lines, which is presented in Chapter 5.

Chapter 2

Methods and Materials

2.1 Purification of human C1q

Human C1q was purified from freshly thawed human plasma (TCS Biosciences; Catalogue # PR100) using affinity chromatography on IgG Sepharose (Tan et al., 2010). Human plasma (100 ml) was made 5 mM EDTA by adding 200 mM sodium EDTA, pH 7.4 and centrifuged at 5000 x g for 10 min. The supernatant was then passed through a Whatmann filter paper (GE Healthcare, UK) to remove any aggregates and lipids. The plasma was then mixed with non-immune human IgG coupled to CNBr-activated Sepharose (20 ml with 20 mg IgG per ml of Sepharose; GE healthcare, UK) on a gentle shaker for 2 h at room temperature. C1q bound to IgG-Sepharose was washed rapidly with 10 mM Hepes, 140 mM NaCl, 0.5mM EDTA, pH 7.4 and the IgG-Sepharose was packed into a column to elute bound C1q with CAPS (N-cyclohexyl-3-aminopropanesulfonic acid) buffer (100 mM CAPS, 1 M NaCl, 0.5 mM EDTA, pH 11). The eluted protein was dialysed against 0.1M HEPES buffer, pH 7.5 to lower the pH. The IgG contaminants were removed from the eluted C1q fractions by passing it through a HiTrap Protein G column (GE Healthcare, UK). The purified protein was then analysed on SDS-PAGE.

2.2 Expression of recombinant proteins

Preparation of competent cells, transformation, pilot scale and large-scale expression steps were common for the purification of all recombinant proteins; rfhSP-D, ghA, ghB, ghC and MBP except the antibiotic resistance, which is mentioned as appropriate in the sections below.

2.2.1 Competent Cells

A single colony of *E. coli* BL21 (λDE3) pLysS (Invitrogen, UK) in the presence of chloramphenicol (50 μg/ml) (Sigma-Aldrich, UK) for rfhSP-D or BL21 (Invitrogen, UK) in the presence of ampicillin (100 μg/ml) (Sigma-Aldrich, UK) for globular head modules was inoculated in 10 ml of Luria Broth (LB) medium at 37^0C on a shaker overnight. On the following day, 500 μl of the primary culture was inoculated into 10 ml of LB medium containing chloramphenicol (50 μg/ml) for BL21 (λDE3) pLysS or ampicillin (100 μg/ml) for BL21 before incubating at 37^0C on a shaker until the optical density (OD_{600nm}) reached between 0.3-0.4 i.e. an early log Phase. The culture was then centrifuged at 2000 x g for 5 min and the pellet was resuspended very gently in 1 ml of 0.1 M $CaCl_2$ and then a final volume of 12.5 ml of $CaCl_2$ was added to the

cell suspension before incubation on ice for 1 h. Then, the cells were centrifuged for 5 min at 2000 x g and the supernatant was discarded. The cell pellet was resuspended in 2 ml of 0.1 M $CaCl_2$ and these cells were competent cells to be transformed.

2.2.2 Transformation of cells

Expression construct rfhSP-D (pUK-D1, containing cDNA sequences for Gly-X-Y repeat, neck and CRD region of human SP-D; Kishore et al., 2006), ghA (pKBM-A), ghB (pKBM-B), ghC (pKBM-C) and MBP, (1-2µg) (Kishore et al.,2003) were added to competent cells separately (200 µl) for incubation on ice for 1 h. Then, bacterial cells were given heat shock at 42^0C for 90 sec followed by an immediate incubation for 5 min on ice. LB (800 µl) was then added to the transformed cells before incubating at 37^0C with gentle shaking at regular intervals for 45 min. After incubation, cells were spread plated on a LB agar plate containing 100 µg/ml of ampicillin and 50 µg/ml of chloramphenicol for rfhSP-D or ampicillin alone for globular head modules and MBP. The transformed cultures were plated for incubation at 37^0C incubator to allow the colonies to grow overnight. Using these plates, colonies were grown for a pilot scale expression analysis to ensure the expression of the protein of interest.

2.2.3 Pilot-Scale Expression

A single colony was inoculated in 4 different sets of 5 ml LB containing ampicillin (100 µg/ml) and chloramphenicol (50 µg/ml) for rfhSP-D or ampicillin (100 µg/ml) alone for globular head modules and MBP to grow overnight in a shaking incubator at 37°C. On the following day, 500 µl of primary culture was added to10 ml LB containing appropriate antibiotics before incubating at 37°C on a shaker until it reached an OD_{600nm} between 0.6–0.8. An un-induced (1 ml) sample was taken as a control and the remaining culture was induced with 0.4mM Isopropyl β-D-1-thiogalactopyranoside (IPTG) (Sigma Aldrich, UK). Both induced culture and an un-induced sample were incubated at 37 °C on a shaker for 3 h. Then, 1 ml of un-induced and induced samples were centrifuged at 13,800 × g for 10 min. The cell pellet was then mixed with 100 µl of 2x treatment buffer (50 mM Tris pH 6.8, 2% β-merceptoethanol, 2% SDS, 0.1% bromophenol blue, and 10% glycerol) and heated at 100°C for 7 min before loading 20 µl of each sample on a 12 % SDS-PAGE to run for 90 min at 120V for analysis of the expression in the induced samples. The primary

culture for the expressed colony was then streaked on a LB agar plate containing appropriate antibiotics for rfhSP-D or globular heads and MBP to grow overnight at 37°C. Using these plates, large scale bacterial cultures were grown for the purification of the recombinant proteins.

2.2.4 Large-Scale Expression

A single colony from the pilot scale was inoculated in 25 ml LB containing ampicillin (100 µg/ml) and chloramphenicol (50 µg/ml) for rfhSP-D or ampicillin (100 µg/ml) alone for globular head modules to grow overnight at 37°C on a shaker. The primary culture (12.5 ml) was added to 500 ml LB medium with appropriate antibiotics for the recombinant proteins and incubated at 37°C on a shaker for 3 h until the OD_{A600} reached between 0.6 and 0.8. An un-induced sample (1 ml) was taken from the culture and the remaining culture was induced with 0.4 mM IPTG before incubating at 37°C on a shaker for further 3 h. After 3 h, 1 ml from induced culture and an un-induced sample were centrifuged at 13,800 x g for 10 min. The cell pellet was mixed with 100 µl of 2x treatment buffer and heated for 7 min at 100°C before running on a 12 % SDS- PAGE for 90 min at 120V to determine the protein expression. In addition, the remaining induced culture was centrifuged at 13,800 x g at 4°C, for 15 min and the cell pellet was stored at −20°C to process for purification later.

2.3 Purification of ghA, ghB, ghC modules of human C1q and MBP

The globular head regions of human C1q A (ghA), B (ghB) and C (ghC) were expressed in *E.coli* as MBP-fused recombinant forms. The cell pellet from the large scale for each fusion protein and MBP was lysed in 25 ml of lysis buffer (20 mM Tris-HCl, pH 8.0, 0.5 M NaCl, 1 mM EGTA pH 7.5, 1 mM EDTA pH 7.5, 5% v/v glycerol, 0.2% v/v Tween 20) containing 0.1 mM PMSF and lysozyme (100 µg/ml) at 4°C for 30 min. The cell suspension was then sonicated at 60 Hz for 30 sec with an interval of 2 min each and it was repeated for 12 cycles. The sonicated cell suspension was then centrifuged at 13,800 x g for 15 min. The supernatant was mixed 5 x 25 ml with buffer I (20 mM Tris-HCl, pH 8.0, 100 mM NaCl, 1 mM EDTA PH 7.5, 0.2% v/v Tween 20 and 5% v/v glycerol). The diluted supernatant was then passed through an amylose resin column (New England Biolabs). The column was then washed extensively with 150 ml of buffer I, followed by buffer II (250 ml of buffer I without

Tween 20). The fusion protein fractions were then eluted with 100 ml buffer II containing 100 mM maltose. The OD_{280} was determined for the concentration of the proteins before running the samples on SDS-PAGE to confirm the purified protein bands. The peak elutions were then passed through Pierce™ High Capacity Endotoxin Removal Resin (Qiagen) to remove lipopolysaccharide (LPS). Endotoxin levels in the purified protein samples were analysed using the QCL-1000 Limulus amebocyte lysate system (Lonza). The assay was linear over a range of 0.1–1.0 EU/ml (1 EU = 0. 1 ng of endotoxin) and the amount of endotoxin levels was measured as <0.5pg/µg of the recombinant proteins.

2.4 Purification of rfhSP-D

A recombinant fragment of human SP-D containing α-helical coiled-coil neck region and three CRDs was purified as discussed below.

2.4.1 Lysis and Sonication

The cell pellet stored at −20°C was lysed using 50 ml of lysis buffer (50 mM Tris-HCl, pH 7.5, 200 mM NaCl, 5 mM EDTA) containing 0.1 mM phenylmethylsulfonyl fluoride (PMSF; Sigma-Aldrich, UK) and 100 µg/ml lysozyme (Sigma-Aldrich, UK) at 4°C for 1 h. The cell suspension was sonicated at 60Hz for 30 sec with 2 min interval and repeated it for 12 cycles. The sonicated cell suspension was then centrifuged at 13,800 x g for 15 min at 4°C and the inclusion bodies enriched with rfhSP-D protein in the cell pellet were stored at -20°C for solubilization later.

2.4.2 Dialysis

The cell pellet was solubilized in 25 ml of solubilisation buffer (50 mM Tris-HCl pH 7.5, 5 mM EDTA and 100 mM NaCl) containing 6 M Urea for 1 h at 4°C. The cell suspension was then centrifuged at 13,800 x g, at 4°C for 15 min. The supernatant was serially dialysed against solubilization buffer containing 4 M, 2 M, 1 M urea with 10mM β-mercaptoethanol and 0 M urea for 2 h each at 4°C. The final dialysis was done in solubilization buffer containing 5 mM $CaCl_2$ for 3 h and centrifuged at 13,800 ×g, 4°C for 15 min to carry out further purification steps.

2.4.3 Protein purification by Affinity Chromatography

The supernatant containing rfhSP-D was passed through the maltose agarose column (Sigma-Aldrich, UK). The column was washed with 50 ml of 1M salt buffer (50 mM Tris-HCL, pH 7.5, 1 M NaCl, 5 mM $CaCl_2$) before eluting the maltose bound protein with solubilisation buffer containing 10mM EDTA, pH 7.5. The OD_{280} was determined for the concentration of the protein in the eluted fractions. The purified protein (20 µl) was mixed with 2 x treatment buffer (50 mM Tris pH 6.8, 2% β-mercaptoethanol, 2% SDS, 0.1% bromophenol blue, and 10% glycerol) and denatured at 100°C for 7 min before running on 12% SDS-PAGE to confirm the purity of the protein.

2.4.4 Endotoxin removal from purified fractions of rfhSP-D and Limulus amebocyte lysate assay

Pierce™ High Capacity Endotoxin Removal Resin (Qiagen) was used to remove lipopolysaccharide (LPS). The column was washed with 50 ml of autoclaved water followed by 50 ml of 1% sodium deoxycholate (Sigma-Aldrich, UK) and then washed again by 50 ml autoclaved water. Then, the purified protein with higher OD_{280} was passed through the column and OD_{280} was determined using a Nanodrop spectrophotometer. To confirm the LPS levels of rfhSP-D, a LAL (Limulus amebocyte lysate) was performed. A standard curve was plotted using 4 E-coli standards provided in the kit and the endotoxin levels were determined by using the optical density 405nm values on Y-axis to the corresponding amount of endotoxin (EU/ml) present in the samples, plotted on x-axis, where 1 endotoxin unit/ml (EU/ml) is equivalent to 0.1ng endotoxin/ml.

2.4.5 SDS (Sodium dodecyl sulfate)-PAGE – 12%

A SDS-PAGE gel consists of two parts: resolving (10 ml) and stacking (5 ml), which were prepared by mixing the components below, with as per quantities listed for 12% gel:

Table 2.1 Resolving and Stacking components for 12% SDS-PAGE

Resolving gel	**12%**	**Stacking gel**	**12%**
Components	**Volume (ml)**	**Components**	**Volume (ml)**
dH_2O	3.3	dH_2O	3.4
30% Bis-Acrylamide mix	4	30% Bis-Acrylamide mix	0.83
1.5M Tris-HCl, pH 8.8	2.5	1.0M Tris-HCl, pH6.8	0.63
10% SDS (Sodium dodecyl sulphate)	0.1	10% SDS	0.05
10% APS (Ammonium Persulfate)	0.1	10% APS	0.05
TEMED (Tetramethylethylenediamine)	0.15	TEMED	0.14

The glass plates were assembled in the casting frames ensuring there was no leakage. The resolving gel solution was first pipetted into the gap between the plates and was left for 10 min to polymerise. The stacking solution was then pipetted on top of the resolving gel and a comb was inserted for the formation of wells. After ensuring the complete polymerisation of the stacking gel, the comb was carefully removed and the glass plates were set in the buffer dam. The running buffer (1x) (25 mM Tris, 192 mM glycine and 0.1% SDS) was poured into the inner chamber and the tank was filled to the required levels in the outer chamber. The samples mixed with 2x treatment buffer (50 mM Tris pH 6.8, 2% β-mercaptoethanol, 2% SDS, 0.1% bromophenol blue, and 10% glycerol), preheated at 100°C for 10 min, were loaded into the wells and a protein marker (Thermo Fisher) was loaded in the first lane to analyse the size of bands. The gel apparatus was then connected to the power pack at 120V for 90 min to run the samples in the gel to separate the proteins for analysis. The gel was stained overnight in the staining solution (0.1% coomassie blue, 10% acetic acid, 40% methanol and 50% H_2O and de-stained the next day using de-staining solution (10% acetic acid, 40% methanol and 50% H_2O) for clearly visible protein bands.

2.5 Cell Culture and treatments

Human cancer cell lines for ovarian clear cell adenocarcinoma cell line: SKOV3 (ATCC, Rockville, MD, USA) and pancreatic cancer: Panc-1, MiaPaCa-2 and Capan-2 (ATCC, Rockville, MD, USA) were used as an *in vitro* model. SKOV3, Panc-1, MiaPaCa-2 and Capan-2 cell lines were cultured in DMEM-F12 media containing 10% v/v fetal calf serum (FCS), 2 mM L-glutamine, and penicillin (100 units/ml)/streptomycin (100 µg/ml) (Thermo Fisher). All cell lines were grown under standard conditions at 37°C and 5% v/v CO_2 until 80-90% confluent.

Table 2.2 Phenotype and Genotype of Cancer Cell lines used in this thesis

Human Cell Line	**Biological Source**	**ATCC** Catalogue #	**Genotype** mt: mutant; wt- wildtype
SKOV3 (Fogh and Trempe, 1975)	Metastasis from ascites in Ovary	HTB-77	$p53^{mt}$
Panc-1 (Lieber et al., 1975)	Primary tumor derived from Pancreas/duct	CRK-1469	$p53^{mt}$ $KRAS^{mt}$ $SMAD4^{wt}$
MiaPaCa-2 (Yunis et al., 1977)	Primary tumor derived from body and tail of pancreas	CRL-1420	$p53^{mt}$ $KRAS^{mt}$ $SMAD4^{wt}$
Capan-2 (Kyriazis et al. 1986)	Primary tumor derived from head of pancreas	HTB80	$p53^{wt}$ $KRAS^{mt}$ $SMAD4^{wt}$

2.6 Cell viability assay

SKOV3 cells ($0.1x10^6$/ml) were grown in DMEM-F12 medium containing 10% FCS overnight in a 12-well plate (Nunc). On the following day, the cells (which were adherent) were washed 2x with PBS and were incubated with C1q, ghA, ghB, ghC, or MBP (10 µg/ml) and an untreated control in serum free DMEM-F12 for 24 h. The cells were then detached using 5mM EDTA (pH 8.0), and centrifuged at 1200 x g for 5 min. The cell pellet was re-suspended in 1 ml of DMEM-F12. The cells were then counted by mixing 10 µl of cell suspension with 10 µl of Trypan Blue (60%; Sigma-Aldrich, UK) using a haemocytometer. The viable cells do not stain whereas the dead cells take up the dye and appear blue under the microscope. The viable cells were counted and an average was taken by counting in five different optical fields. Average of three independent experiments was used for analysis.

2.7 MTT assay

SKOV3 cells ($0.1x10^5$/ml) were grown in a 96-well plate (Nunc) in DMEM-F12 containing 10% FCS. Next day, the cells were washed twice with PBS. MTT (3-[4,5-dimethylthiazol-2-yl]-2,5-diphenyltetrazolium bromide) (Thermo Fisher, Catalogue # M6494) assay was performed by incubating SKOV3 cells ($0.1x10^5$) with C1q, ghA, ghB, ghC or MBP (10 µg/ml each) along with an untreated control in serum-free DMEM-F12 medium for 24 h. Then, cells were incubated with 50 µg/µl MTT (5 mg/ml stock in PBS) per well for 4 h at 37°C. Media was discarded from the wells, leaving behind 25 µl per well, which was mixed gently with 50 µl of dimethyl sulfoxide (DMSO) and incubated for another 10 min at 37°C. The absorbance was read at 570 nm using a plate reader.

2.8 Cell morphological Studies

Morphological alterations were examined in order to determine the optimal dose of rfhSP-D for the treatment of pancreatic cell lines. Panc-1 cells were seeded at a low density (0.1×10^4/ml) and grown overnight in DMEM-F12 containing 10% FCS in a 12 well plate (Nunc). The cells were washed twice with PBS and incubated in serum free media with and without rfhSP-D (5, 10 or 20 µg/ml). An area of 5-10 cells was selected for each condition for analysis and images were taken at 0 h, 6 h and 24 h using phase contrast Axioscope microscope.

2.9 Matrigel Invasion Assay

The invasion assay was performed using Corning™ BioCoat™ Matrigel™ Invasion Chamber (Fisher; Catalogue # 08-774-122). Inserts pre-coated with basement membrane, extracted from Engelbreth-Holm-Swarm mouse tumor, were reconstituted in serum free DMEM-F12 media at 37°C for 2 h. 35,000 cells, resuspended in 500 µl serum free DMEM-F12 media, were added to the top wells of the inserts with and without rfhSP-D (20 µg/ml) and 500 µl of media containing serum was added to the bottom of the inserts in a 24-well plate and incubated at 37°C for 22 h. Next, medium containing non-evaded cells were discarded and remaining cells were scraped off from the membrane using a sterile cotton bud ensuring cells at the bottom of the membrane remained intact for fixing. Fixing was done using 100% methanol for 2 min, followed by 2 min incubation with toluidine blue (Thermo Fisher) to stain the

evaded cells. The membrane was cut using a sterile scalpel and mounted on the slide to count the evaded cells.

2.10 Fluorescence Microscopy

Cell lines ($0.5x10^5$/ml) were grown on coverslips overnight in DMEM-F12 medium containing 10% FCS. On the following day, the cells were washed twice with PBS and incubated with human C1q, ghA, ghB, ghC, MBP (10 μg/ml; SKOV3) or rfhSP-D (20 μg/ml; Panc-1, MiaPaCa-2, and Capan-2) in a serum free DMEM-F12 medium for appropriate time as per the experiment requirements as discussed below.

2.10.1 Protein Binding

Cell lines ($0.5x10^5$/ml) were grown on coverslips overnight in DMEM-F12 medium containing 10% FCS. Next day, the cells were washed twice with PBS and incubated with human C1q, ghA, ghB, ghC (10 μg/ml; SKOV3) or rfhSP-D (10 μg/ml; Panc-1, MiaPaCa-2, and Capan-2) separately in a serum free DMEM-F12 medium for 1 h at 4°C to allow protein binding. After 1 h, the cells were washed twice with PBS to remove any unbound proteins. The cells were then probed with appropriate primary antibody (1:200; rabbit anti-human C1q; MRC Immunochemistry Unit, Oxford, rabbit anti-human MBP for globular head modules (Thermo Fisher, UK) or mouse anti-human SP-D; MRC Immunochemistry Unit, Oxford) for 1 h at room temperature. The cells were then washed twice with PBS to remove excess antibody before incubation with appropriate secondary antibody (1:500; goat anti-rabbit IgG Alexa Flour 488 (Thermo Fisher; Catalogue # R37116) or goat anti-mouse IgG conjugated with CY5 (Abcam; Catalogue # ab6563) and Hoechst 33342 (1:10,000, Thermo Fisher; Catalogue # 10150888) for 1 h at room temperature. The cells were then washed twice with PBS to remove excess secondary antibody and were fixed with 4 % paraformaldehyde (PFA; Thermo Fisher) for 10 min. The anti-fade (5 μl; Citiflour, UK; Catalogue # AF1) was added on top of the coverslips and the slides were prepared to view them under HF14 Leica DM4000 microscope for fluorescence analysis.

2.10.2 Intracellular staining

Cell lines ($0.5x10^5$/ml) were grown on coverslips overnight in DMEM-F12 medium containing 10% FCS. Next day, the cells were washed twice with PBS and incubated with human C1q, ghA, ghB, ghC, MBP (10 μg/ml; SKOV3) or rfhSP-D (20 μg/ml; Panc-1, MiaPaCa-2, and Capan-2) in a serum free DMEM-F12 medium. The cells were then fixed and permeabilized by adding 500 μl of ice-cold 100% methanol for 10 min at -20°C. Intracellular staining was performed as per incubation time and antibodies for each cell line as listed in Table 2.3. The cells were washed twice with PBS in between each step. The permeabilized cells were incubated with primary antibody for 1 h at room temperature followed by 1 h incubation with goat anti-rabbit IgG Alexa Flour 488 (1:500, Thermo Fisher) or anti-rabbit conjugated with CY3 (1:500; Thermo Fisher) and Hoechst (1: 10,000; Thermo Fisher) before preparing the slides for fluorescence microscopy analysis using HF14 Leica DM4000 microscope.

Table 2.3 List of cell lines and antibodies

Cell Line (Treatment)	**Primary Antibody /Dilution**	**Source & Catalogue #**	**Secondary Antibody/Dilution**	**Source & Catalogue #**
SKOV3 (C1q & globular head modules)	Rabbit anti-human mTOR (1:200)	Cell Signalling #2972	Goat anti-rabbit IgG Alexa Flour 488 (1:500)	Thermo Fisher # R37116
	Rabbit anti-human caspase 3 (1:500)	Cell Signalling #9664	Goat anti-rabbit IgG, CY3 (1:500)	Thermo Fisher # A10520
Panc-1, MiaPaCa-2, & Capan-2 (rfhSP-D)	rabbit anti-human Vimentin (1:200)	Cell Signalling #5741S	Goat anti-rabbit IgG Alexa Flour 488 (1:500)	Thermo Fisher # R37116
	Rabbit anti-human snail1 (1:200)	Cell Signalling #3879S		
	Rabbit anti-human Zeb1 (1:200)	Cell Signalling #3396S		
	Rabbit anti-human mTOR (1:200)	Cell Signalling #2972		
	Rabbit anti-human TGF-β (1:200)	R&D system #AB-100-NA		
	Rabbit anti-human Smad2/3 (1:200)	Cell Signalling #3102	Goat anti-rabbit IgG, CY3 (1:500)	Thermo Fisher #A10520

2.10.3 Apoptosis Microscopy

After 24 h (SKOV3: C1q and g heads) and 48 h (Panc-1, MiaPaCa-2, and Capan-2: rfhSP-D) incubation with proteins, the coverslips were washed twice with PBS and then incubated with annexin V binding buffer containing FITC annexin V (1:200) and propidium iodide (1:200) (FITC Annexin V apoptosis detection kit with PI, Biolegend; Catalogue #: 640914) for 15 min. The coverslips were then washed twice with PBS and fixed with 4% PFA before preparing the slides to view under HF14 Leica DM4000 microscope.

2.11 Flow Cytometry

Cell lines ($0.1x10^7$) were plated in culture petri dishes (Nunc) using DMEM-F12 containing 10% FCS. Next day, the cells were washed twice with PBS and incubated with proteins separately; C1q, ghA, ghB, ghC (10 μg/ml; SKOV3) or rfhSP-D (20 μg/ml; Panc-1, MiaPaCA-2 and Capan-2), along with an untreated control in a serum free DMEM-F12 medium for 1 h for protein binding analysis, 24 h for apoptosis and growth arrest analysis or 48 h for apoptosis analysis. The cells were detached using 5 mM EDTA and centrifugation at 1200 x g for 5 min for various analysis as discussed below.

2.11.1 Protein Binding

For protein binding analysis, SKOV3 cells ($0.5x10^6$) were incubated with C1q, ghA, ghB and ghC (10 μg/ml), using BSA treated cells as a negative control. Cells were incubated with proteins at 4°C for 1 h and washed twice with PBS. Then, cells were incubated with primary polyclonal antibodies, rabbit anti-human C1q polyclonal antibody (1:200) for C1q and rabbit anti-human MBP (Thermo Fisher, 1:200; Catalogue # PA1-989) for globular head module treated cells as well as their respective BSA treated controls for 1 h at room temperature. The cells were then incubated with goat anti-rabbit IgG Alexa Flour 488 (1:1000, Thermo Fisher) for 1 h, and then washed with PBS twice between each step. Compensation parameters were acquired using unstained, untreated goat anti-rabbit IgG Alexa Flour 488 stained SKOV3 cells. 10,000 cells were acquired for each experiment and compensated before plotting the acquired data.

2.11.2 Apoptosis

For apoptosis analysis via flow cytometry, FITC annexin V apoptosis detection kit with propidium iodide (FITC/annexin V apoptosis detection kit with PI, Biolegend; Catalogue # 640914) was used, as per manufacturer's instructions. Both treated and untreated cells were incubated with annexin V conjugated with FITC (5 µl) and propidium iodide (5 µl) for 15 min at room temperature. The cells were then washed twice with PBS before analysing the samples using a Novocyte flow cytometer. Compensation parameters were acquired using unstained, untreated FITC stained, and untreated propidium iodide stained cells. 10,000 cells were acquired for each experiment and compensated before plotting the acquired data.

2.11.3 Cell Cycle Analysis

Cell lines (Panc-1, MiaPaCa-2 and Capan-2) were plated in culture petri dishes (Nunc) ($0.1x10^7$/3 ml) and incubated with rfhSP-D (20 µg/ml), along with an untreated control, for 24 h and 48 h, followed by cell detachment using 5 mM EDTA, pH 8, and centrifugation at 1200 x g for 5 min. For cell cycle analysis, the cells were fixed in 70% v/v ethanol for 30 min at 4°C, followed by a PBS wash twice at 850 x g. The cells were then treated with ribonuclease (100 µg/ml; Sigma; Catalogue # R4875) to ensure DNA staining without RNA contamination before staining with propidium iodide (50 µg/ml; Thermo Fisher; Catalogue # P3566). 10,000 cells were then acquired for both treated and untreated samples and the propidium iodide histograms were plotted using the set markers within the analysis program of Novocyte Flow Cytometer.

2.11.4 Intracellular staining

Cell lines (Panc-1, MiaPaCa-2 and Capan-2) were plated in culture petri dishes (Nunc) ($0.1x10^7$/3 ml) and incubated with rfhSP-D (20 µg/ml), along with an untreated control, for 24 h followed by cell detachment using 5 mM EDTA, pH 8, and centrifugation at 1200 x g for 5 min. The cells were then fixed and permeabilized by adding 500 µl of ice-cold 100% methanol for 10 min at -20°C. The cells were washed twice with PBS in between each step. The permeabilized cells were incubated with primary antibody (rabbit anti-human Vimentin, rabbit anti-human Zeb1, rabbit anti-human Snail) for 1 h at room temperature followed by 1 h incubation with goat anti-

rabbit IgG Alexa Flour 488 (1:500, Thermo Fisher). 10,000 cells were acquired for each experiment and compensated before plotting the acquired data.

2.12 Quantitative Real-time Polymerase Chain Reaction Analysis

2.12.1 Time-points

Cell lines (0.3 x 10^7/ml) were grown overnight in DMEM-F12 medium containing 10% FCS in 12 well plates (Nunc). Next day, cells were washed twice with PBS and incubated with C1q, ghA, ghB or ghC (10 µg/ml) or rfhSP-D (20 µg/ml) in serum free DMEM-F12 medium for various times. At each time-point the cells were detached using trypsin (Sigma) and centrifuged at 1500 x g for 5 min. The cell pellets were stored at -80°C for RNA extraction later.

2.12.2 Total RNA extraction

GenElute Mammalian Total RNA Purification Kit (Sigma-Aldrich, UK; Catalogue # RTN350) was used, as per manufacturer's instructions, to extract total RNA. The cells were lysed using 250 µl of lysis solution and 2.5 µl of 2-mercaptoethanol and vortexed until clumps disappeared. The lysate was mixed with 250 µl of 70% ethanol, gently vortexed and added to the binding column. The columns were then centrifuged for 15 sec at 13, 000 x g. Then, columns were washed twice using washing buffer I and followed by twice with washing buffer II, provided in the kit. The columns were then transferred to the fresh eppendorf tube for elution. 50 µl of elution solution was added to each column and centrifuged for 1 min to elute total RNA.

2.12.3 DNase Treatment

DNase treatment with DNase I (Sigma-Aldrich, UK, Catalogue # AMPD1-1KT) was carried out to remove any DNA contaminants. 5 µl of 10 x buffer and 5 µl of Dnase I enzyme was added to 50 µl RNA elutions and mixed gently. The samples were then incubated at room temperature for 15 min. Then, 5 µl stop solution was added and mixed gently to stop the reaction. The samples were heated at 70°C for 10 min and placed on ice. The concentration and purity of total RNA was determined by measuring the absorbance at 260 nm and 260:280 nm ratio, using a NanoDrop 2000/2000c spectrophotometer (Thermo-Fisher).

2.12.4 cDNA Synthesis

Total RNA (2 µg) was used to synthesize cDNA using High Capacity RNA to cDNA Kit (Applied Biosystems; Catalogue # 4387406). Master mix of 2 x RT buffer (10 µl) and 20 x enzyme mix (1 µl) was added to the RNA samples (9 µl) and converted to cDNA for target analysis later.

2.12.5 Gene expression analysis

The qPCR reactions were performed to measure the mRNA expression level of various target genes. Each reaction was conducted in triplicate and consisted of 5 µl Power SYBR Green MasterMix (Applied Biosystems; Catalogue # 4309155), 75 nM of forward and reverse primers and 500 ng cDNA, making up to a 10 µl final volume per well. Relative mRNA expression was determined by qPCR using the 7900HT Fast Real-Time PCR System (Applied Biosystems). Samples were initially incubated at 50°C and 95°C for 2 and 10 min respectively, followed by amplification of the template for 40 cycles (each cycle involved 15 seconds at 95°C and 1 min at 60°C). The gene expression was normalized using the expression of human 18S rRNA as an endogenous control. The Ct (cycle threshold) mean value for each target gene was used to calculate the relative expression using the Relative Quantification (RQ) value and formula: $RQ = 2^{-\Delta\Delta Ct}$, which was compared with the relative expression of untreated.

2.12.6 Primers

Forward and Reverse Primer sequences were designed using the web based Basic Local Alignment Search Tool and Primer-BLAST (http://blast.ncbi.nlm.nih.gov/Blast.cgi). The primers used in this thesis are listed in Table 2.4.

Table 2.4 Target genes and primers used in the qPCR analysis

Target Gene	Forward Primer	Reverse Primer
18S	5'-ATGGCCGTTCTTAGTTGGTG-3'	5'-CGCTGAGCCAGTCAGTGTAG-3'
Bax (mitochondrial apoptosis marker)	5'-TGCTTCAGGGTTTCATCCAGG-3'	5'- GGAAAAAGACCTCTCGGGGG-3'
Fas (extrinsic apoptosis marker)	5'- ACACTCACCAGCAACACCAA-3'	5'- TGCCACTGTTTCAGGATTTAA-3'
mTOR (cell survival pathways marker)	5'- TGCCAACTATCTTCGGAACC-3'	5'- GCTCGCTTCACCTCAAATTC-3'
RICTOR (cell survival pathways marker)	5'- GGAAGCCTGTTGATGGTGAT-3'	5'- GGCAGCCTGTTTTATGGTGT-3'
RAPTOR (cell survival pathways marker)	5'- ACTGATGGAGTCCGAAATGC-3'	5'- TCATCCGATCCTTCATCCTC-3'
TNF-α (role in apoptosis induction)	5′-GTATCGCCAGGAATTGTTGC-3′	5′-AGCCCATGTTGTAGCAAACC-3′
NF-κB (role in apoptosis induction)	5′-TGAGGTACAGGCCCTCTGAT-3′	5′-GTATTTCAACCACAGATGGCACT-3′
Snail (EMT marker)	5'- GAGCTGACCTCCCTGTCAGA-3'	5'- GTTGAAGGCCTTTCGAGCCT -3'
Vimentin (EMT marker)	5'-CTCTGGCACGTCTTGACCTT- 3'	5'-TCTTGGCAGCCACACTTTCA- 3'
Zeb1 (EMT marker)	5'- AAGGGCAAGAAATCCTGGGG- 3'	5'-ATGACCACTGGCTTCTGGTG- 3'
TGF- β (EMT inducer)	5'-GTACCTGAACCCGTGTTGCT-3'	5'-GTATCGCCAGGAATTGTTGC-3'
P53 (role in cell growth arrest and apoptosis)	5'- AGCACTGTCCAACAACACCA -3'	5'- CTTCAGGTGGCTGGAGTGAG -3'

2.13 Western Blot

Cells (10^6/2 ml) were plated in a 6-well plate (Nunc) in DMEM-F12 containing 10% FCS. Next day, the cells were washed twice with PBS and incubated with proteins; C1q, ghA, ghB, or ghC (10 μg/ml; SKOV3) or rfhSP-D (20 μg/ml; Panc-1, MiaPaCA-2 and Capan-2), along with an untreated control in a serum free DMEM-F12 medium for 12 h, 24 h or 48 h. After the appropriate time-point, the SKOV3 cells were lysed using lysis buffer (50mM Tris-HCL, pH 7.5, 10% glycerol, and 150 mM NaCl, 1% TritonX-100) and kept over ice for 10 min, before gently transferring to pre-cooled microcentrifuge tube and centrifuged for 15 min at 13,000 x g at 4°C. The supernatant was mixed with the treatment buffer (50 mM Tris pH 6.8, 2% β-merceptoethanol, 2% SDS, 0.1% bromophenol blue and 10% glycerol) and heated for 10 mins at 100°C in order to run on SDS-PAGE (12% w/v). Panc-1, MiaPaCa-2 and Capan-2 cells were lysed using 2x treatment buffer and scraped off from the plates, followed by sonication for 15 sec and heated for 10 mins at 100°C in order to run on SDS-PAGE. The rainbow marker (5 μl, Thermo Fisher) was run in the first well for protein size determination. The SDS-PAGE separated proteins were then electrophoretically transferred onto a nitrocellulose membrane (Sigma) using transfer buffer (25 mM Tris, 190 mM glycine and 20% methanol, pH 8.3) for 2 h at 320 mA or iBLOT (Thermo Fisher), followed by blocking with 5% w/v dried milk powder (Sigma) in 100 ml PBS at room temperature for 2 h on a rotatory shaker. The membrane was washed with PBST (PBS + 0.05% Tween 20) three times, 10 min each, and incubated with primary polyclonal antibody (1:1000) such as anti-human SP-D (Immunobiochemistry, MRC Unit, Oxford), rabbit anti-human caspase 3, rabbit anti-human cleaved caspase 3, rabbit anti-human cleaved caspase 8, rabbit anti-human Fas, (Cell Signalling Technology) or rabbit anti-human TGF-β (R&D systems) or anti-β actin (as loading control; Thermo Fisher, Catalogue # PA1-183) at 4°C overnight with gentle shaking. Next day, the membrane was washed with PBST (3 times, 10 min each) before incubating with secondary anti-rabbit IgG HRP-conjugate (1:1000; Promega; Catalogue # W4011) for 1 h at room temperature. Anti-GAPDH/HRP (Thermo Fisher, Catalogue # PA1-987-HRP) was used a loading control for pancreatic cancer experiments. The bands were visualized using Enhanced Chemiluminescence (ECL; Thermo Fisher; Catalogue # 32106) in the BioRad

ChemiDoc MP imaging system, or using 3,3'-diaminobenzidine (DAB) substrate kit (Sigma; Catalogue # D4293).

2.14 Statistical Analysis

Graphpad Prism 6.0 was used to make graphs, and the statistical analysis was carried out using an unpaired one-way ANOVA test. Significant values were considered based on *$p<0.05$, *$p<0.01$ and ***$p<0.001$ between treated and untreated conditions. Error bars show the standard deviation or standard error of mean, as indicated in the figure legends.

Chapter 3

Effects of Complement protein C1q and its globular head modules on an ovarian cancer cell line, SKOV3

3.1 Abstract

Complement protein C1q is the first subcomponent of the complement classical pathway. It plays an important role in the clearance of immune complexes, pathogens and apoptotic cells. C1q has been shown to be expressed locally in the tumour microenvironment in a wide range of human malignant tumours, where it promotes cancer cell adhesion, proliferation and migration, which is a complement independent role of C1q. The complement components including C1q have been found in the ascitic fluid produced in ovarian cancers. In this study, the effects of human C1q and its globular head modules on an ovarian cancer cell line, SKOV3 have been examined, and it was found that C1q and the recombinant globular head modules induce apoptosis in SKOV3 cells. C1q expression was not detected in SKOV3 cells either at transcriptional level, or at the protein level. Treatment of SKOV3 cells with exogenous C1q and its globular head modules (10 μg/ml) induced apoptosis in ~55% cells, as revealed by fluorescence microscopy and flow cytometry. qPCR and caspase cascade analysis via western blot suggested that C1q and globular head modules trigger upregulation of TNF-α and Fas. The pro-survival pathways mTOR, RICTOR and RAPTOR, which are usually overexpressed in ovarian cancer, were significantly downregulated upon treatment with C1q and globular head modules. In conclusion, C1q and globular head modules induced apoptosis in an ovarian cancer cell line, SKOV3 via a TNF-α mediated apoptosis pathway.

3.2 Introduction

C1q, the first subcomponent of the C1 complex, recognises IgG or IgM- containing immune complexes and activates the complement classical pathway. It can bind a huge range of self and non-self ligands to bring about a variety of homeostatic functions such as clearance of pathogens and apoptotic cells (Kishore et al., 2004). Recently, several immunomodulatory functions of C1q have been reported, which are independent of its participation in the complement pathways (Kouser et al., 2015; Kishore et al., 2016). These include regulation of dendritic cell (DC) functions (van Kooten et al., 2008), cancer development (Bulla et al., 2016), and neuronal synapse pruning (Stevens et al., 2007).

Ovarian cancer is the sixth most commonly diagnosed cancer with the highest mortality rate compared to any other cancer associated with the reproductive system among women worldwide. Nearly 70% of the ovarian tumours are detected at an advanced stage (III or IV), with ~85% expected mortality (Permuth-Wey and Sellers, 2009). The presence of complement activation markers such as C3a and soluble C5b-9, have been shown in the intraperitoneal ascitic fluid (AF) produced during ovarian cancer, suggesting the possibility of complement activation *in vivo*. However, this complement activation seems to be dampened as membrane regulators such as CD46, CD55 and CD59 are overexpressed on the ovarian cancer cells, which makes the complement system ineffective of complete immune surveillance mechanism. Interestingly, the malignant ovarian cancer cells derived from the ascitic fluid exhibit C1q and C2 deposits on their surface. These cells become susceptible to complement dependent cytotoxicity by ascitic fluid, when CD59 expression is neutralised using anti-CD59 neutralising antibody (Bjorge et al., 2005). A recent study revealed that C1q is present in the stroma and vascular endothelium of various human malignant tumours. These include adenocarcinomas of lung, colon, breast, pancreas and melanoma (Bulla et al., 2016). This locally synthesized C1q was shown to promote cancer growth by enhancing adhesion, proliferation and migration.

The cancer immunotherapies involving complement molecules have emerged to be very successful recently. The identification of a range of cell surface tumour-associated antigens, which are either overexpressed or mutated, in comparison to normal tissues, has presented various antibody mediated therapies in various cancers (Ramsland et al., 2015). These anti-tumour antibodies work either via receptor or

checkpoint blockade/agonist, induction of apoptosis, immune-mediated cytotoxicity either via CDC, or antibody-dependent cellular cytotoxicity (ADCC), and regulation of T cell function. Additionally, antibodies that target growth factors and their associated receptors including epidermal growth factor receptor (EGFR), tumour necrosis factor (TNF)-related apoptosis-inducing ligand receptors, insulin-like growth factor 1 receptor (IGF1R), and receptor activator nuclear factor-κB ligand (RANKL) have also been used for cancer treatments (Scot et al., 2012).

In this chapter, the complement independent effects of exogenous C1q and recombinant globular head modules (ghA, ghB and ghC) on an ovarian cancer cell line, SKOV3 have been investigated. This chapter has been published as below:

Kaur A, Sultan S, Murugaiah V, Pathan A, Alhamlan F, Karteris E, Kishore U., Human C1q Induces Apoptosis in an Ovarian Cancer Cell Line via Tumor Necrosis Factor Pathway. Frontiers in Immunology. 2016;7: 599.

3.3 Results

3.3.1 Purification of Human C1q

Human C1q was purified as described in section 2.1 and analysed for purity by running on 12% SDS-PAGE (Figure 3.1).

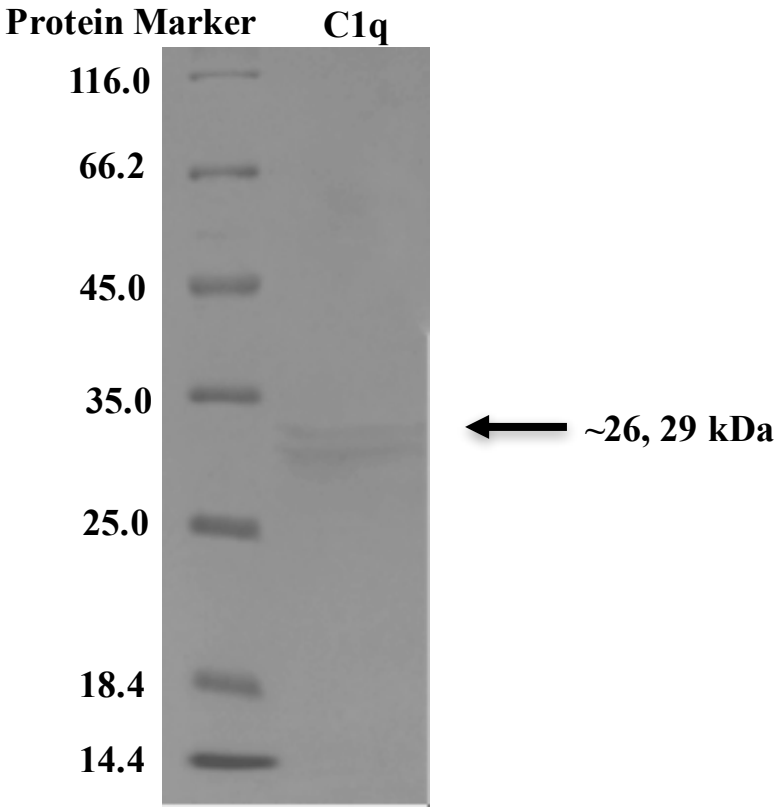

Figure 3.1 SDS-PAGE (12% w/v) for analysis of purified C1q fractions from human plasma. The chain A and B bands appeared at ~26 and 29 kDa whereas C chain remains trapped in the well due to its larger size.

3.3.2 Expression and Purification of C1q globular head chains and MBP

The recombinant globular head chains of human C1q, MBP-ghA, ghB and ghC were expressed using pKBM-A, pkBM-B, pkBM-C, transformed in *Escherichia coli* BL21. Initially, the expression of these proteins was analyzed in a pilot scale (Figure 3.2) and the colony with the maximum expression was then inoculated to produce the large-scale batches (Figure 3.3). The large-scale pellet was lysed using 50 ml lysis buffer for 30 min followed by sonication. The sonicated sample was then centrifuged (10,000 x g for 30 min) and the supernatant was diluted 5-fold in buffer I to pass through an amylose resin column. The column was then washed with buffer I (150 ml), followed by buffer II (250 ml of buffer I without Tween 20). The protein fractions were eluted with 100 ml of buffer II containing 10 mM maltose. The concentration of the protein was determined by measuring the OD_{280} absorbance and quality confirmed by running 12% SDS-PAGE gel with bands appearing at ~60 kDa (Figure 3.3). The peak elutions were then passed through Pierce™ High Capacity Endotoxin Removal Resin (Qiagen) to remove lipopolysaccharide (LPS) and the amount of endotoxin levels were found to be <4pg/µg of the rfhSP-D protein (Figure 3.4).

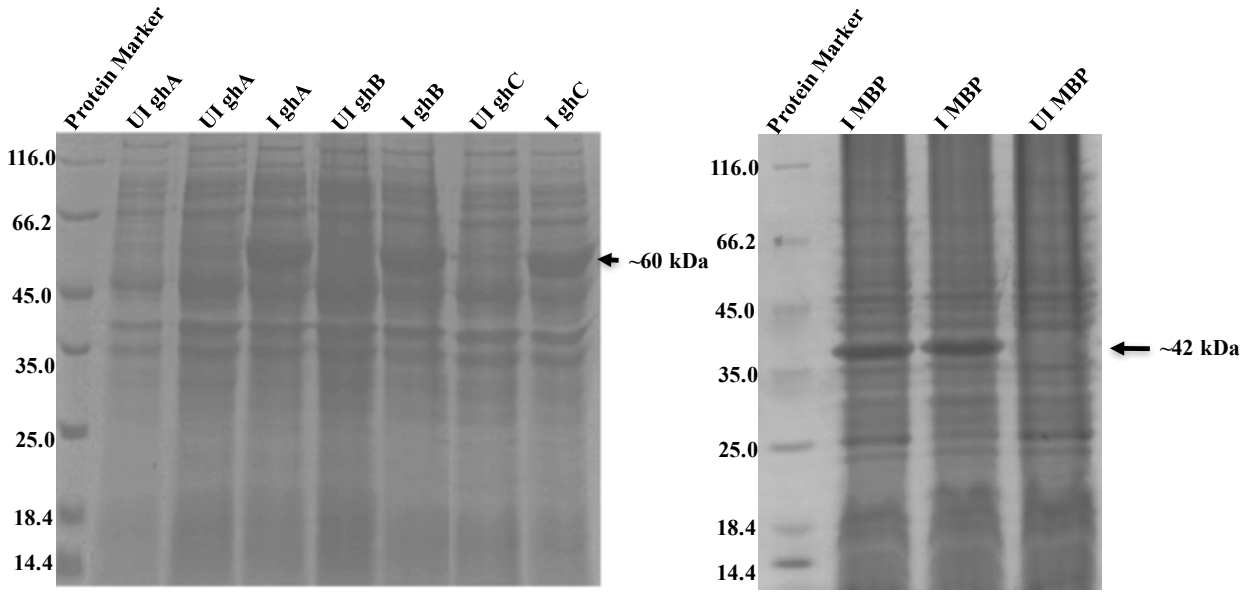

Figure 3.2 Pilot scale expression of ghA, ghB, ghC and MBP on a 12% w/v SDS-PAGE. 1 ml of bacterial culture was centrifuged at 2000 x g and the pellet was mixed with 100 µl of 2x treatment buffer to load 20 µl on 12% SDS-PAGE for 90 min at 120V. The gel was stained and then de-stained to determine the expression. The protein expression bands were visible at ~60 kDa for globular heads and ~ 42 kDa for MBP in the induced (I) sample, which is not observed in the un-induced (UI) samples.

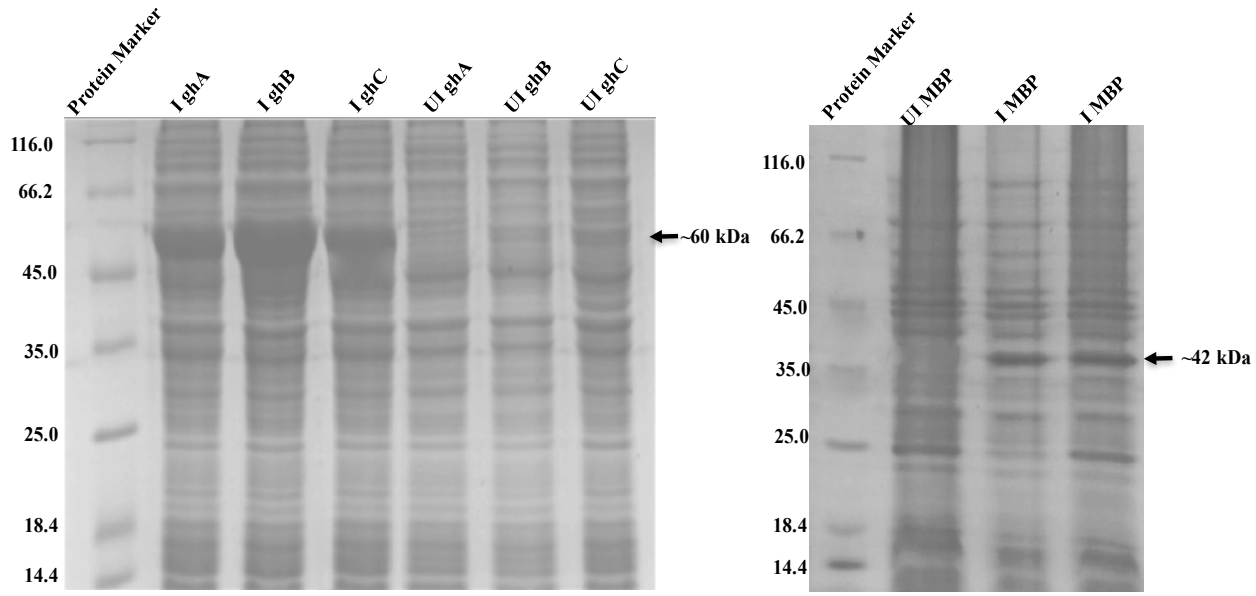

Figure 3.3 Large-scale expression of ghA, ghB and ghC and MBP on 12% w/v SDS-PAGE. 1 ml of bacterial culture was centrifuged at 2000 x g and the pellet was mixed with 100 µl of 2x treatment buffer to load 20 µl on 12% SDS-PAGE for 90 min at 120V. The gel was stained and then de-stained to determine the expression. The protein expression bands were visible at ~60 kDa for globular head modules and ~ 42 kDa for MBP in the induced (I) sample, which is not observed in the un-induced (UI) samples.

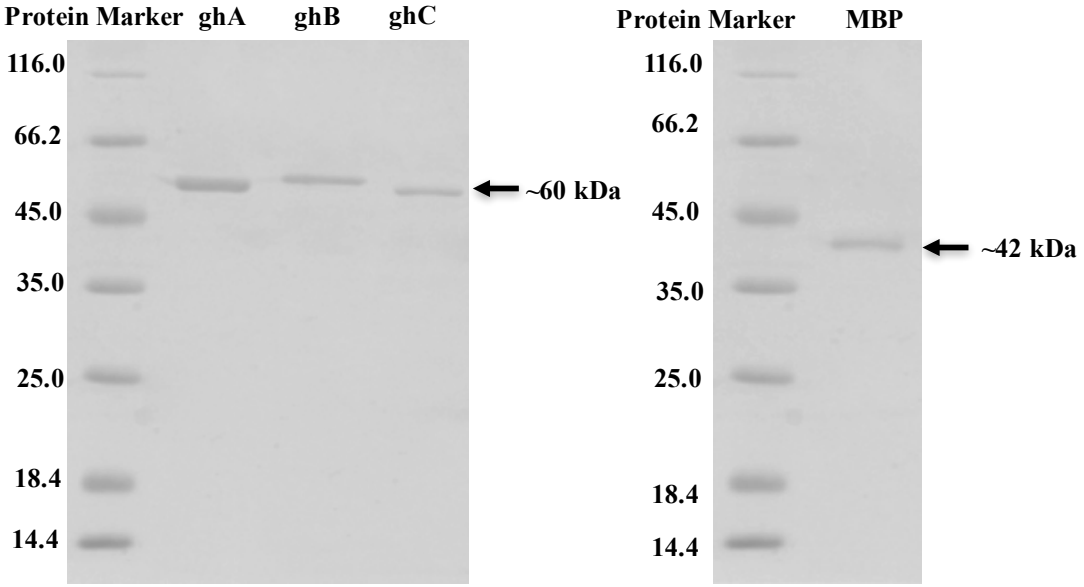

Figure 3.4 SDS-PAGE (12% w/v) analysis of purified globular head fractions. Purified fractions (20 µl) for each protein was mixed with 20 µl of 2x treatment buffer to run on SDS-PAGE for 90 min at 120V. The gel was then stained and detained to analyse the purity of the fractions, ghA, ghB and ghC appeared at ~60kDa and MBP appeared at ~42kDa.

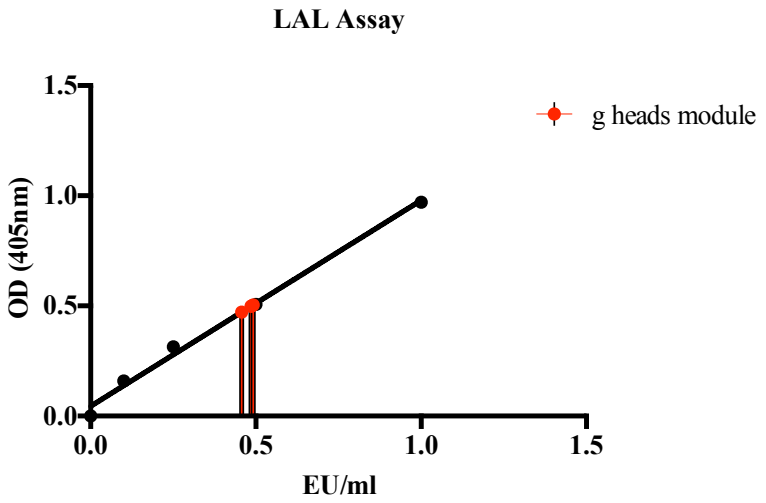

Figure 3.5 Measurement of endotoxin levels in the purified g head modules and MBP. The endotoxins activate Factor C proteolytic activity present in LAL, which is photometrically measured using chromogenic substrate at optical density (OD_{405}). A standard curve is plotted using 4 *E. coli* endotoxin standards, which were plated in parallel to the test sample. Using standard curve, where 1 EU/ml is equivalent to 0.1ng endotoxin/ml, the endotoxin levels in g head modules and MBP were found to be ~0.5 pg/µg.

3.3.3 Human C1q and recombinant globular head modules bind SKOV3

SKOV3 cells ($0.5x10^5$/ml) were grown on coverslips overnight and were incubated with C1q and individual recombinant globular head modules (ghA, ghB and ghC; 10 µg/ml) for 1 h at 4°C to analyse their cellular binding using fluorescence microscopy. All proteins were localized on the cell membrane uniformly in the treated cells, whereas no fluorescence was detected in the BSA treated cells, which were used as control (Figure 3.6, Panel B). In addition, no fluorescence was detected in an untreated, MBP treated and a secondary only control. The nucleus was stained positively with Hoechst (Figure 3.6; panel A). The protein binding was further quantified using flow cytometry analysis, which showed similar binding pattern, as seen under fluorescence microscopy as C1q and globular head modules treated cells over 90% positive in the FITC positive quadrant, as compared to the BSA treated cells used a control protein (Figure 3.7).

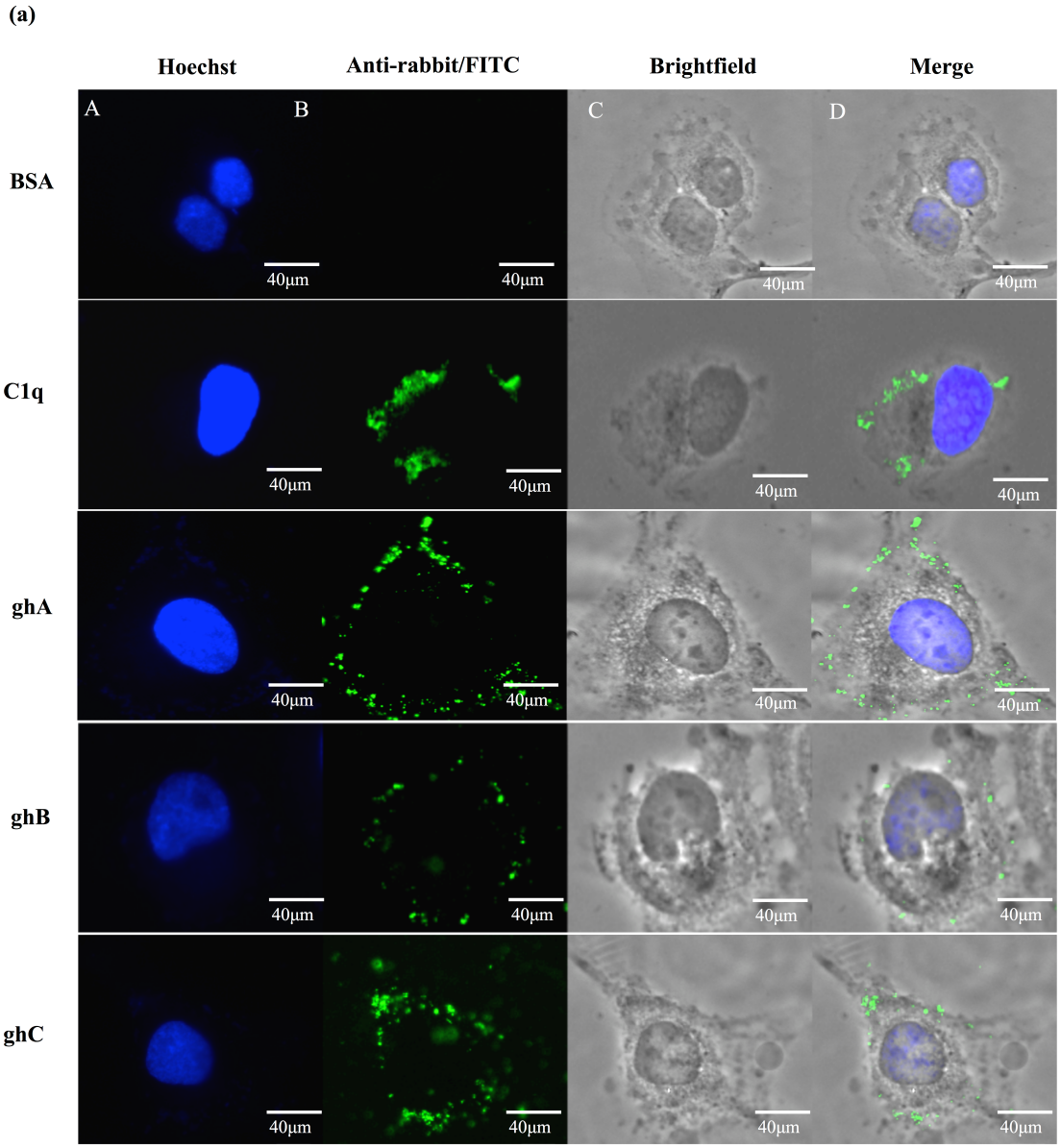

Figure 3.6 Fluorescence microscopy analysis to show binding of human C1q and individual recombinant globular head modules (ghA, ghB and ghC; 10 µg/ml) to SKOV3 cells. Panel A: shows the positive staining for nucleus using Hoechst. Panel B shows the cell membrane localization of proteins in SKOV3 cells probed with rabbit anti-human C1q (C1q) and rabbit anti-human MBP (globular head modules) antibodies, followed by goat anti-rabbit IgG Alexa 488; Panel C shows the cell images taken in brightfield and Panel D shows the merge, where proteins are visible bound to the cell membrane.

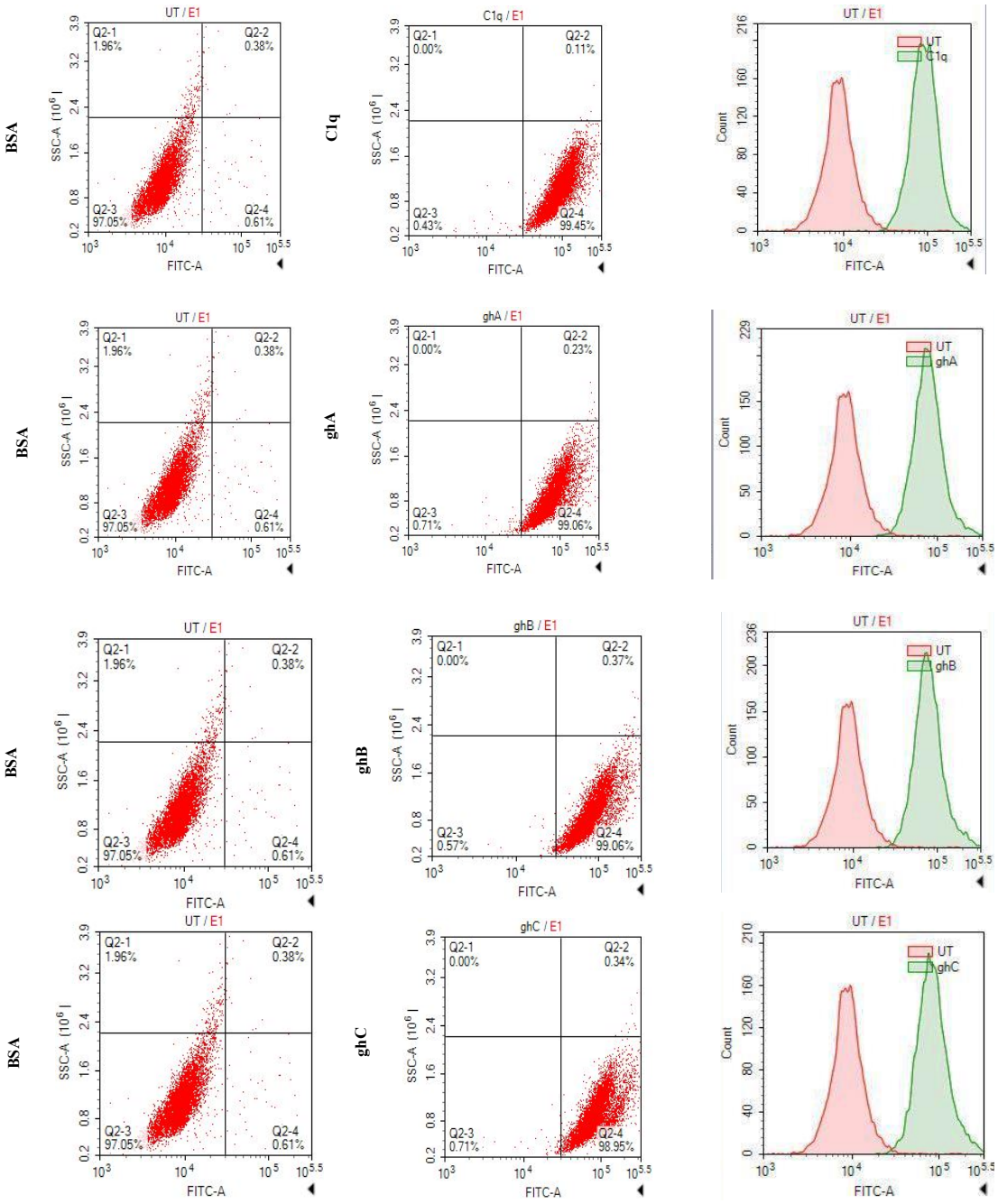

Figure 3.7 Flow Cytometry analysis to quantify the binding of human C1q and individual globular head modules (ghA, ghB and ghC; 10 µg/ml) to SKOV3 cells. Both treated and untreated cells were probed with rabbit anti-human C1q (C1q) and rabbit anti-human MBP (globular head modules) antibodies for 1 h, followed by 1 h incubation with goat anti-rabbit IgG Alexa 488. Panel (a) shows over 90% treated cells in FITC positive quadrant cells, as compared to the untreated cells. Panel (b) The shift in the mean fluorescent intensity to show a difference between untreated and treated cells is presented.

3.3.4 C1q and individual recombinant globular head modules reduce cellular viability in SKOV3 cells

SKOV3 cells (0.1×10^6/ml) were incubated with C1q and individual globular head modules (10 μg/ml) for 24 h. The untreated cells and MBP treated cells were used as controls. The cells were then detached and stained with trypan blue for counting using a haemocytometer. A significant decrease in the cell viability was observed using trypan blue dye exclusion following incubation with C1q (~50%), ghA (~50%), ghB (~40%), and ghC (~55%) (Figure 3.8). These results were further confirmed via MTT assay by growing SKOV3 cells in a 96-well microtiter plate and treating with C1q and globular head modules (10 μg/ml) for 24 h. As above, the NAD(P)H-dependent cellular oxidoreductase enzymes in the viable cells reduces the MTT into soluble purple colour formazan product and the concentration was determined at OD_{570}, which showed ~ 50% reduction in cell viability of treated cells (Figure 3.8).

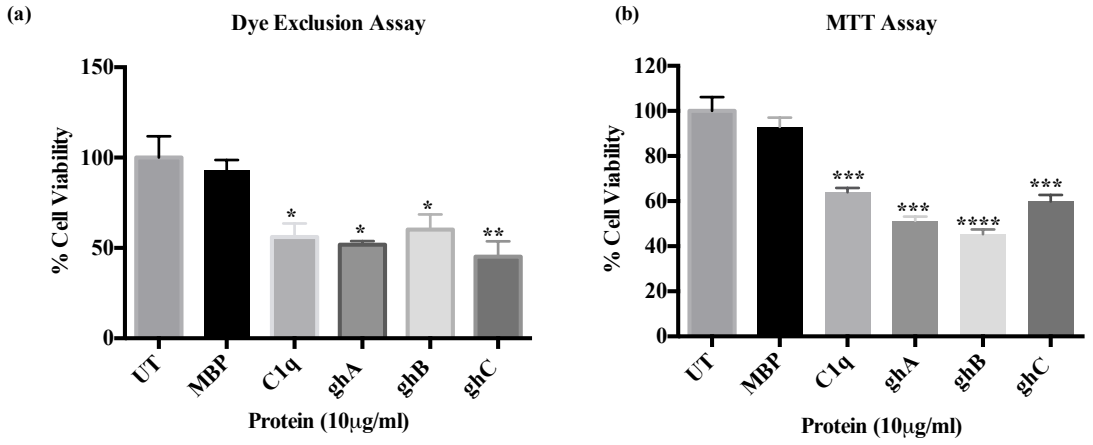

Figure 3.8 Trypan Blue Exclusion (a) and MTT (b) assay to analyse SKOV3 cell viability. Following the treatment with human C1q, ghA, ghB, ghC (10 μg/ml) and controls as MBP (10 μg/ml) and untreated for 24 h (±SEM, of three independent experiments), the cell viability was reduced by approximately 50% in the treated cells as compared to untreated and MBP control. All experiments were done in triplicate and the significance was established using the unpaired one-way ANOVA test (*$p<0.05$, *$p<0.01$ and ***$p<0.001$).

3.3.5 C1q and recombinant globular head modules induce apoptosis as shown via fluorescence microscopy in SKOV3 cells

The decrease in cell viability following treatment with C1q and globular heads was then further analysed to determine whether the cell death occurred via apoptosis using a FITC-annexin V apoptosis detection kit with propidium iodide. Fluorescence microscopy showed a significant proportion of SKOV3 cells, when treated with C1q and globular head modules (10 μg/ml) for 24 h, stained positive for annexin V (conjugated to FITC), which binds to phosphatidylserine (PS) of the cell membrane, which is exposed during apoptosis (Figure 3.9; panel B). The nucleus was positively stained using Hoechst (Figure 3.9; panel A). No FITC was observed in the untreated cells, suggesting that the cell membrane was still intact and the untreated cells were still viable (Figure 3.9).

3.3.6 C1q and recombinant globular head modules induce apoptosis as shown via flow cytometer in SKOV3 cells

Fluorescence microscopy results were then quantified via flow cytometer analysis, which showed that approximately 58% SKOV3 cells (C1q, quadrant Q2-2; Figure 3.10) were positive for both FITC (annexin V marker) and propidium iodide (stains DNA) quadrant following the treatment with C1q (10 μg/ml) for 24 h, which was significantly higher than 1.42% observed in untreated control cells (UT, quadrant Q2-2; Figure 3.10). The cells positive for both FITC and propidium iodide suggested that these cells were in the late apoptosis stage as the propidium iodide staining was internalized to stain the DNA due to pores in the cell membrane. In addition, 16% of cells stained positive for FITC only (C1q, quadrant Q2-4; Figure 3.10), which suggested that some cells were still in an early apoptosis stage.

Additionally, treatment of SKOV3 cells with individual globular head modules (ghA, ghB and ghC) for 24 h induced apoptosis in ~50% (ghA and ghC) and 40% (ghB) of cells as shown in quadrant Q2-2 (Figure 3.10). Approximately, 15-20% were stained positive for FITC alone (quadrant Q2-4; Figure 3.10), suggesting early apoptotic cell population. Approximately 90% of the untreated cell population was negative for both FITC and propidium iodide (UT, quadrant Q2-3; Figure 3.10). A shift in the mean fluorescence intensity of the treated SKOV3 cells in comparison to the untreated cells, further confirmed this observation (Figure 3.10).

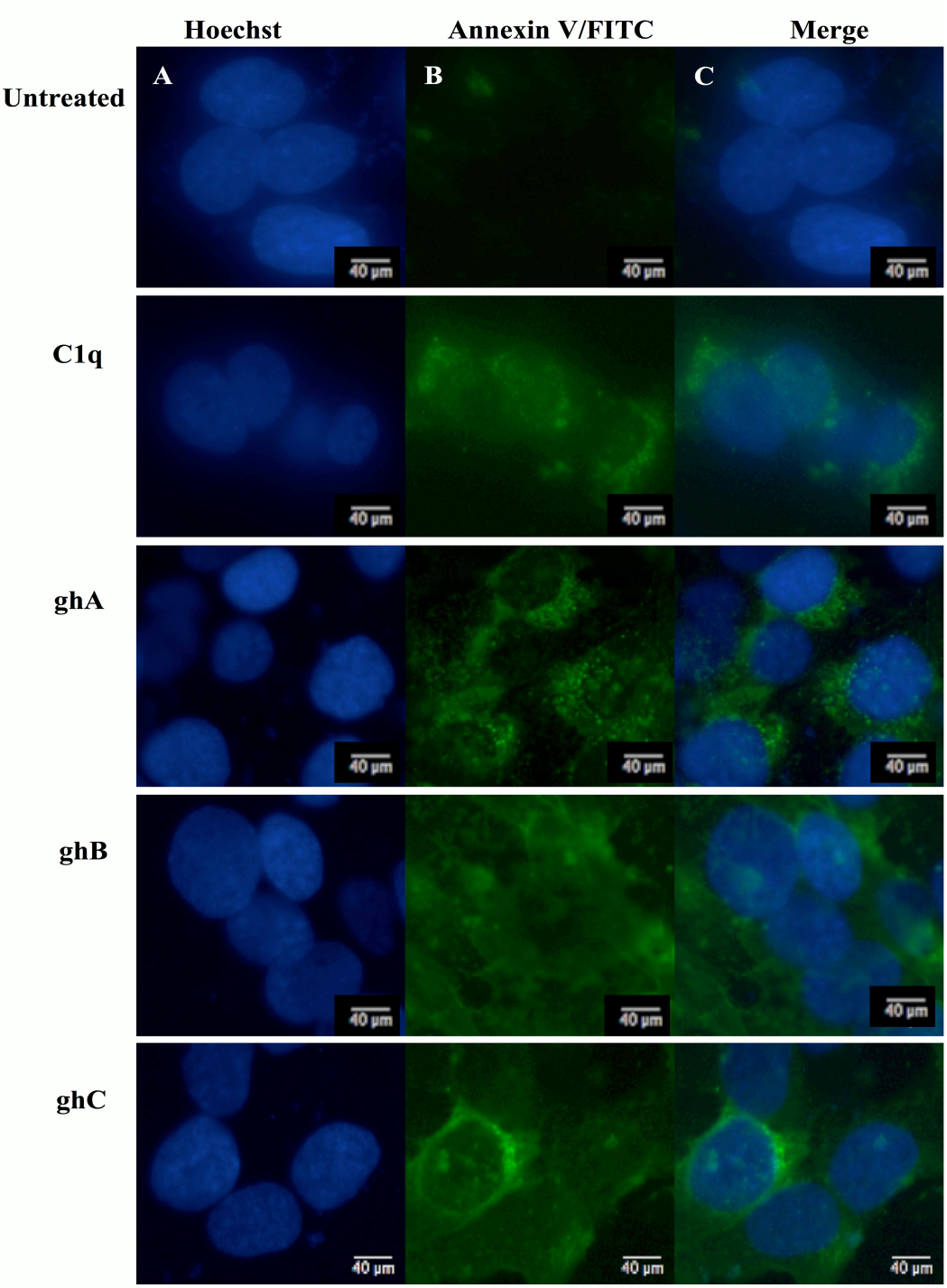

Figure 3.9 Fluorescence microscopy to analyze apoptosis in SKOV3 cells. Following the treatment with human C1q and ghA, ghB, ghC (10 µg/ml) and untreated cells, as a control, for 24 h, Panel A shows the nucleus stained positively with Hoechst. Panel B shows positive staining for PS, a cell integrity marker, which becomes exposed during apoptosis, available for binding annexin V labeled with FITC. No fluorescence was detected in the untreated SKOV3 cells, suggesting that the viability of these cells was not affected.

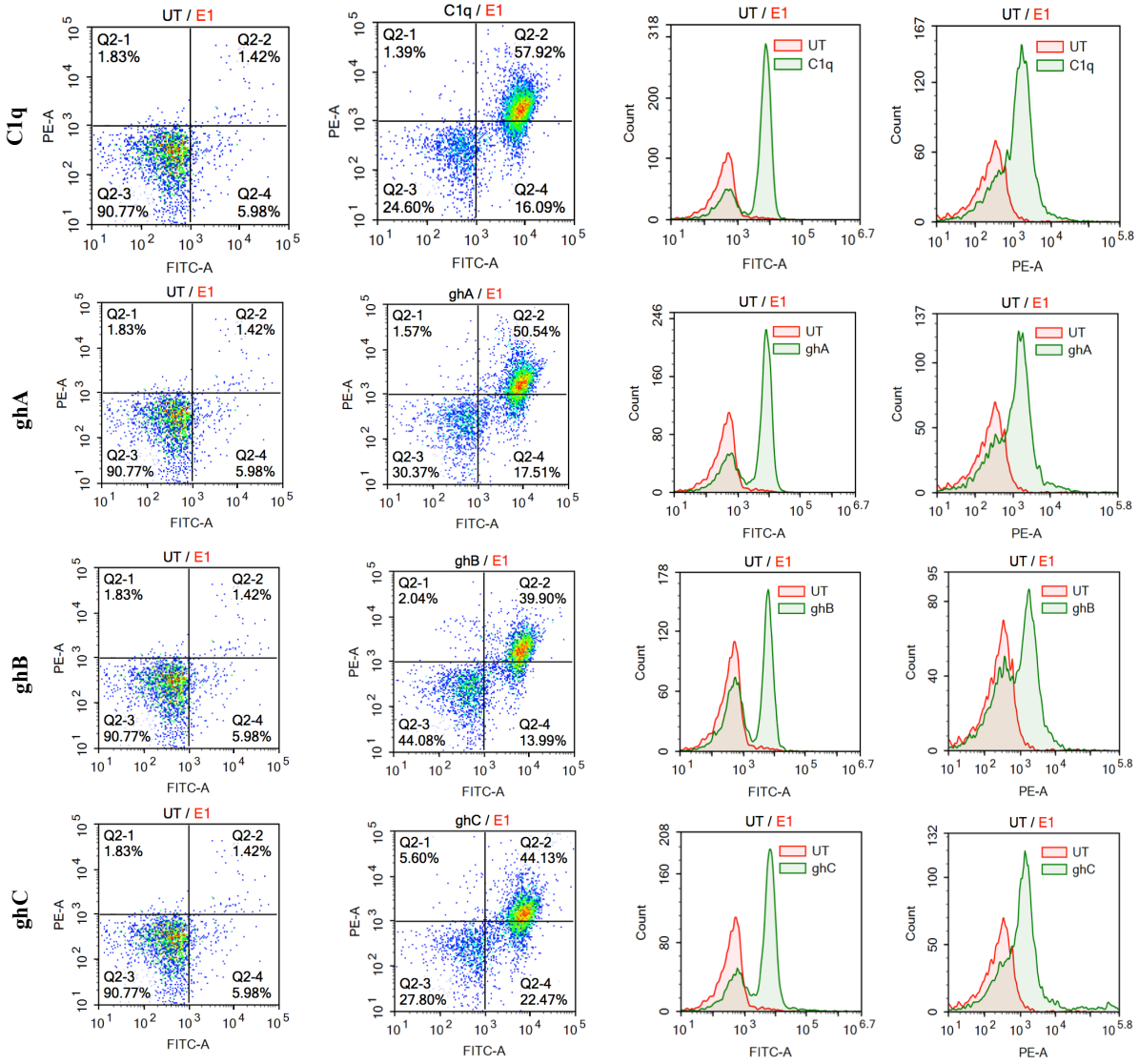

Figure 3.10 Flow Cytometer analysis to quantify SKOV3 cells undergoing apoptosis following treatment with C1q and individual globular head modules for 24 h. Approximately 50% (C1q, ghA, ghB, ghC; quadrant Q2-2) SKOV3 cells were stained positive for both FITC and PI, which was significantly higher than 1.42% of untreated control cells (untreated, quadrant Q2-2). Approximately 20% SKOV3 cells were stained positive for FITC only (C1q, ghA, ghB, ghC; quadrant Q2-4).

3.3.7 C1q and individual globular head modules upregulate TNF-α production by SKOV3 cells with concomitant upregulation of NF-κB

To determine the apoptosis pathway involved, the mRNA expression levels of pro-inflammatory cytokine, TNF-α and NF-κB was analysed for various time points. Interestingly, mRNA expression level of TNF-α was not affected at earlier time points up to 6 h but it was significantly upregulated at 12 h following treatment with C1q (~log 1.2-fold), ghA (~log 0.4-fold), ghB (~log 1-fold) and ghC (~log 0.7-fold) in comparison to an untreated control, as analysed by qPCR (Figure 3.11). As anticipated and consistent with TNF-α upregulation, NF-κB was also significantly upregulated (log 0.7-fold) in all the treated SKOV3 cells at 12 h. (Figure 3.11).

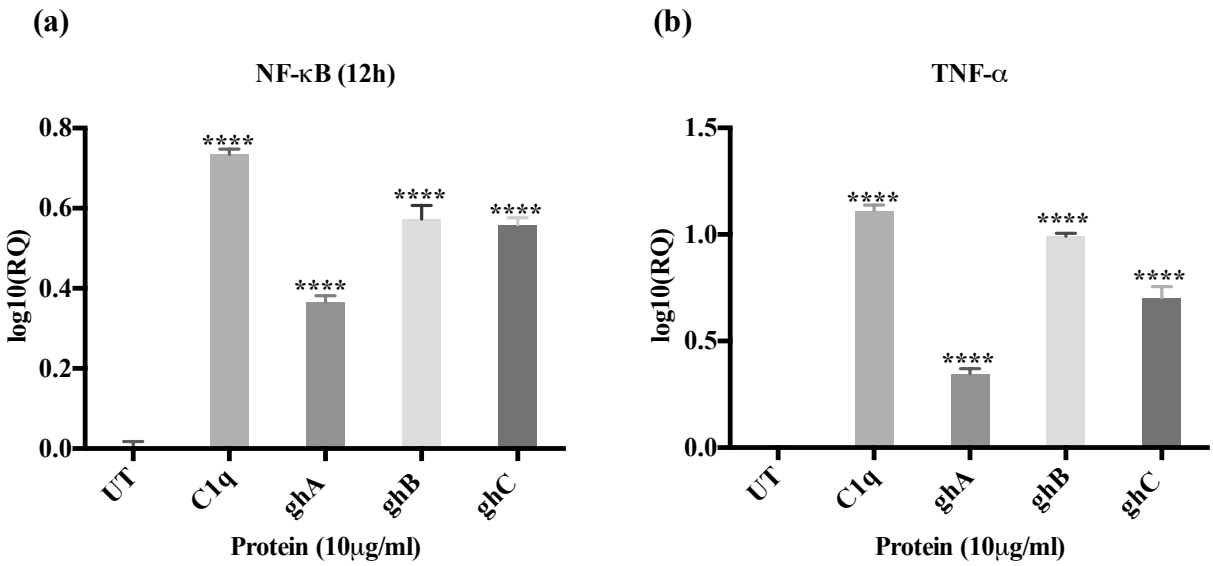

Figure 3.11 Relative quantification of TNF-α (a) and NF-κB (b) mRNA expression in SKOV3 cells treated with C1q, and globular head modules (ghA, ghB and ghC; 10 μg/ml) at 12 h. Both TNF-α and NF-κB were upregulated (~log 0.5-1 fold) in all the treated SKOV3 cells compared to untreated. The gene expression of the treated was normalized using the expression of both human 18S rRNA and untreated cells. All experiments were done in triplicate and the significance was established using the unpaired one-way ANOVA test (*$p<0.05$, *$p<0.01$ and ***$p<0.001$).

3.3.8 C1q upregulates expression of pro-apoptotic Bax and Fas in SKOV3 cells

C1q and globular head modules induced apoptosis was further analyzed by determining the mRNA expression of pro-apoptotic genes, Bax (intrinsic marker) and Fas (extrinsic marker), via qPCR. Fas was upregulated in the C1q (log 0.4-fold) treated SKOV3 cells, most significantly at 12 h and 24 h compared to the untreated cells (Figure 3.12), whereas in globular heads treated cells, the significant upregulation of Fas was seen at 24 h (log 0.4-fold) (Figure 3.12). Similarly, significant upregulation of Bax was observed in the case of C1q, ghA, ghB and ghC at 24 h (Figure 3.12). The cell membrane integrity is lost during apoptosis, which was seen in the Fluorescence microscopy at 24 h and is consistent with the upregulation of mRNA expression of pro-apoptotic genes Fas and Bax.

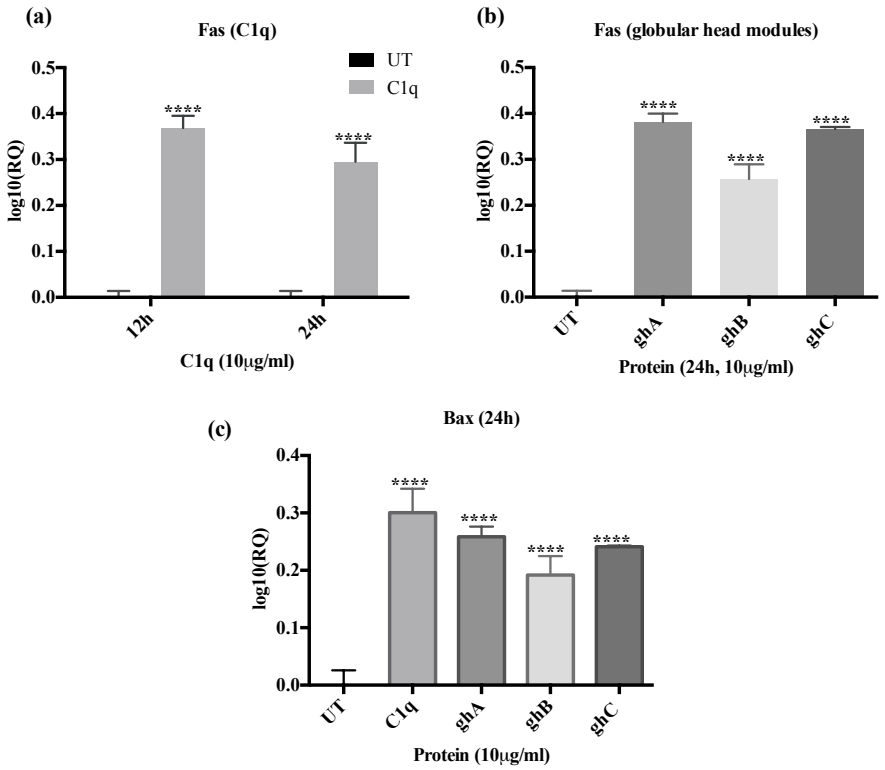

Figure 3.12 Relative quantification expression of Fas (a) and Bax (b) mRNA expression in SKOV3 cells treated with C1q, ghA, ghB and ghC (10 μg/ml) at 12 h and 24 h. Fas mRNA expression was upregulated at 12 h and 24 h following C1q treatment (~log 0.5 fold), whereas upregulation following globular head modules treatment was seen at 24 h only. Bax mRNA expression was upregulated (~log 0.5 fold) at 24h across all the treated cells compared to untreated. The gene expression of the treated was normalized using the expression of both human 18S rRNA and untreated cells. All experiments were done in triplicate and the significance was established using the unpaired one-way ANOVA test (*$p<0.05$, *$p<0.01$ and ***$p<0.001$).

3.3.9 C1q and the globular head modules activate caspase 3 in SKOV3 cells

The cleavage of caspase 3 is the final molecular event in the apoptosis pathway, therefore caspase 3 and cleaved caspase-3, were analysed in the SKOV3 cells treated with C1q and globular head modules, compared with untreated cells. The cleaved caspase 3 bands were seen at 17 kDa after 24 h treatment of SKOV3 cells with C1q, ghA and ghB in the western blot (Figure 3.13). A reduction in the full-length caspase 3 bands at 32 kDa was seen after 24 h in comparison to 12 h in the treated samples (Figure 3.13). Additionally, the activation of caspase 3 was also observed by fluorescence along with apoptosis staining for annexin V-FITC at 24 h following treatment with C1q and globular head modules. Activated caspase 3 was detected in the cytoplasm probed with rabbit anti-human cleaved caspase 3, followed by goat anti-rabbit/CY3, which further confirmed the final molecular event of apoptosis as the membrane was stained positively for annexin V-FITC, as compared to the untreated control where no fluorescence was detected (Figure 3.14). The cleaved caspase 3 in the ghC treated sample was not be detected via western blot; however, positive staining was observed for activated caspase 3 via fluorescence microscopy (Figure 3.14).

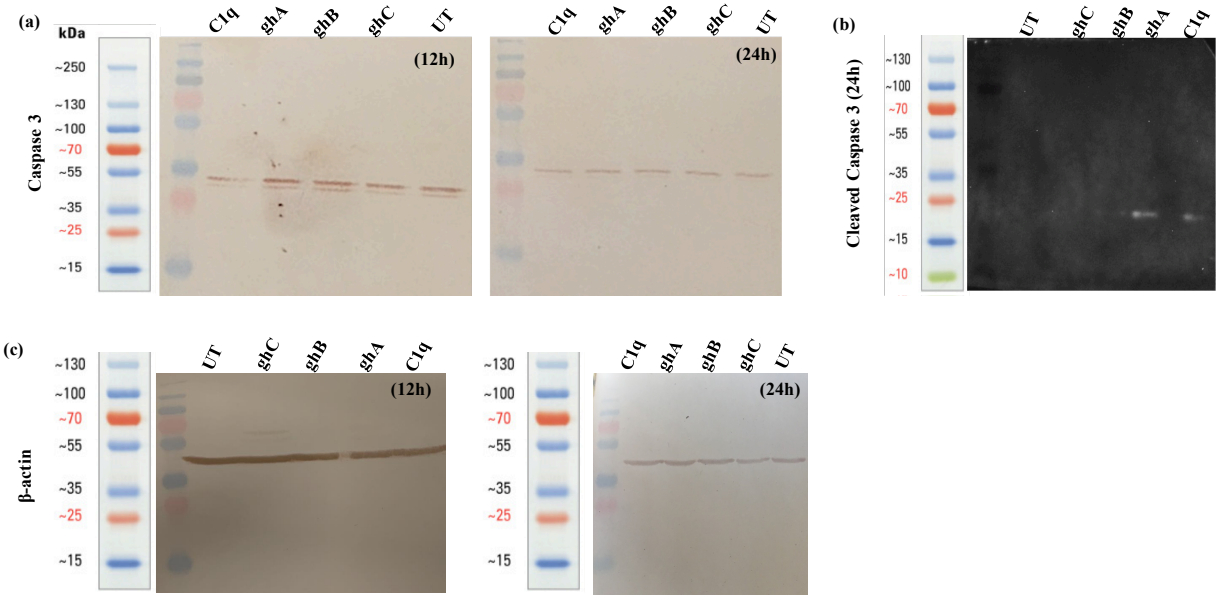

Figure 3.13 Western Blot analysis of caspase 3 activation in SKOV3 cells treated with C1q and globular head modules. (a) Western blot analysis of full-length caspase 3 at 32 kDa after 12 h and 24 h of the treatment with C1q, ghA, ghB, ghC and untreated as indicated. (b): The cleaved caspase 3 was observed at 17 kDa after 24 h of treatment with C1q, ghA, ghB, ghC and untreated. (c) β-actin was used a loading control.

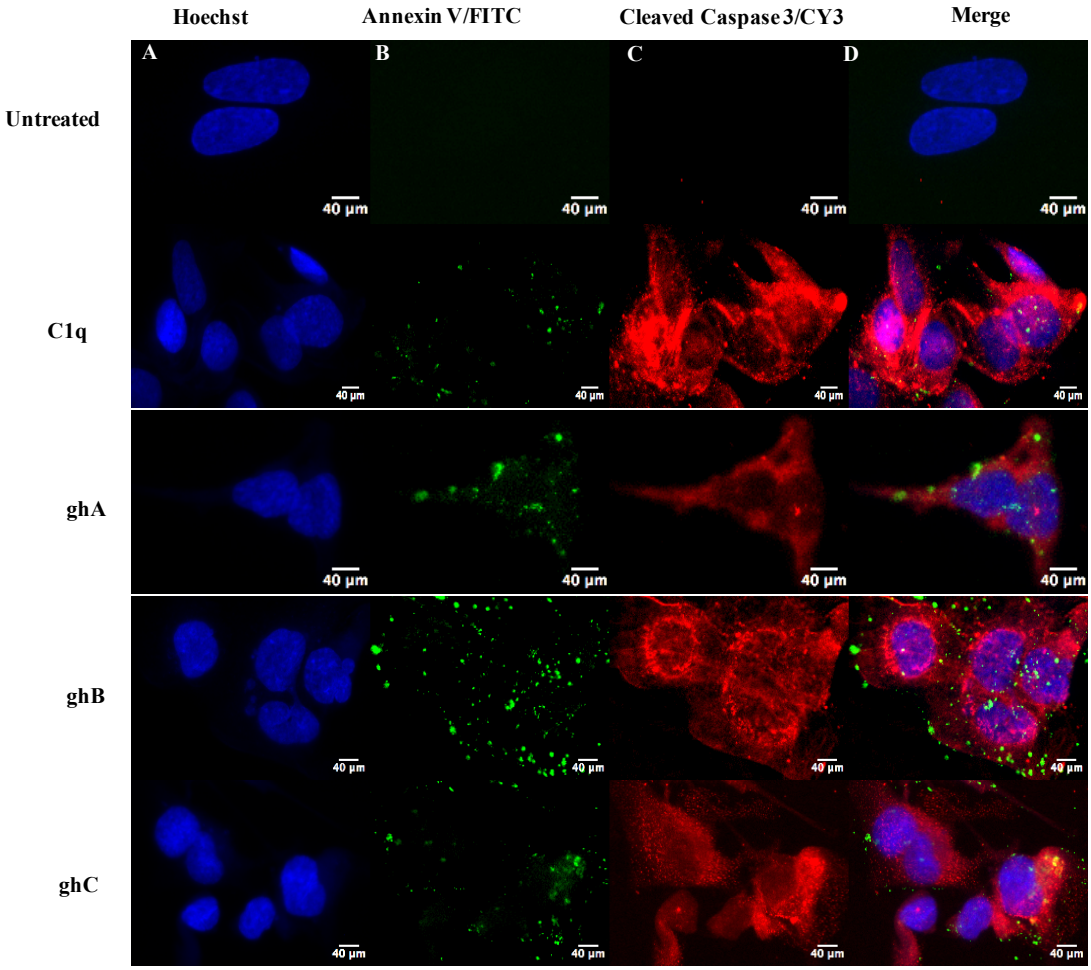

Figure 3.14 Fluorescence microscopy to analyze the activation of caspase 3 at 24 h. Panel C shows apoptosis staining with annexin V/FITC along with cleaved caspase 3/CY3, where activated caspase 3 was clearly seen in the cytoplasm probed with CY3 at 24 h. Panel B shows positive staining for annexin V/FITC, suggesting that cells were undergoing apoptosis. The nucleus was stained positively with Hoechst as seen in Panel A. Panel D shows merged images.

3.3.10 C1q and globular head modules down-regulate pro-survival factors such as RICTOR, mTOR and RAPTOR

The mRNA expression of pro-survival pathway, mTOR signalling pathway, was also determined since it is frequently overexpressed in ovarian cancers (Altomare et al., 2004). A significant downregulation of mRNA expressions of mTOR, RICTOR and RAPTOR (~log 0.5-fold) at 6 h was observed (Figure 3.15), which suggested that the treatment with C1q and globular head modules can intervene in mTOR signalling within the first few hours. Additionally, mTOR probed with anti-rabbit mTOR, followed by goat anti-rabbit IgG Alexa 488, was seen abundantly in the cytoplasm of the untreated cells as compared to SKOV3 cells treated with C1q and globular heads at 15 h time point via fluorescence microscopy (Figure 3.16).

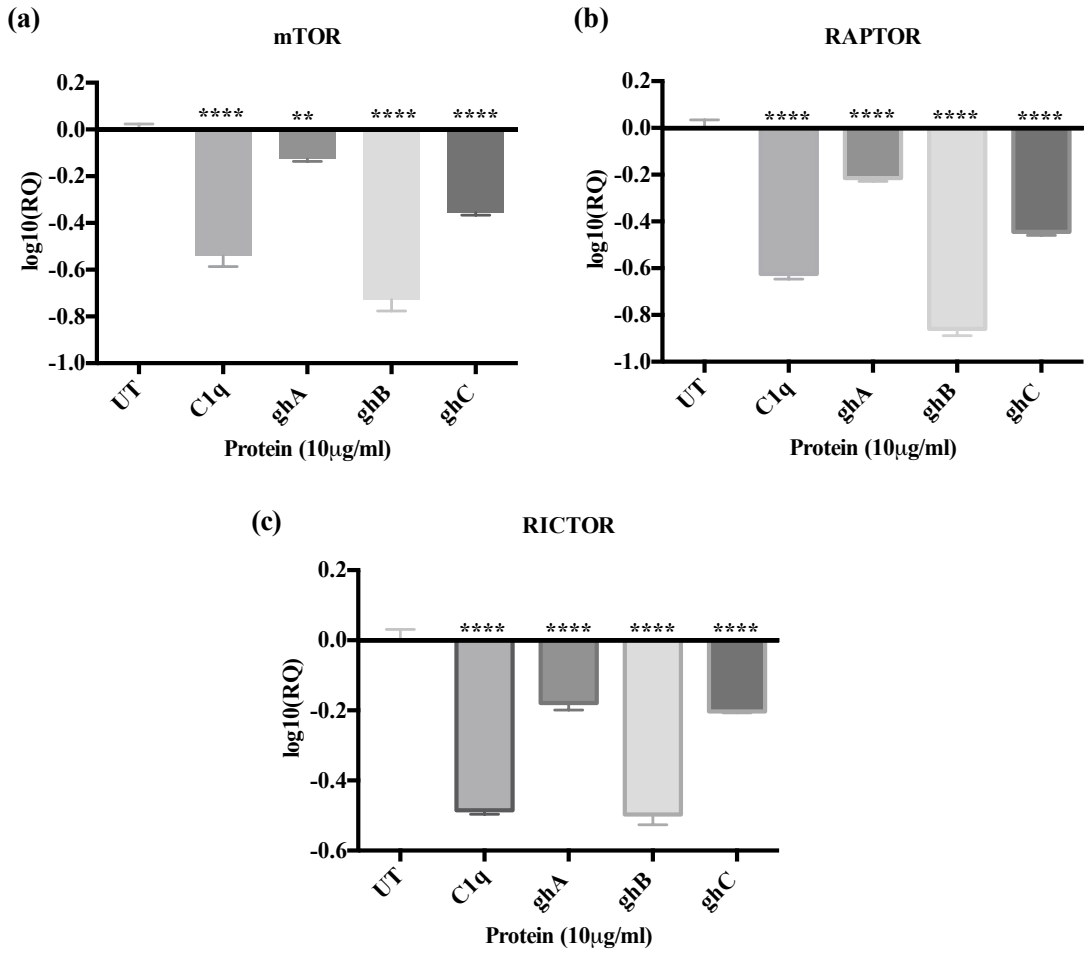

Figure 3.15 Relative quantification by comparisons of mTOR (a), RAPTOR (b) and RICTOR (c). mRNA expression in SKOV3 cells treated with C1q, ghA, ghB, and ghC (10 μg/ml) at 6 h was downregulated after the treatment. The gene expression of the treated was normalized using the expression of both human 18S rRNA and untreated cells. Significance was obtained using the unpaired one-way ANOVA test (*$p<0.05$, *$p<0.01$ and ***$p<0.001$) (n=3).

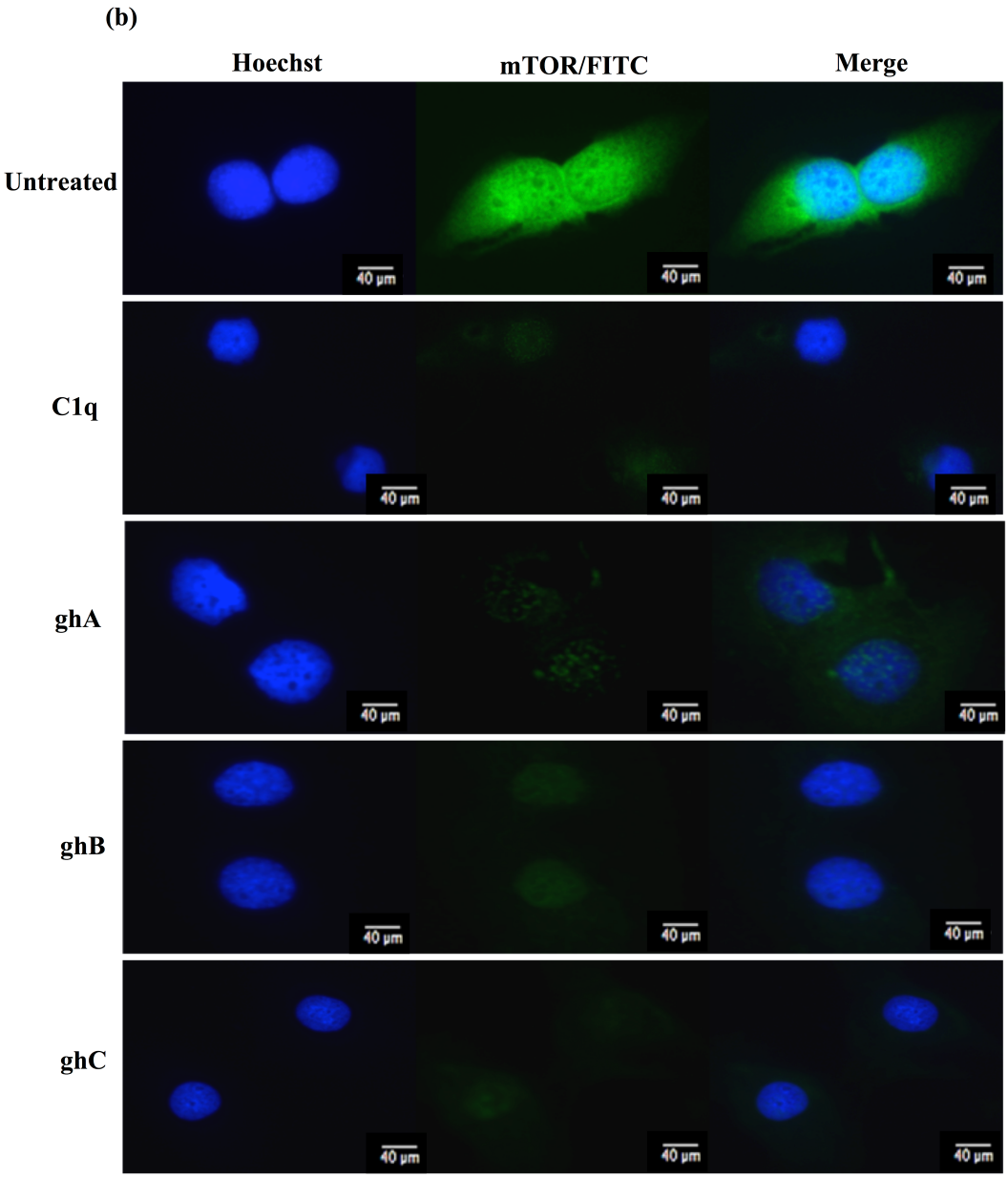

Figure 3.16 Fluorescence Microscopy analysis of mTOR expression. The presence of Mtor was detected using anti-human mTOR (1:200, 1 h) followed by secondary antibody goat anti-rabbit IgG Alexa Flour 488 and Hoechst (1:10,000) (nucleus staining) was analysed. It showed that mTOR was abundantly present in the cytoplasm of the untreated cells, as compared to the C1q and globular head modules treated SKOV3 cells at 15 h.

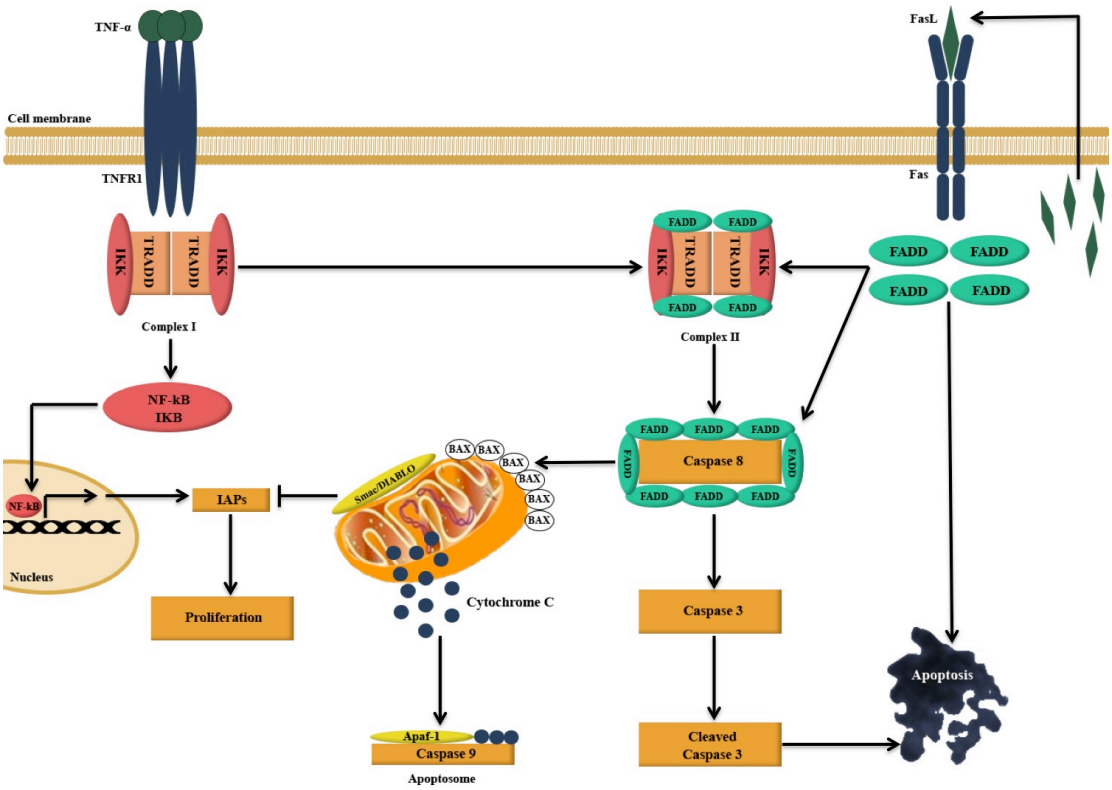

Figure 3.17 Illustration of the potential apoptotic pathway following the exogenous treatment of SKOV3 cells with C1q and globular head modules. TNF-α and Fas were upregulated. TNF-α binds to TNF type I receptor (TNFR1), which is internalized and forms a complex with TNFR1-associated DEATH domain (TRADD) (complex I), stimulating the upregulation of NF-κB. Then, a complex II is formed upon binding of complex I to Fas-Associated protein with Death Domain (FADD), which is available when Fas is activated. Subsequently, Complex II activates downstream caspase cascade, which causes the cleavage of caspase 8 followed by effector caspase 3 cleavage, which brings about apoptosis. NF-κB upregulation may interfere with apoptosis pathway, as it may promote the activation of apoptosis inhibitors including inhibitor of apoptosis protein (IAP). Bax, a marker of mitochondria mediated apoptosis, causes the release of pro-apoptosis factors such as cytochrome c, Smac (second mitochondria-derived activator of caspase)/DIABLO (direct inhibitor of apoptosis protein (IAP)-binding protein) from the mitochondria. Release of these factors into cytosol promotes a caspase cascade by antagonizing the (IAPs) (Figure 3.17 was taken from Kaur et al, 2016)

3.4 Discussion

This study reports, for the first time, that human C1q and recombinant globular head module (ghA, ghB and ghC) treatment induces apoptosis in an ovarian cancer cell line, SKOV3. A significantly higher number of Annexin V/FITC positive cells were observed via fluorescence microscopy and flow cytometry. Moreover, cleaved caspase 3 was detected via western blot. The transcriptional upregulation of pro-apoptotic genes, such as TNF-α, Fas and Bax was also seen. These results indicated that C1q and individual globular head modules induce apoptosis in SKOV3 cells via TNF-α mediated apoptosis pathway. However, other apoptosis pathways may potentially be involved.

During early stages of apoptosis, the cell membrane integrity is lost and phosphatidylserine (PS) is exposed, which is a target for annexin V binding (Lee at al, 2013). A significantly higher number of SKOV3 cells were stained Annexin V positive, when observed under fluorescence microscope, which indicated that the cell membrane was no longer intact as annexin V conjugated with FITC could bind PS, which normally exists intracellularly in the healthy cells. This provided the first indication that C1q and globular head module treated SKOV3 cells underwent apoptosis at 24 h. MTT, Trypan Blue exclusion assay and flow cytometry analysis of treated SKOV3 cells further validated induction of apoptosis. Thus, the alterations in the levels of pro-apoptosis genes such as Fas and Bax were further investigated following C1q and globular head module treatment of SKOV3 cells. This subsequently provided evidence for the involvement of the TNF-mediated apoptosis pathway.

TNF-α, is a pro-inflammatory cytokine, that plays a key role in various pathways associated with inflammation and cell death (Ashkenazi and Dixit, 1998). TNF family members play a key role in cancer immune surveillance, for example; TNF-α can regulate apoptosis induction selectively in tumour cells via death receptors; TRAIL/FasL ligands (Chan et al., 2000). C1q and globular head module treatment of SKOV3 cells, triggers the transcriptional upregulation of TNF-α at 6 h (C1q only) and 12 h (both C1q and globular head modules), and the cells subsequently underwent apoptosis by 24 h. TNF-α interaction with TNFR1 causes upregulation of NF-κB, which was observed in this study. Fas transcriptional upregulation was seen, as anticipated. This suggested that Fas, a receptor for FasL and

also a TNF receptor family member, may have been also involved in the apoptosis pathway. Interestingly, the transcriptional upregulation of Bax, a marker of mitochondria mediated apoptosis, was also observed. Bax activation causes the release of pro-apoptosis factors such as cytochrome c, apoptosis-inducing factor (AIF), Smac (second mitochondria-derived activator of caspase)/DIABLO (direct inhibitor of apoptosis protein (IAP)-binding protein), Omi/HtrA2 or endonuclease G from the mitochondria. Release of these factors into cytosol promotes a caspase cascade by antagonizing the inhibitor of apoptosis proteins (IAPs), which are produced due to NF-κB upregulation (Saelens et al., 2004). This indicated that Bax upregulation in this study may have negated the pro-apoptotic effects of NF-κB signalling pathway. (Saelens et al., 2004; Yuan et al., 2011; Wurstle et al., 2011; Janicke et al., 1998).

Akt/Mammalian target of rapamycin (mTOR) survival pathway are usually overexpressed in ovarian cancer cells, including the SKOV3 cancer cell line, thus protecting the cancer cells from undergoing apoptosis (Peng et al., 2010). mTOR, is a serine-threonine kinase, which upon activation by AKT, forms two complexes, mTOR complex I (mTORC1) and mTOR complex II (mTORC2). mTORC1 phosphorylates p70S6K, which is required for cell proliferation and progression into G1 cell cycle phase (Altomare et al., 2004, Laplante and Sabatini, 2009). Hence, the effect of C1q and globular heads module treatment of SKOV3 cells on the gene expression of mTOR and components of mTORC1 (regulatory-associated protein of mTOR; RAPTOR) (Hara et al., 2002) and mTORC2 (rapamycin-insensitive companion of mTOR; RICTOR) (Sarbassov et al., 2004) were investigated. The transcriptional levels of mTOR, RICTOR and RAPTOR were significantly downregulated at 6 h. This was further validated via fluorescence microscopy, which revealed that mTOR diminished in the cytoplasm following the treatment with C1q and globular head module. These results further supported that C1q and globular head module treatment not only triggered an apoptosis signalling pathway, but also downregulated the cell survival pathways. In conclusion, treatment with C1q and recombinant globular head module (ghA, ghB and ghC) induce transcriptional upregulation of TNF-α and Fas, and subsequently induce apoptosis, in addition to downregulation of mTOR cell survival pathways in SKOV3 cells.

Based on the jellyroll topology of the gC1q domain (Shapiro and Schener 1998), it became evident that C1q is potentially a prototypical molecule of the TNF

family. Hence, the C1q-TNF superfamily came into existence (Kishore et al., 2004). This study adds an additional layer of criss-cross mechanism, establishing that C1q can regulate TNF-α in cancer, to induce apoptosis in the target cells. Moreover, a cytokine – like property of C1q has been shown recently (Ghebrehiwet et al., 2012). It is perhaps no co-incidence that the recombinant fragments of the gC1q domain of human C1q (ghA, ghB and ghC) are also able to stimulate apoptosis in SKOV3 cells. It will be interesting to measure levels of C1q in serum and ascitic fluid of the ovarian cancer patients and establish a correlation with the classification of the severity of the ovarian cancer.

Chapter 4

Effect of rfhSP-D on epithelial-to-mesenchymal transition in pancreatic cancer cell lines

4.1 Abstract

Human Surfactant Protein-D (SP-D), an innate immune molecule, links innate and adaptive immunity during which it influences a range of other factors which may either be pro-or anti-tumorigenic such as TNF-α, TGF-β and NFκB, which collectively play an important role in immunomodulation and immunosurveillance against cancer. The inflammatory tumour microenvironment contributes in epithelial-to-mesenchymal transition (EMT) invasion and metastases in pancreatic cancer. In this study, we provide the first evidence that Surfactant Protein-D within the tumour-microenvironment blocks the mesenchymal-invasive properties of highly aggressive pancreatic cancer cells. Mechanistically, a recombinant form of SP-D (rfhSP-D) inhibits TGF-β expression and reduces the invasive potential of pancreatic cancer cell lines. In response to rfhSP-D, Smad2/3 expression appeared diminished in the cytoplasm of treated cells as compared to untreated, suggesting interrupted signal transduction required to initiate transcription of key mesenchymal genes such as Vimentin, Zeb1 and Snail. Interestingly, expression of Vimentin, Zeb1 and Snail was also downregulated upon rfhSP-D treatment in pancreatic cancer cell lines. Furthermore, TGF-β blocking showed similar downregulation of mesenchymal markers as seen with rfhSP-D treatment. An aberrant form of SP-D in a very low quantity was secreted by all pancreatic cancer cell lines tested, which may not have been able to initiate effective immune surveillance. Thus, this study presents yet another novel role of rfhSP-D to interfere with EMT induction by attenuating TGF-β pathway in pancreatic cancer cell lines.

4.2 Introduction

Pancreatic ductal adenocarcinoma (PDA) is one of the most lethal of all human malignancies with dismal 5-year survival rate below 7%; and it is estimated to become the third leading cause of cancer-related death by end of 2030 (Siegel et al., 2016). PDA is associated with high rates of mortality due to metastasis, resistance to conventional chemotherapy, and high tumor recurrence rate after surgery (Ansari et al., 2016). Metastasis requires Epithelial-to-Mesenchymal transition (EMT), which is considered a cause of tumour recurrence and resistance to conventional therapies (Brabletz et al., 2005; Brabletz, 2012; Rhim et al., 2012, Singh et al., 2015). EMT is a complex and hierarchical mechanism during tumor progression as it enables the tumor cells to acquire increased motility, leading to invasion of adjoining tissue and infiltration of systemic circulation and subsequent penetration into the adjacent tissues by tumour cells resulting in macroscopic secondary tumours (Fidler, 2003, Maier et al., 2010). A number of EMT markers have been identified that regulate the invasion-metastatic process in tumor cells. Aberrant activation of EMT has been attributed to over-expression of mesenchymal markers, such as Zeb1 (zinc finger E-box binding homeobox 1) (Wellner et al., 2009), Snail (Nishioka et al., 2010; Hotz et al., 2007) and Vimentin (Nishioka et al., 2010), as well as repression of E-cadherin, an epithelial marker (Singh et al., 2015) in the pancreatic cancer cells. During the EMT process, E-cadherin expression is lost whereas mesenchymal markers, including fibronectin and vimentin are over-expressed (Beuran et al., 2015). Snail1, Slug, Zeb1, Zeb2 and Twist, to name a few, have been shown to suppress E-cadherin. The Snail1 expressing metastatic tumors are associated with poor prognosis, drug and immune resistance; offering limited opportunity for therapeutic strategies (Kaufhold and Bonavida, 2014).

Recent studies have shown that the inflammatory tumor microenvironment influences early tumour dissemination, EMT and metastasis in pancreatic cancer (Rhim et al., 2012; Singh et al., 2015; Noll et al., 2016). Pro-tumorigenic cytokines such as TGF-β have also been linked to EMT, invasion, metastasis and drug resistance in many types of cancer (Heldin et al., 2012; Oshimori et al., 2015). In PDA, elevated TGF-β expression has been linked to highly invasive (metastatic) phenotype, acquired through SMAD signalling pathway. Importantly, TGF-β signalling regulates EMT-gene signatures, thereby promoting cell motility and

invasiveness in the pancreatic cancer cells (Friess et al., 1993, Ellenrieder et al., 2001, Maier et al., 2010; Peinado et al., 2003, Roshani et al., 2014).

Human Surfactant Protein D (SP-D), a soluble collagen containing C-type lectin (collectin), is a potent innate immune molecule, found at the pulmonary and extra-pulmonary mucosal surfaces. As a link between innate and adaptive immunity, SP-D is known for its role in immune surveillance and immunomodulation in asthma and pulmonary allergy (Kishore et al., 2006). SP-D has been considered for quite some time as a modulator of inflammatory response. However recent studies have shown not only anti-proliferative properties against cancer but also that its deficiency can trigger serious adverse clinical outcome in a number of diseases such as emphysema in mice (Ishii et al., 2012), chronic and infectious lung diseases in human (Foreman et al., 2011), Crohn's disease and ulcerative colitis in human (Tanaka et al., 2009), pneumococcal lung disease (Lingappa et al., 2011) and tuberculosis (Silveyra et al., 2012). An extension to defense mechanism of SP-D became evident when a recombinant fragment of human SP-D comprising the homotrimeric neck region and carbohydrate recognition domain (rfhSP-D), was shown to selectively induce apoptosis in the sensitized eosinophils derived from allergic patients, whereas eosinophils derived from healthy individuals were unaffected (Mahajan et al., 2008). Proteomics analysis of an eosinophil-like leukemic cell line, AML14.3D10, treated with rfhSP-D, showed that it induced cell cycle arrest via activation of G2/M checkpoints, and subsequently apoptosis via p53 mediated apoptosis pathway (Mahajan et al., 2013). More recently, treatment of human lung adenocarcinoma A549 cell line with SP-D has been shown to suppress the epidermal growth factor (EGF) signalling by interrupting the EGF-EGFR interaction, thus reducing cell proliferation, invasion and migration (Hasegawa et al., 2015).

In this study, for the first time, an anti-tumorigenic role of SP-D in EMT and modulation of mesenchymal-invasive phenotype in pancreatic cancer has been demonstrated. rfhSP-D inhibits the invasive functions of TGF-β/SMAD expressing pancreatic cancer cells. Mechanistically, rfhSP-D blocks the EMT-related gene signatures (Vimentin, Zeb1 and Snail), and hence pancreatic cancer cell invasion, mainly by attenuating TGF-β signalling pathway.

4.3 Results

4.3.1 Expression and Purification of rfhSP-D

The construct pUK-D1 containing 8 Gly-X-Y repeats, neck region and CRD region was transformed into BL21 (λDE3) pLysS. The expression of rfhSP-D was analysed via a pilot scale as shown in Figure 4.1 before producing large-scale batches (Figure 4.2) for purification of rfhSP-D. The inclusion body pellet containing insoluble rfhSP-D was sonicated, solubilized and serially dialysed to denature and refold the protein as described in Methods and Materials in Section 2.4. The supernatant was then passed through a maltose-agarose column to capture rfhSP-D. The concentration of the eluted fractions was determined by measuring the OD_{280} absorbance and the quality was confirmed by running the purified fractions on SDS-PAGE 12% gel (Figure 4.3). The peak elutions were then passed through Pierce™ High Capacity Endotoxin Removal Resin (Qiagen) to remove lipopolysaccharide (LPS) and the amount of endotoxin was found to be <0.4pg/µg of the rfhSP-D protein (Figure 4.4).

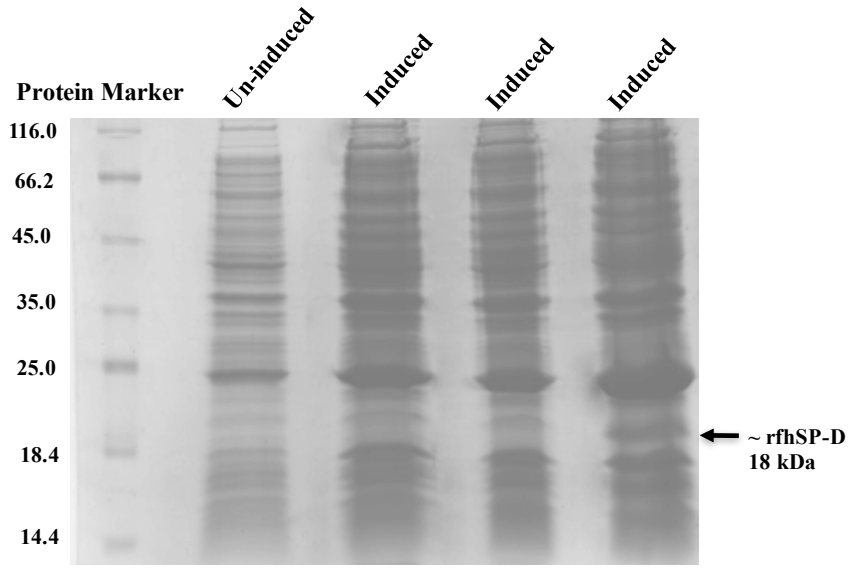

Figure 4.1 SDS-PAGE 12% analysis for rfhSP-D expression in the pilot-scale batches. The cell pellet centrifuged from 1 ml culture was mixed with 100 µl of the 2x treatment buffer. 20µl for each sample was loaded on SDS-PAGE and run for 90 min at 120V. The gel was stained and then de-stained to determine the expression. A clear band was visible ~18kDa in the last well for expressed rfhSP-D, which was not seen in the un-induced sample.

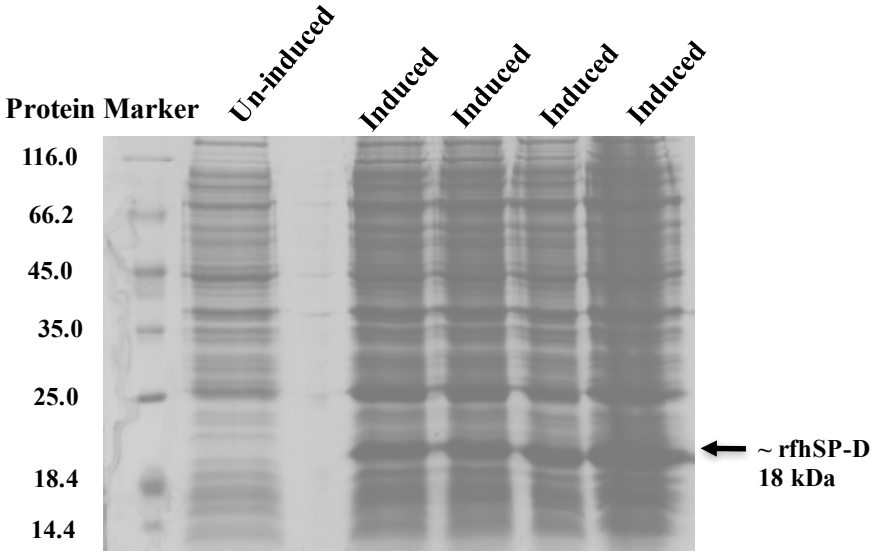

Figure 4.2 SDS-PAGE 12% analysis for rfhSP-D expression in large-scale batches. The cell pellet centrifuged from 1 ml culture was mixed with 100 µl of the 2x treatment buffer. 20µl for each sample was loaded on 12% SDS-PAGE and run for 90 min at 120V. The gel was stained and then de-stained to determine the expression. A clear band was visible ~18kDa in the induced wells for expressed rfhSP-D, which was not seen in the un-induced sample.

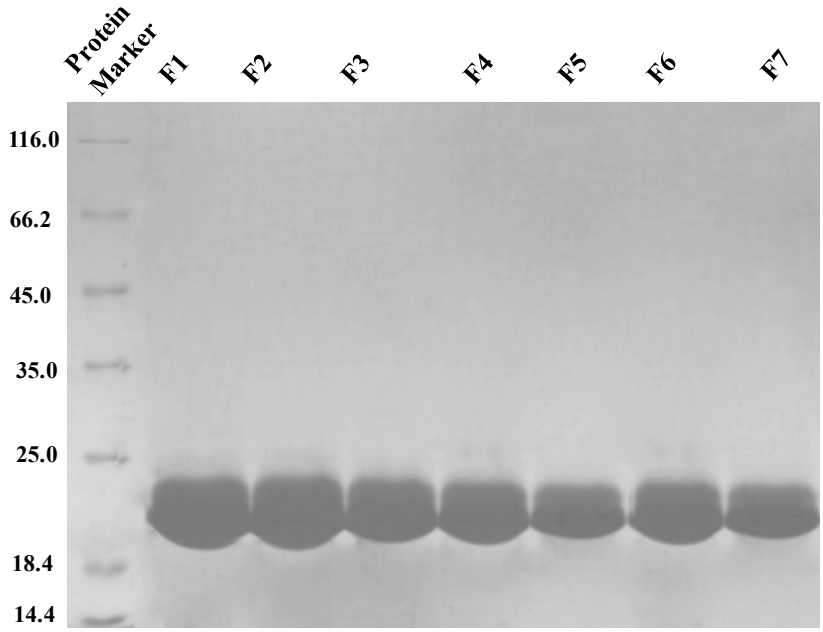

Figure 4.3 SDS-PAGE (12% w/v) analysis of purified fractions of rfhSP-D. The large-scale pellets were lysed, sonicated and the insoluble inclusion bodies were solubilized, refolded and affinity purified on maltose-agarose. 10 µl of purified protein was mixed with 10µl of 2x treatment buffer for each fraction and run on SDS-PAGE for 90 min at 120V. The gel was stained and de-stained and the bands were seen at ~18kDa.

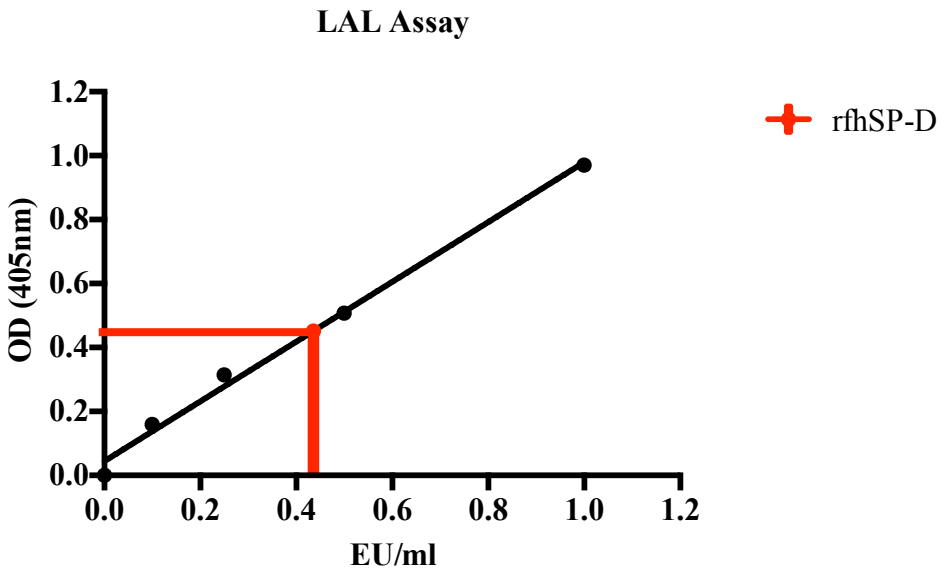

Figure 4.4 Measurement of endotoxin levels in the purified rfhSP-D. The endotoxins activate Factor C proteolytic activity present in LAL, which is photometrically measured using chromogenic substrate at optical density (OD_{405}). A standard curve is plotted using 4 *E. coli* endotoxin standards, which were plated in parallel to the test sample. Using standard curve, where 1 EU/ml is equivalent to 0.1ng endotoxin/ml, the endotoxin levels in rfhSP-D were found to be ~0.4pg/µg.

4.3.2 Human pancreatic cancer tissues and cell lines secrete SP-D

Fluorescence studies of human pancreatic cancer tissues probed with anti-human SP-D polyclonal antibody showed positive staining confirming the presence of an SP-D epitope in the tissues (Figure 4.5). These images were produced as a part of our collaboration by Dr Shiv K Singh, Department of Gastroenterology and Gastrointestinal Oncology, University Medical Center, Gottingen, Germany. Additionally, the tissues were probed with rabbit anti-human Vimentin, which also showed positive staining. This prompted further characterization of SP-D, which may be secreted into the tumour microenvironment. Subsequently, SP-D was purified via maltose affinity chromatography using supernatant from 80-90% confluent Panc-1, MiaPaCa-2 and Capan-2 cell lines. Interestingly, the western blot analysis of purified fractions probed with rabbit anti-human SPD antibody revealed that all pancreatic cancer cell lines secreted a very low quantity of an aberrant form of SP-D, which appeared above 60 kDa, as compared to normally found human SP-D at ~43 kDa. The rfhSP-D (~18 kDa) was used as a positive control for the western blotting (Figure 4.6). Therefore, inability of this abnormal SP-D secreted by pancreatic cancer cells to contribute to defense mechanism against cancer cells was further investigated by

incubating the cell lines with purified rfhSP-D. Initially, it was established if rfhSP-D binds to these cell lines using fluorescence microscopy.

(a)

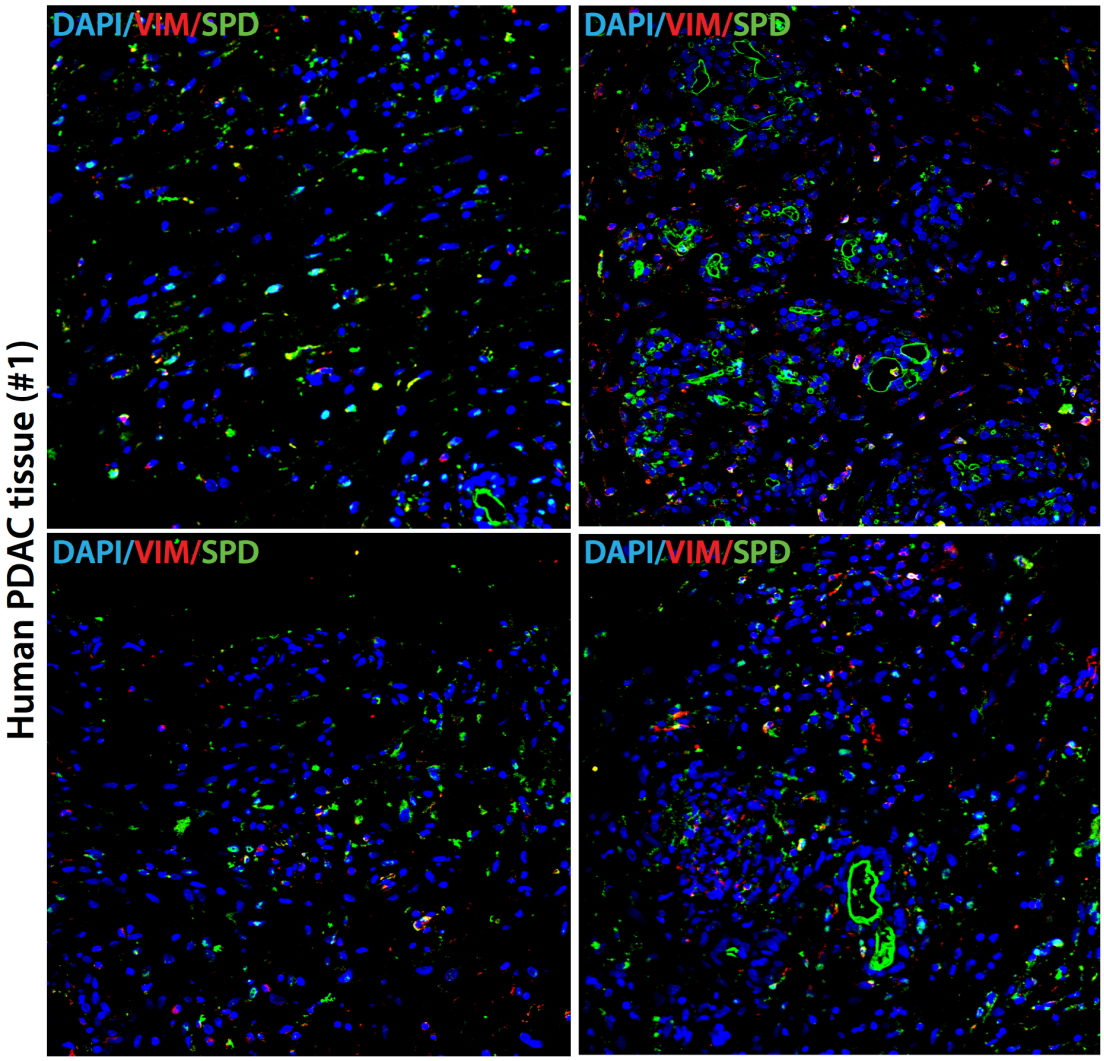

Figure 4.5 Fluorescence analysis of SPD in human pancreatic cancer tissues. The tissue slides were probed with rabbit anti-human SP-D (1:500) and rabbit anti-human Vimentin (1:500) followed by secondary goat anti-rabbit IgG Alexa 488 (1:500) and DAPI (for nucleus staining; 1;1000) showed positive staining for the presence of SP-D and Vimentin in the human pancreatic cancer tissue. These images have been used, with permission, for completeness. These images were produced as a part of our collaboration by Dr Shiv K Singh, Department of Gastroenterology and Gastrointestinal Oncology, University Medical Center, Gottingen, Germany.

(b)

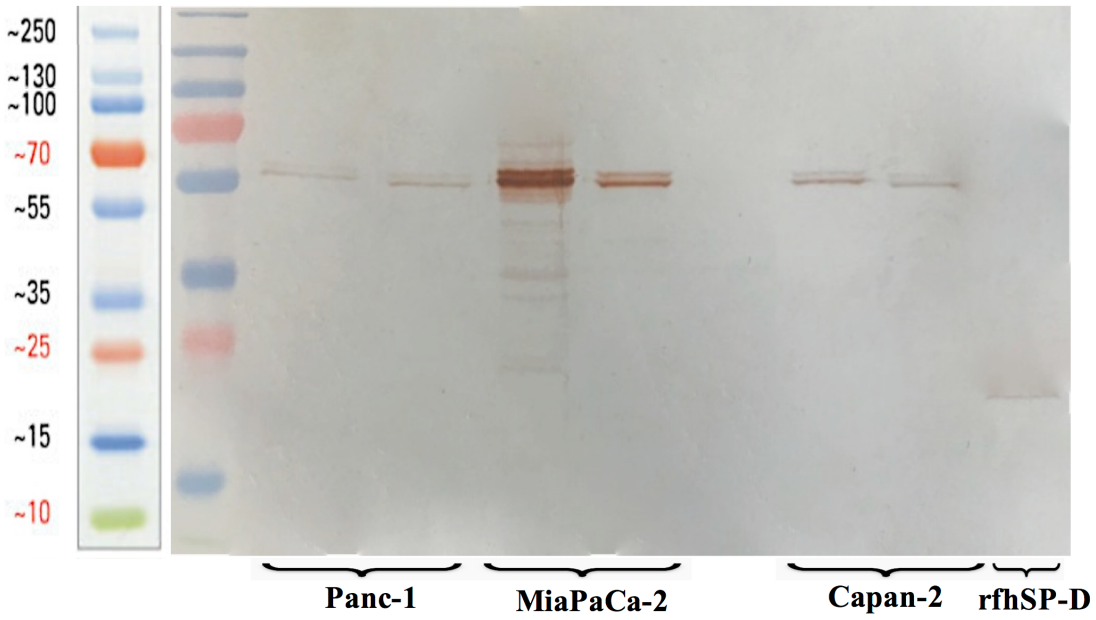

Figure 4.6 Western blot analysis of purified SP-D fractions from all pancreatic cancer cell lines. SP-D was purified using supernatant from 80-100% confluent cells and two fractions for each cell line were subjected to western blot analysis by probing the membrane with rabbit anti-human SP-D (1:1000) for 1 hr, followed by anti-rabbit conjugated with HRP (1:1000) for 1 hr and the colour was developed using DAB substrate kit. The bands appeared above 60 kDa for Panc-1, MiaPaCa-2 and Capan-2 and rfhSP-D (~18Kda) was used a positive control.

4.3.3 rfhSP-D binds to a range of pancreatic cell lines

The fluorescence analysis of rfhSP-D binding to Panc-1, MiaPaCa-2 and Capan-2 revealed its membrane localization following 1 h incubation at 4°C (Figure 4.7). The rfhSP-D probed with mouse anti-human SP-D/CY5 antibody appeared evenly bound in clusters on the cell membrane, along with nuclei stained positively with Hoechst. All cell lines showed a similar rfhSP-D binding pattern. No CY5 fluorescence was detected in the untreated controls, probed with primary and secondary antibodies, for each cell line, suggesting the rfhSP-D binding observed in the treated cell lines was protein-specific. To determine whether rfhSP-D influences the cellular morphology and EMT phenotypic expression, we treated highly invasive pancreatic cancer cells (e.g. Panc-1) with exogenous rfhSP-D in a dose-dependent manner.

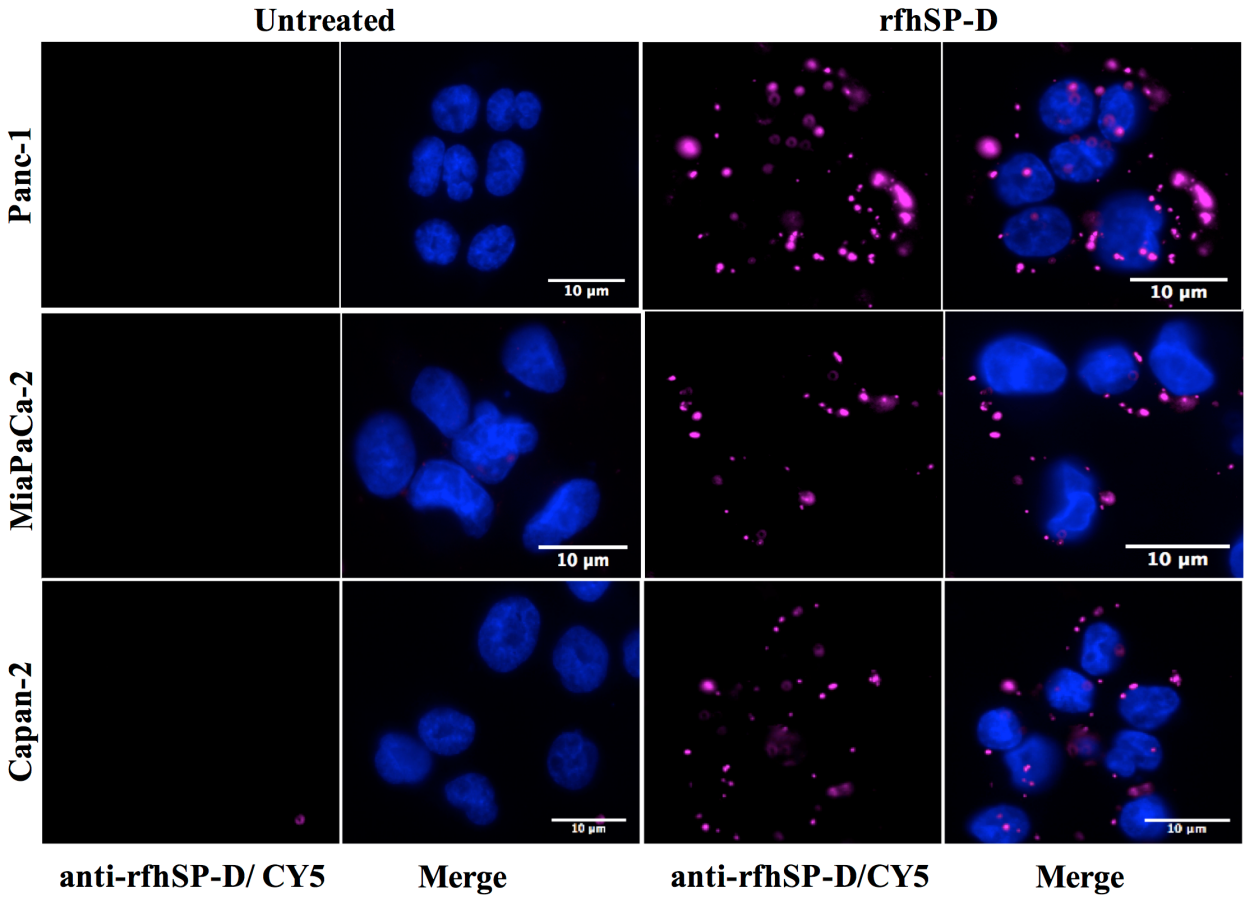

Figure 4.7 rfhSP-D binds to a range of pancreatic cell lines. All cell lines, Panc-1, MiaPaCa-2 and Capan-2 ($0.5x10^5$/ml) were grown on coverslips and incubated with and without rfhSP-D (10 µg/ml) for 1 h, followed by incubation with primary antibody (mouse anti-human SP-D, 1:200) for 1 h and then probed with Goat Anti-Mouse IgG H&L (Cy5 ®) (1:500,) and Hoechst (1: 10,000) for fluorescence analysis. rfhSP-D was seen bound on the cell membrane in the treated cells whereas no Cy5 fluorescence was detected in the untreated cells. Hoechst positively stained the nuclei.

4.3.4 rfhSP-D induces morphological alterations in the pancreatic cell line Panc-1 in a dose and time-dependent manner

To determine the optimal dose of rfhSP-D, Panc-1 cells were incubated with 0, 5, 10, and 20 µg/ml. Colonies of 10-15 cells were selected for each protein dose to observe the effect of rfhSP-D on cell morphology and cell division. The images of the selected cell colonies were taken at 0 h, 6 h and 24 h (Figure 4.8). Panc-1 cells treated with rfhSP-D (5 µg/ml) acquired spindle type cell morphology, reduced cell-cell contact and continued to divide in a time dependent manner. These alterations were similar to the untreated cells. Panc-1 cells treated with rfhSP-D (10 and 20 µg/ml) did not acquire spindle shape and appeared to be static. However, cell morphology at 10

µg/ml appeared to be regaining the spindle shape and reduced cell-cell contact and some cell division by 24 h. At 20 µg/ml, the non-spindle effect continued up to 24 h. Although some cell division was noted, cells remained in close contact with each other and static. Interestingly, some dead cells were also seen at 20 µg/ml as compared to the other dose conditions. Therefore, 20 µg/ml dose was selected to further investigate a possible effect on EMT by rfhSP-D in Panc-1, MiaPaCa-2 and Capan-2. This finding was then investigated qualitatively and quantitatively using a matrigel invasion chambers.

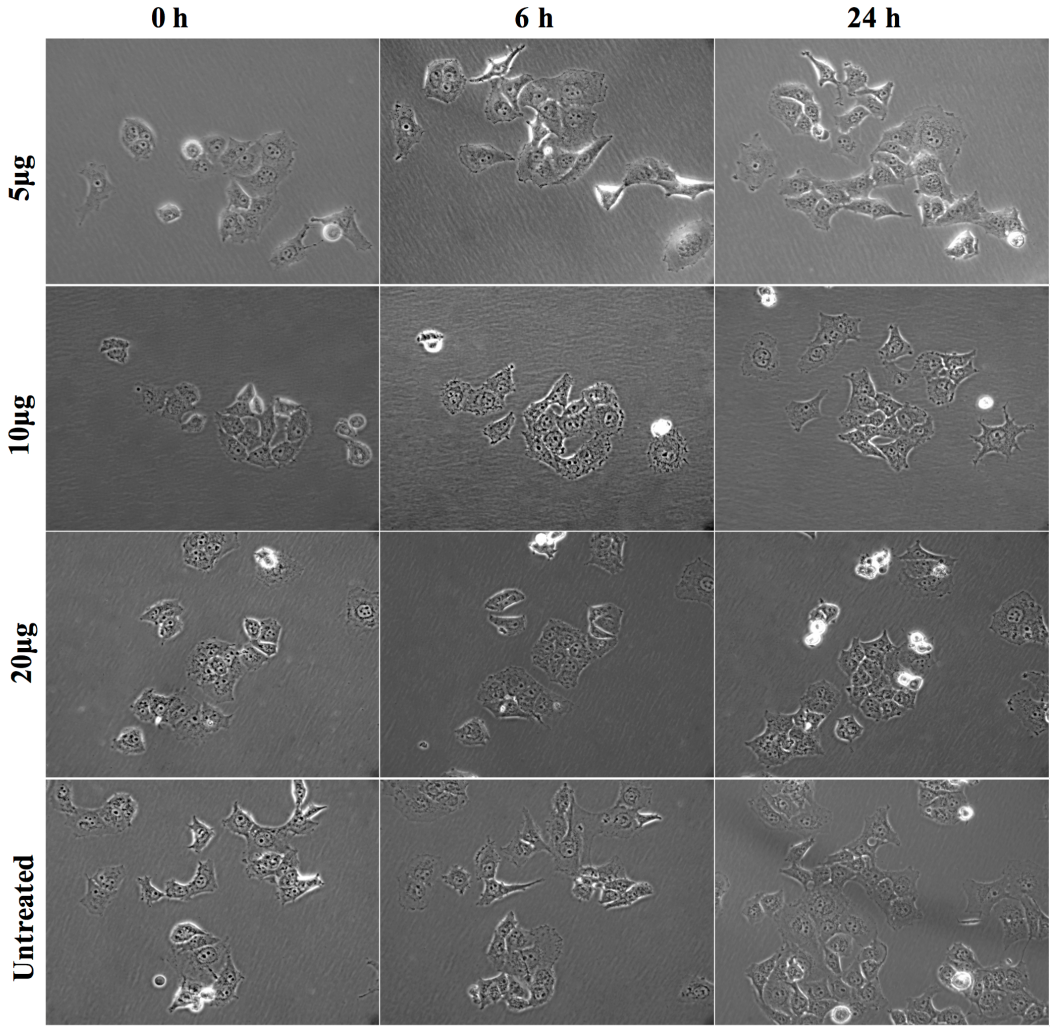

Figure 4.8 Exogenous treatment with rfhSP-D of Panc-1 cells induced morphology changes in a time and dose- dependent manner. Panc-1 cells ($0.1x10^4$/ml) were grown overnight in a 12 well plate and colonies of 5-10 cells were selected for analysis with and without rfhSP-D (5, 10, 20 µg/ml) at 0, 6 and 24 h. The cells treated with 5 µg/ml and untreated appeared to undergo EMT as they acquired spindle shape and showed reduced cell-cell contact whereas cells treated with 10 and 20 µg/ml appeared static, did not acquire spindle shape and some dead cells were also seen.

4.3.5 rfhSP-D suppresses the invasion ability/capacity in pancreatic cancer cell lines

The matrigel invasion chambers pre-coated with extracellular matrix proteins were used to incubate the pancreatic cancer cells (3.5 x 10^4/0.5ml) in presence and absence of rfhSP-D (20 µg/ml) in the upper surface of the chamber and serum containing media as a chemo-attractant in the bottom surface for 22 h. Both Panc-1 and MiaPaCa-2 cell lines treated with rfhSP-D (20 µg/ml) showed significantly reduced invasion in the matrigel (Figure 4.9); however almost no invasion occurred in Capan-2 whether treated or untreated, which was anticipated since it is a low-grade cancer cell line. MiaPaCa-2 was most affected as the invasion was reduced by 65%, followed by Panc-1 cell line, which was approximately 50% less than the untreated cells (Figure 4.10). Since pancreatic cancer cells are well known to overexpress TGF- β, which has a prominent-role in inducing EMT, the expression of TGF- β in the cell lines was investigated following the treatment with rfhSP-D (20 µg/ml).

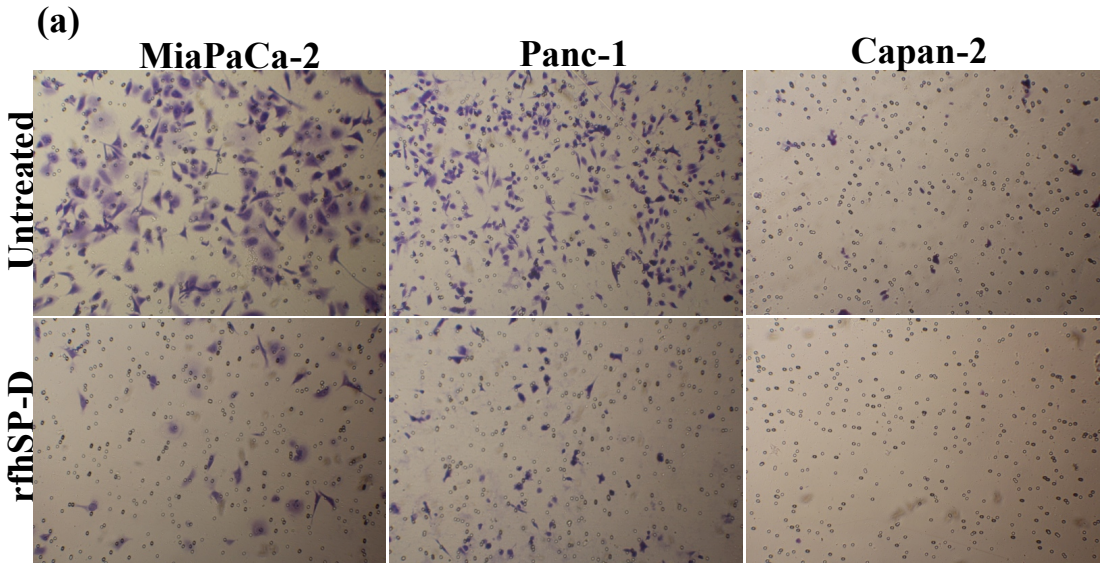

Figure 4.9 rfhSP-D suppresses the invasion in pancreatic cancer cell lines. The cell invasion was analysed by incubating 35,000 cells, with and without rfhSP-D (20 µg/ml) in the BioCoat™ Matrigel™ Invasion Chambers at 37°C for 22 h. The metastasized cells were fixed and stained before mounting the membrane on the slide for cell counting. The images show the difference between treated and untreated.

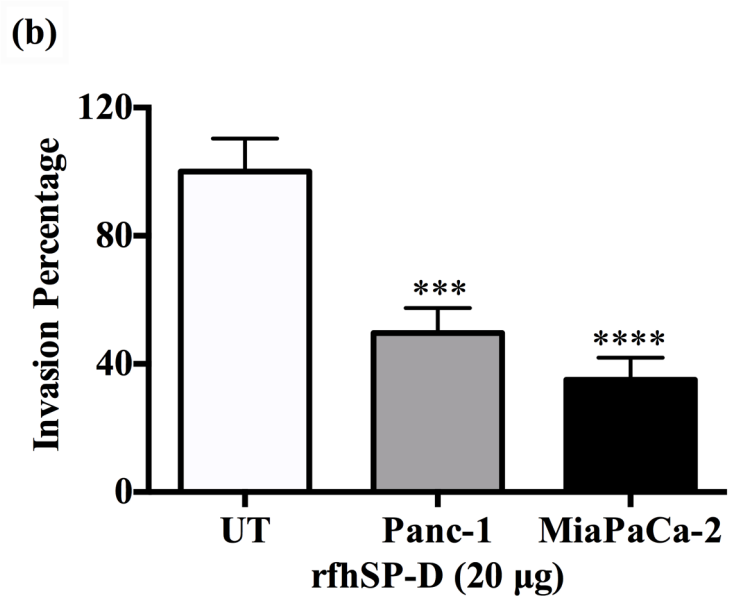

Figure 4.10 Treatment with rfhSP-D significantly reduced the cell invasion by Panc-1 (~50%) and MiaPaCa-2 (~65%) measured by counting the number of cells that penetrated through the matrigel. However, as anticipated, no invasion was detected in Capan-2 cell line, neither in treated nor untreated.

4.3.6 rfhSP-D downregulates TGF-β gene expression

The gene expression of TGF-β was significantly downregulated in Panc-1 (~$\log_{10}$ 0.5-fold) and MiaPaCa-2 (~$\log_{10}$ 0.3-fold) at 12 h (Figure 4.11) whereas Capan-2 showed no difference between treated and untreated. This suggested that reduced TGF-β transcripts were being made following the rfhSP-D treatment. Thus, the total cell extracts for all cell lines were then analyzed by western blot. The rabbit anti-human TGF-β antibody bands detected at 60 kDa at 24 h treatment and a reduction in the amount of TGF-β in the rfhSP-D treated Panc-1 and MiaPaCa-2 samples was observed as compared to the untreated cells; the amount of TGF-β in Capan-2 was unaffected (Figure 4.12). The qualitative analysis by fluorescence microscopy showed TGF-β expression at 24 h diminished considerably within the cytoplasm Panc-1 and MiaPaCa-2 cell lines following rfhSP-D treatment (Figure 4.13). During TGF-β induced EMT pathway, Smad2/3 are phosphorylated in the cytoplasm, followed by translocation into nucleus, however Smad2/3 staining appeared very weak in the cytoplasm of the treated Panc-1 and MiaPaCa-2 cell lines (Figure 4.14). Then, key regulators of EMT were examined.

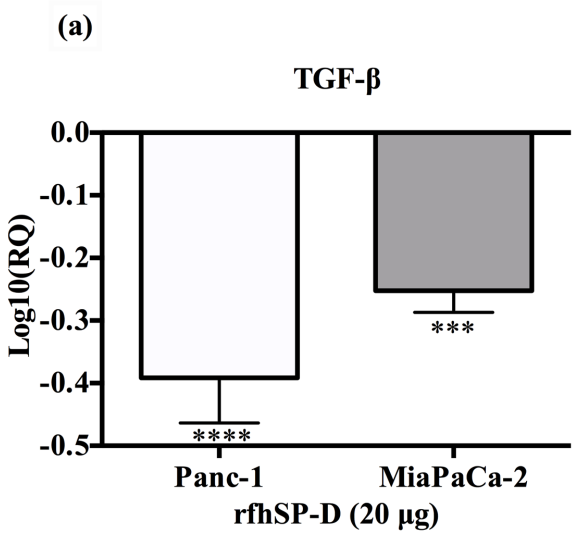

Figure 4.11 TGF- β gene expression as determined by qPCR was significantly downregulated at 12 h in both Panc-1 and MiaPaca-2 cell lines. The gene expression of the treated was normalized using the expression of both human 18S rRNA and untreated cells. Significance was obtained using the unpaired one-way ANOVA test (*p<0.05, *p<0.01 and ***p<0.001)(n=3).

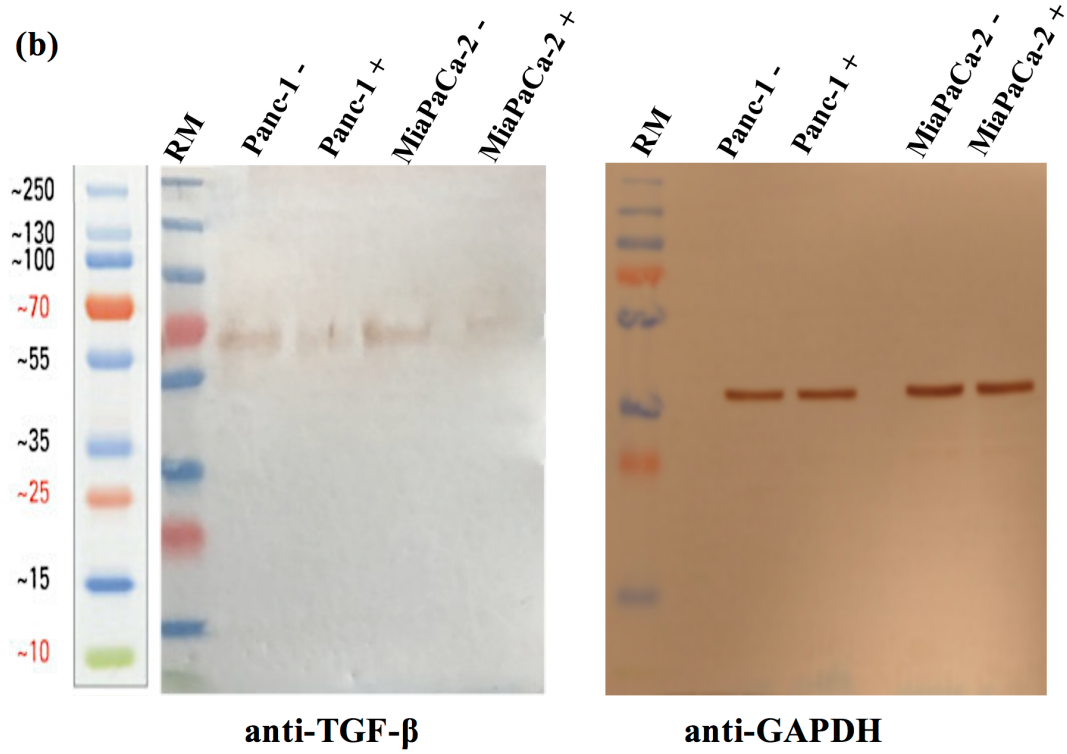

Figure 4.12 Western Blot analysis confirmed this results as the bands (~60Kda) in the treated samples (+) appeared very faint as compared to untreated (-), when probed with rabbit anti-human TGF- β (1:1000) for 1 h followed by anti-rabbit conjugated with HRP and the colour was developed using DAB. Anti-GAPDH was used as a loading control.

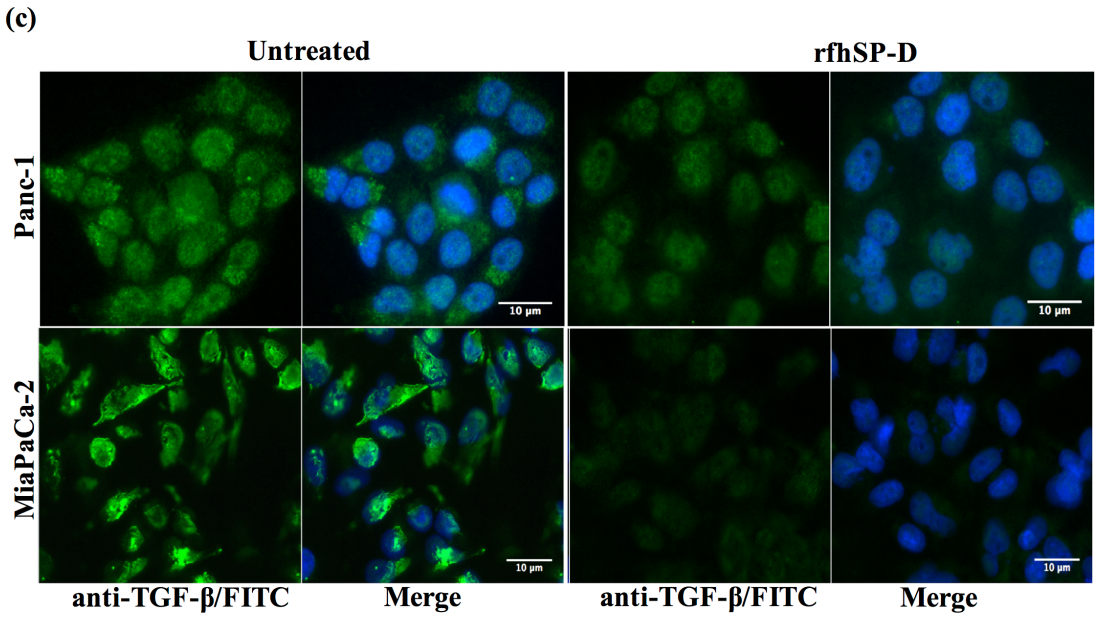

Figure 4.13 TGF- β intracellular staining for all cell lines using $0.5x10^5$ cells/ml incubated with and without rfhSP-D (20 µg/ml) for 24 h followed by probing with rabbit anti-human TGF- β1antibody (1:500) and then probed with goat anti-rabbit IgG Alexa Flour 488 (1:500) and Hoechst (1:10,000) for fluorescence analysis showed bright green fluorescence in the cytoplasm of the untreated cells as compared to minor staining in the treated cells.

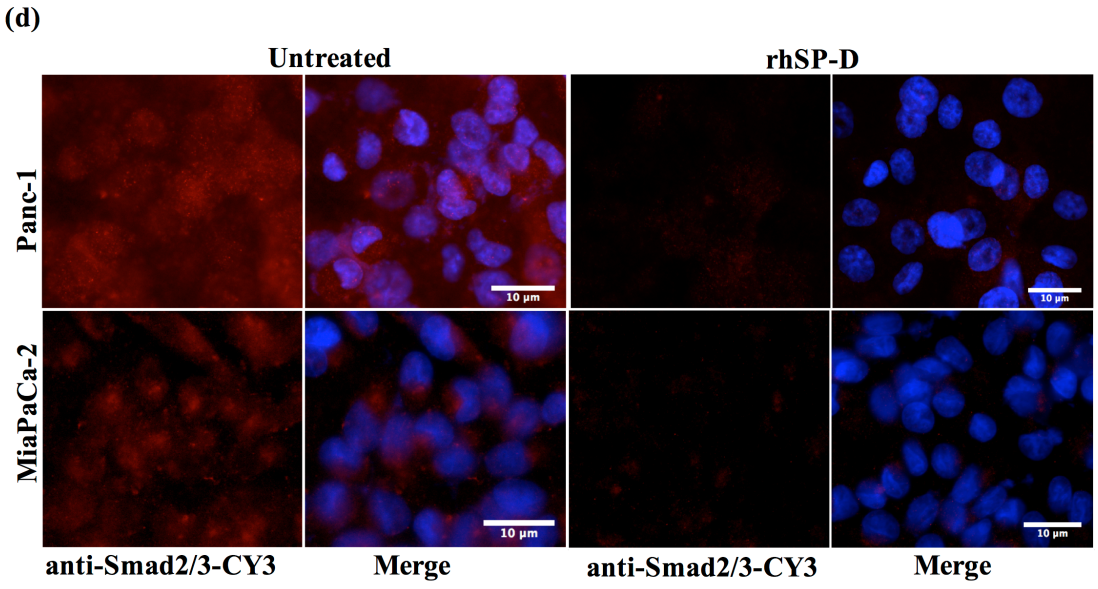

Figure 4.14 Smad 2/3 intracellular staining for Panc-1 and MiaPaCa-2 cell lines with and without rfhSP-D (20 µg/ml) for 24 h using rabbit anti-human Smad2/3 antibody (1:500) and then probed with goat anti-rabbit IgG/CY3 (1:1000) showed the presence of Smad2/3 in the cytoplasm of untreated cells, however no CY3 fluorescence was detected in the treated cells.

4.3.7 rfhSP-D reduces the expression of EMT markers

To determine whether exogenous rfhSP-D was affecting the key regulators of EMT, we examined the gene expression of Vimentin, Zeb1 and Snail at various time points. All of these markers were downregulated in all the cell lines; however, variations in the transcript levels and the time of downregulation in each cell line were observed. Vimentin was significantly downregulated in Panc-1, ~$\log_{10}$ 1-fold at 1 h, and ~$\log_{10}$ 0.5-fold at 6 h (Figure 4.15). MiaPaCa-2 had downregulation of ~$\log_{10}$ 0.5-fold at 1 h that remained constant at 6 h (Figure 4.15). Vimentin downregulation occurred at later time-point, as compared to Panc-1 and MiaPaCa-2, at 6 h in Capan-2 (~$\log_{10}$ 0.5-fold) cell line (Figure 4.15). All cell lines showed a similar pattern of decrease in levels of downregulation of Vimentin at 12 h compared to earlier time-points.

Snail was significantly downregulated in Panc-1 (~$\log_{10}$ 1-fold), MiaPaCa-2 (~$\log_{10}$ 0.5-fold), and Capan-2 (~$\log_{10}$ 1-fold) at 1 h and remained downregulated at 6 h and 12 h (Figure 4.15). Zeb1 transcript level was significantly reduced in Panc-1 (~$\log_{10}$ 0.5-fold) at 1 h at 6h and MiaPaCa-2 (~$\log_{10}$ 2-fold) at 12h (Figure 4.15). No difference in Zeb1 gene expression was seen in Capan-2. Since TGF-β regulates these markers and rfhSP-D downregulates TGF-β, rfhSP-D mediated downregulation of EMT markers (Vimentin, Snail and Zeb1) was clearly evident. To further establish the TGF-β association, we used neutralizing antibody in order to block TGF-β in all cell lines and assessed the expression of these markers.

4.3.8 Fluorescence and flow cytometry Analysis of EMT markers

The qualitative analysis of Vimentin (Figure 4.16) and Zeb1 expressions (Figure 4.17) in Panc-1 and MiaPaCa-2 cell lines via fluorescence microscopy revealed a significant difference in the cytoplasmic presence of these proteins in treated and untreated cells. Furthermore, the quantitative analysis using flow cytometry was carried out to further confirm the downregulation of the Vimentin, Zeb1 and Snail in Panc-1 and MiaPaCa-2 (Figure 4.18) following 24 h treatment with rfhSP-D. The mean fluorescence for Vimentin, Zeb1 and Snail was approximately 50% less in the rfhSP-D treated cells as compared to the untreated counterparts and a clear shift was seen in the fluorescent intensity between treated and untreated (Figure 4.18).

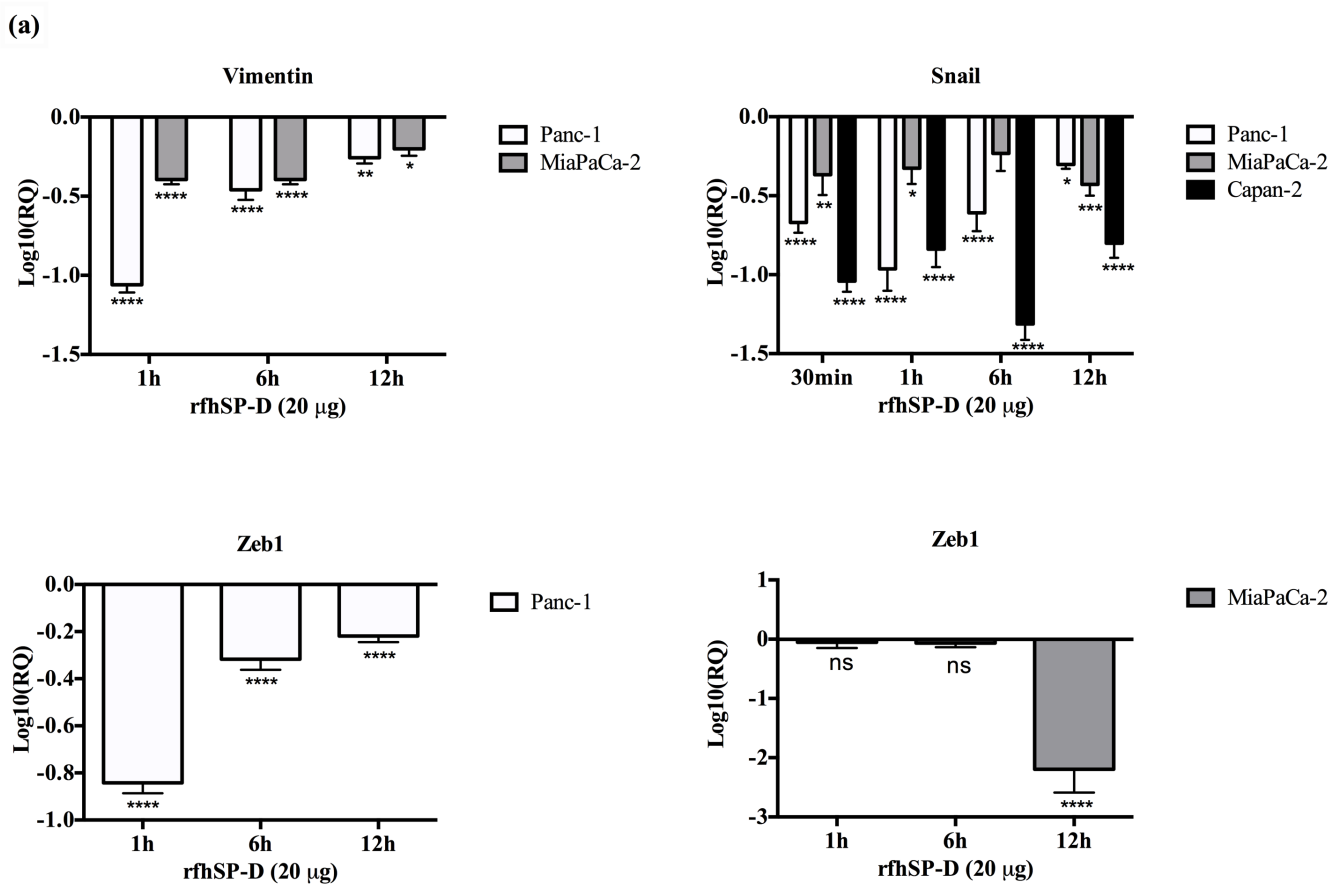

Figure 4.15 rfhSP-D affected the EMT markers (Vimentin, Snail and Zeb1) gene expression. All cell lines were incubated with and without rfhSP-D (20 μg/ml) for various time points and total RNA was extracted to make cDNA. Each qPCR reaction was carried out in triplicate and human 18S RNA, an endogenous control, was used to normalize the gene expressions. The cycle threshold (ct) mean was used to calculate the relative expression to compare treated and untreated. The gene expression of the treated was normalized using the expression of both human 18S rRNA and untreated cells. EMT inducers i.e. Vimentin, Snail, and Zeb1 were significantly downregulated across the cell lines.

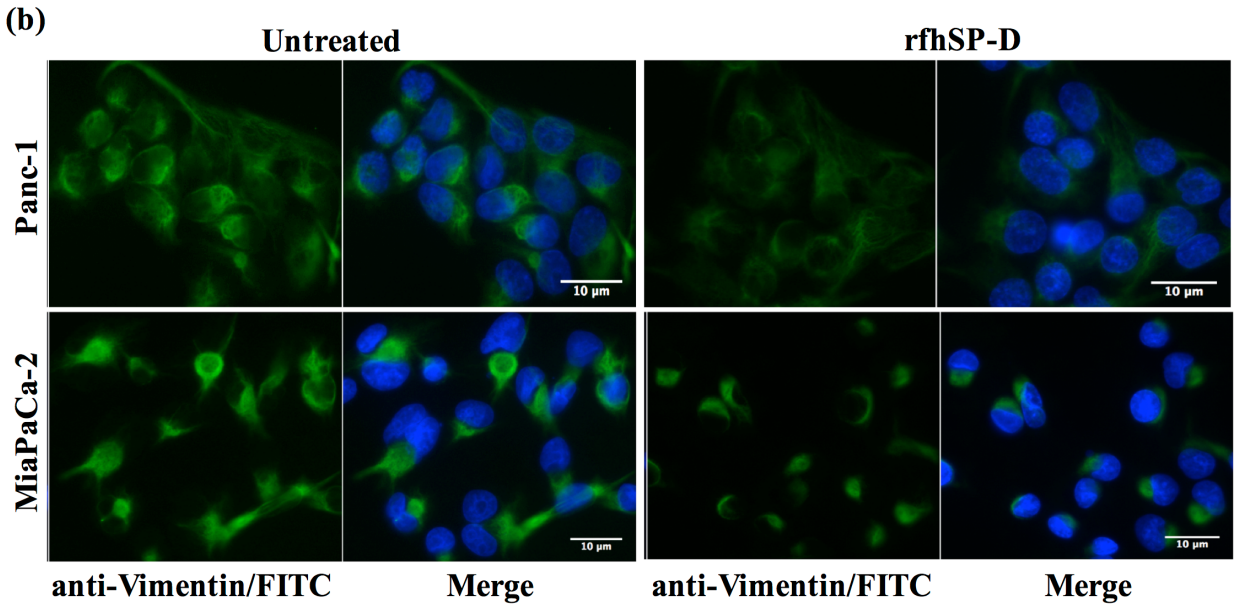

Figure 4.16 Vimentin intracellular staining for all cell lines using $0.5x10^5$ cells/ml incubated with and without rfhSP-D (20 µg/ml) for 24 h followed by probing with rabbit anti-human Vimentin antibody (1:500) and then probed with goat anti-rabbit IgG Alexa Flour 488 (1:500) and Hoechst (1:10,000) for fluorescence analysis showed bright green fluorescence in the cytoplasm of the untreated cells as compared to minor staining in the treated cells.

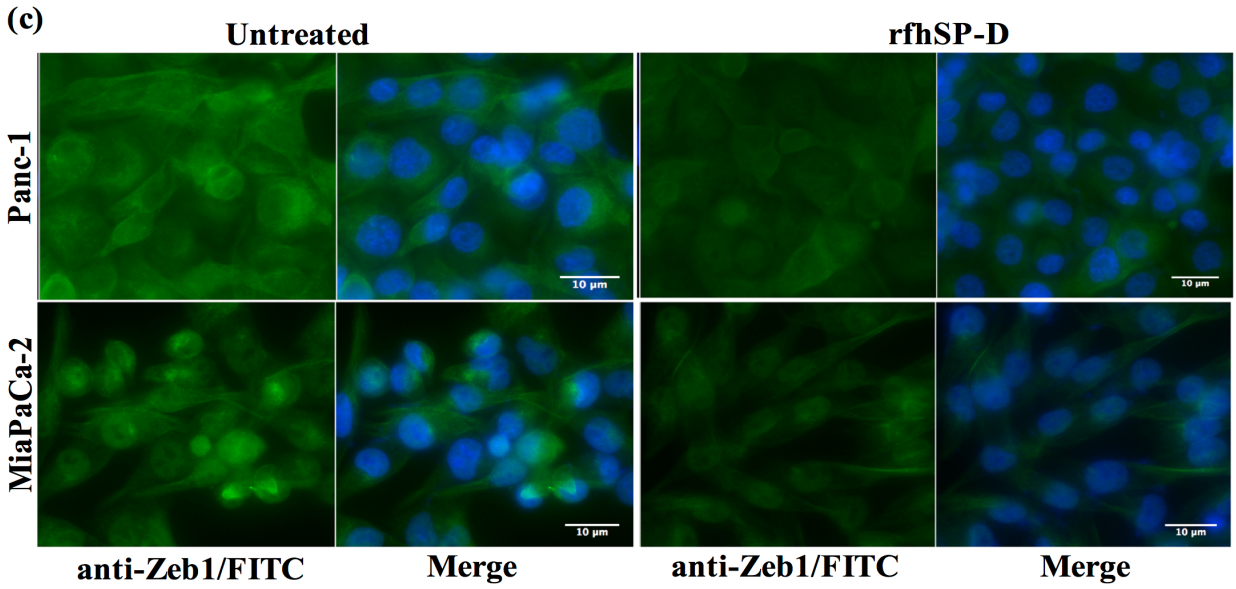

Figure 4.17 Zeb1 intracellular staining for all cell lines using $0.5x10^5$ cells/ml incubated with and without rfhSP-D (20 µg/ml) for 24 h followed by probing with rabbit anti-human Zeb1 antibody (1:500) and then probed with goat anti-rabbit IgG Alexa Flour 488 (1: 500) and Hoechst (1:10,000) for fluorescence analysis showed bright green fluorescence in the cytoplasm of the untreated cells of all cell lines compared to minor staining in the treated cells of Panc-1 and MiaPaCa-2.

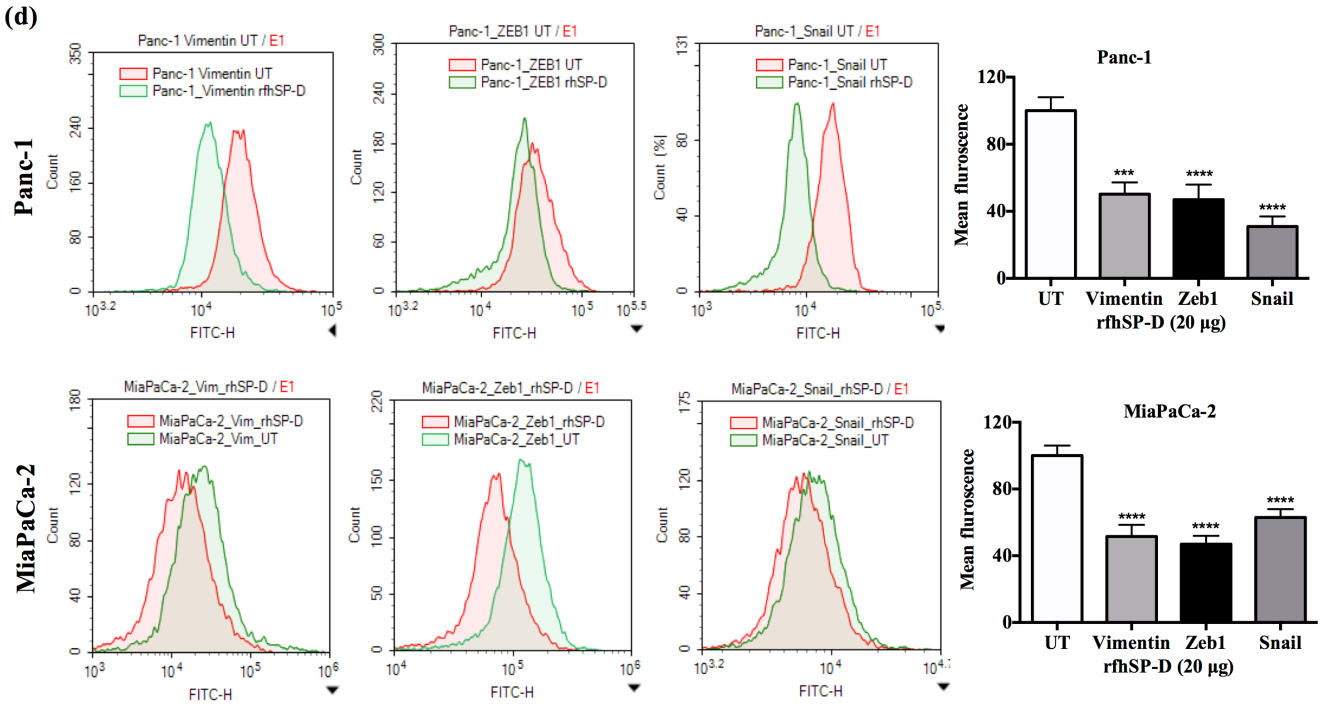

Figure 4.18 The quantitative analysis of mean fluorescence of Vimentin, Zeb1 and Snail of Panc-1 and MiaPaCa-2 cell lines showed a significant reduction in the treated cells compared to untreated. 10,000 cells were acquired via flow cytometer for intracellular staining. A shift of fluorescence intensity suggested that the expression of these proteins was higher in the untreated as compared to treated. The mean of fluorescence intensity was also plotted.

4.3.9 Blocking TGF-β via neutralizing antibody reduces the expression of EMT markers in a similar trend as rfhSP-D

All cell lines were incubated with TGF- β neutralizing antibody (1 µg/ml) for 6 h and the mRNA expression for EMT markers (Vimentin, Snail and Zeb1) was measured by qPCR. Interestingly, blocking TGF- β showed a similar downregulation trend to that seen following the rfhSP-D treatment, which further validated that rfhSP-D treatment causes downregulation of TGF- β, which in turn suppresses EMT regulators (Figure 4.19). The images were taken for Panc-1 cell line to analyze the cell morphological differences following treatment with rfhSP-D, rabbit anti-human TGF-β antibody, or both added together, to compare with untreated at 6 h (Figure 4.20). Fewer branches and cell movement was observed in all the treated cells compared to the untreated, which suggested that suppressed EMT effects become apparent as early as 6 h following the treatment. Interestingly, the effect was even more prominent when rfhSP-D and rabbit anti- human TGF- β were added together (Figure 4.20).

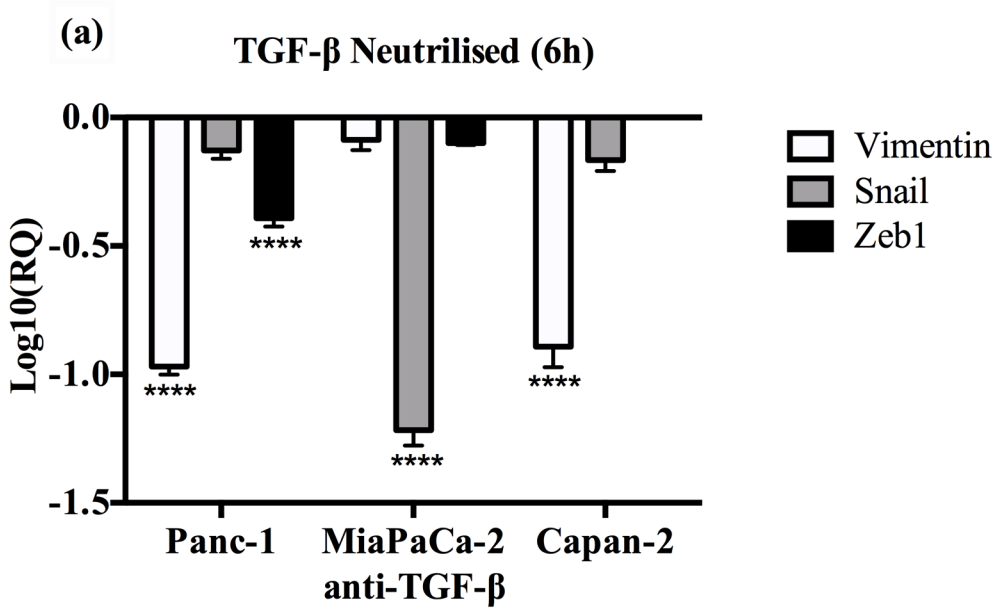

Figure 4.19 TGF- β blocking caused downregulation of EMT markers. All cell lines were incubated with TGF-β neutralizing antibody for 6 h to analyse the gene expression of Vimentin, Snail and Zeb1, which showed that all markers were downregulated in a similar pattern as rfhSP-D treatment. The gene expression of the treated was normalized using the expression of both human 18S rRNA and untreated cells. Significance was obtained using the unpaired one-way ANOVA test (*p<0.05, *p<0.01 and ***p<0.001) (n=3).

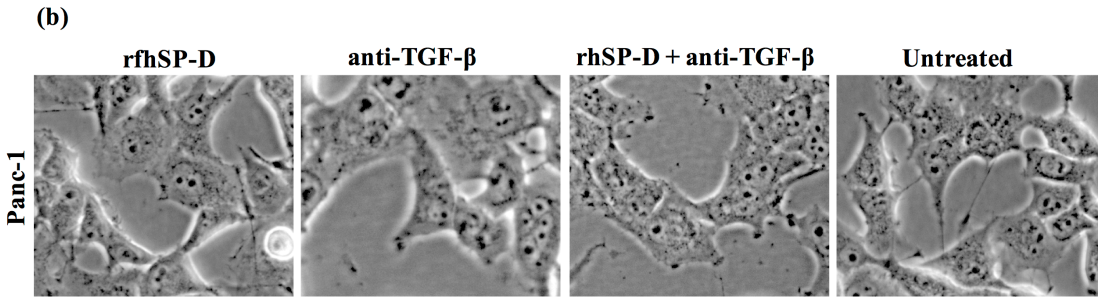

Figure 4.20 TGF- β blocking caused downregulation of EMT markers. Panc-1 cells were incubated with TGF-β neutralizing antibody, rfhSP-D, both rfhSP-D and anti-human TGF-β neutralizing antibody and an untreated control for 6 h and the images were taken to visualize the differences in the EMT morphological changes. rfhSP-D and cells with neutralized TGF- β morphology appeared very similar whereas untreated cells continued to branch out.

4.4 Discussion

EMT induction is characterized by morphological alterations, enhanced motility, reduced cell-cell contact (Ellenrieder et al., 2001), and upregulation of mesenchymal markers such as Vimentin (Maier et al., 2010), Snail (Peinado et al., 2003), and Zeb1 (Wellner et al., 2009). In this study, we report, for the first time, a novel anti-EMT role of rfhSP-D. rfhSP-D which interferes with TGF-β induced EMT by blocking Smad phosphorylation, using two poorly differentiated pancreatic cancer cell lines, Panc-1, and MiaPaCa-2, and a well-differentiated cell line Capan-2 (Deer et al., 2010). The rfhSP-D treatment of these cell lines for up to 24 h prevented the cell morphological alterations associated with EMT, reduced tumor cell invasion in the matrigel, downregulated TGF-β production, downregulated key mesenchymal genes such as Vimentin, Zeb1 and Snail, which suggested that it may have attenuated the TGF-β pathway to suppress EMT. SP-D was found in human pancreatic tissues and all three pancreatic cancer cell lines included in this study secreted very low levels of an aberrant form of SP-D (hyper-glycosylated) (Foreman et al., 2011; Ishii et al., 2012; Silveyra et al., 2012; Tanaka et al., 2009).

Overexpression of TGF-β1 in tumor microenvironment suppresses immune surveillance and facilitates the escape, migration and increased resistance to anti-tumor immune responses (Sun et al., 1994; Beauchamp et al., 1990; Reiss, 1999) by exerting anti-proliferative effects on natural killer (NK) cells and cytotoxic T cells (Kehrl et al., 1986a; 1986b; Rook et al., 1986; Wahl et al., 1989). TGF-β1 has also been shown to upregulate VEGF production, thus increasing the liver metastasis of pancreatic cancer by regulating angiogenesis in a mouse model (Teraoka et al., 2001). It is understood that TGF-β binds to heterotetrameric receptor complex consisting of type I receptors (TβRI/ALK5) and type II receptors (TβRII) to activate downstream Smads, which act as signal transducers from the receptors to the nucleus (Massague and Wotton, 2000; Massague, 2000). TGF-β expression, as analysed by qPCR and western blots of total cell extracts, showed downregulation in Panc-1 and MiaPaCa-2 cell lines, whereas Capan-2 was unaffected since it is unable to produce TGF- β (Subramanian et al., 2004), thus acting as a negative control in this study. In addition, minimal presence of Smad2/3 was detected in the cytoplasm and no translocation to the nucleus was detected in the rfhSP-D treated cells as compared to untreated Panc-1 and MiaPaCa-2 cell lines, which suggested that the downregulation of TGF-β had

prevented the recruitment of Smads, the signal transduction molecules into the nucleus. Previous studies have shown that TGF-β stimulation causes the phosphorylation of Smad2/3, which then accumulate in nucleus to drive transcription of various target genes (Maasague and Wotton, 2000), including key mesenchymal markers such as Vimentin (Nishioka et al., 2010), Snail (Nishioka et al., 2010; Horiguchi et al., 2009), and Zeb1 (Wellner et al., 2009) in pancreatic cancer, which regulate EMT by either direct or indirect effect on epithelial cell adhesion markers such as E-cadherin (Imamichi et al., 2007). The treatment of Panc-1, MiaPaCa-2 and Capan-2 with rfhSP-D resulted in downregulation of Snail and Zeb1, however Vimentin downregulation was only seen in Panc-1 and MiaPaCa-2. Capan-2 has been previously shown not to express Vimentin (Diaferia et al., 2016). This suggests that due to downregulation of TGF-β, phosphorylation of Smads is affected, since no Smad2/3 was seen either in the cytoplasm or nucleus, which then further causes the downregulation of EMT inducing genes resulting in a static state and loss of key EMT- associated morphological features. Moreover, when TGF-β was blocked for 6 h by a neutralizing antibody, gene expressions of Vimentin, Snail and Zeb1 were downregulated similar to rfhSP-D treatment, re-affirming that rfhSP-D suppressed EMT by downregulation of TGF-β pathway. These results thus explain the significantly reduced invasion of rfhSP-D treated Panc-1 and MiaPaCa-2 in the matrigel matrix pre-coated with extracellular matrix proteins that promotes invasion, whereas a non-invasive Capan-2 remained unaffected.

It has been previously shown that stable, short hairpin RNA (shRNA)-mediated Zeb1-knockdown in Panc-1 and MiaPaCa-2 with overexpressed Zeb1 showed a reduced sphere formation, a hallmark of self-renewal and differentiation (Wellner et al., 2009). In addition, Zeb1 knockdown in orthotopic mouse xenograft models, significantly affected the tumor growth and EMT by switching the expression of vimentin and E-cadherin (Wellner et al., 2009). Similarly, downregulation of Snail in Panc-1 cells has been shown to increase sensitivity to chemotherapeutics or radiation (Zhang et al., 2010). Therefore, downregulation of mesenchymal markers can be crucial to target the EMT driven by TGF-β signalling pathway, which is emerging as a critical event in the progression of pancreatic cancer. In view of this study, rfhSP-D offers potentially a novel therapeutic approach to restore the polarized epithelial phenotype in pancreatic cancer. Interestingly, rfhSP-D was effective in the invasive cancer cells lines i.e. Panc-1 and MiaPaCa-2, but less so in the non-invasive

Capan-2 cell line, which indicates that it selectively targets the mesenchymal-differentiated cells. This is consistent with previous studies where rfhSP-D did not affect the eosinophils derived from healthy individual whereas it induced apoptosis in the sensitized eosinophils from allergic patients (Mahajan et al., 2008; Mahajan et al., 2013). Targeting EMT pathway using rfhSP-D could not only lead to decreased invasiveness but also promote drug sensitivity. As mentioned earlier, Zeb1 knockout Panc-1 clones were more susceptible to chemotherapy and their proliferation was significantly reduced (Wellner et al., 2009). Silencing of Zeb1 in Panc-1 and MiaPaCa-2 reversed the E-cadherin expression and significant increase in apoptotic cell death was measured following gemcitabine, 5-FU and cisplatin treatment (Arumugam et al., 2009). Therefore, it will be interesting to explore the EMT suppressor role of rfhSP-D in combination with conventional chemotherapy as a therapeutic strategy.

Chapter 5

Induction of apoptosis in pancreatic cancer cell lines by rfhSP-D

5.1 Abstract

Human Surfactant Protein (SP-D) is a potent innate immune molecule, known as a key molecule in recognizing and clearing altered and non-self targets. Previous studies have shown that a recombinant fragment of human SP-D (rfhSP-D) induced apoptosis via a p53 mediated apoptosis pathway in an eosinophilic leukemic cell line, AML14.3D10. However, in this study, we report the ability of rfhSP-D to induce apoptosis via TNF-α/Fas-mediated apoptosis pathway regardless of the p53 status in human pancreatic adenocarcinoma using Panc-1 ($p53^{mt}$), MiaPaCa-2 ($p53^{mt}$), and Capan-2 ($p53^{wt}$) cell lines. Treatment of these cell lines with rfhSP-D for 24 h caused growth arrest in G1 cell cycle phase and triggered transcriptional upregulation of pro-apoptotic factors such as TNF-α and NF-κB. Translocation of NF-κB from the cytoplasm into the nucleus following treatment with rfhSP-D compared to the untreated cells was seen via fluorescence microscopy. The rfhSP-D treatment caused upregulation of a pro-apoptotic marker Fas, as analyzed by qPCR and western blot, which then triggered caspase cascade, as evident from cleavage of caspase 8 and 3 analyzed by western blot at 48 h, and subsequent apoptosis of the cells. The cell number following the rfhSP-D treatment was reduced in ~70% of Panc-1 and MiaPaCa-2 cells and ~43% in Capan-2. All these cell lines secrete an aberrant form of SP-D in very low quantities, however, rfhSP-D (20 μg/ml) treatment induced apoptosis in all pancreatic cancer cell lines at 48 h.

5.2 Introduction

Human Surfactant Protein D (SP-D), a member of soluble C-type lectin family, plays a vital role in linking the innate and adaptive immunity to protect against infection, allergy and inflammation (Kishore et al., 2006). Although its homeostatic role in lungs has been widely studied, its specific functions at extrapulmonary tissues such as kidney, human trachea, brain, testis, heart, prostate, kidneys, and pancreas are poorly understood (Madsen et al., 2000; Kishore et al., 2006; Nayak et al., 2012). SP-D deficiency is associated with significant clinical outcome in a number of diseases (Schaub et al., 2004; Wert et al., 2000; Ikegami et al., 2005). SP-D gene knockout mice showed chronic inflammation and fibrosis due to accumulation of surfactant phospholipids in the lungs, monocyte infiltration, and activation of pro-inflammatory alveolar macrophages (Wert et al., 2000; Ikegami et al., 2005). SP-D deficiency in children makes them more susceptible to frequent pneumonia as compared to SP-D sufficient children (Griese et al., 2008). SFTPD polymorphisms increase the susceptibility to chronic and infectious lung diseases (Foreman et al., 2011), pneumococcal lung disease (Lingappa et al., 2011), emphysema in mice (Ishii et al., 2012), tuberculosis (Silveyra et al., 2012), Crohn's disease and ulcerative colitis (Tanaka et al., 2009).

SP-D has been shown to be a potent innate immune molecule at pulmonary as well as extrapulmonary mucosal surfaces by virtue of its ability to control inflammatory response and helper T cell polarization (Nayak et al., 2012). The first clue came via a murine model of allergic hypersensitivity, when therapeutic treatment with a recombinant fragment of human SP-D (rfhSP-D) lowered peripheral and pulmonary eosinophilia, in addition to specific IgE levels and Th2 cytokines in the spleen (Madan et al., 2001; Singh et al., 2003). It turned out that rfhSP-D was able to selectively induce apoptosis in sensitized eosinophils derived from allergic patients (Mahajan et al., 2008). The molecular mechanisms involved in apoptosis induction were further delineated by proteomics analysis using an eosinophilic leukemia cell line AML14.3D10, which revealed involvement of the p53 pathway in SP-D mediated apoptosis induction (Mahajan et al., 2013; Mahajan et al., 2014). Subsequently, involvement of SP-D in the control of cancer has recently been examined. Human lung adenocarcinoma cells (A549 cell line), when exogenously treated with SP-D, showed suppressed epidermal growth factor (EGF) signalling by reducing the EGF

binding to EGFR, which subsequently reduced the cell proliferation, invasion and migration of cancer cells (Hasegawa et al., 2015).

This chapter examines a possible pro-apoptotic role of SP-D in pancreatic cancer. Pancreatic cancer is the fourth leading cause of cancer-related mortality in the western world (Malvezzi et al., 2015; Siegal et al., 2016) and its five-year survival rate is ~5% (Wolfgang et al., 2013). The poor prognosis has been attributed to the silent nature of the tumor in early stages, aggressive phenotype, surgical complications, and lack of targeted efficacious therapies (Ansari et al., 2016). In this study, we show that a rfhSP-D composed of homotrimeric neck and carbohydrate recognition domains (CRDs), induces cell growth arrest in G1 phase and subsequently apoptosis in human pancreatic adenocarcinoma using Panc-1, MiaPaCa-2 and Capan-2 cell lines. The apoptosis induction appears to involve TNF-α, NF-κB and Fas axis, revealing a p53 independent route of apoptosis induction in the tumour cells by SP-D.

5.3 Results

5.3.1 rfhSP-D induces cell cycle arrest in G1 phase in Panc-1 and MiaPaCa-2

Panc-1, MiaPaCa-2, Capan-2 cell lines were individually treated with rfhSP-D (20 μg/ml) for 24 h to assess if the cytostatic effect seen in Chapter 4 could be due to growth arrest following rfhSP-D treatment. DNA binding dye, PI, was used to analyse the cell cycle for both treated and untreated cells via DNA quantitation. rfhSP-D induced inhibition of DNA synthesis in treated Panc-1 (68%) and MiaPaCa-2 (50%) in comparison to untreated Panc-1 (3%) and MiaPaCa-2 (2%) cells, respectively, as the cells were arrested in G1 phase (Figure 5.1). DNA synthesis was unaffected in the untreated cells for both cell lines since Panc-1 (43%) and MiaPaCa-2 (31%) were seen in S phase and Panc-1 (32%) and MiaPaCa-2 (33%) in the G2 phase of cell cycle. The growth arrest was, however, not seen in Capan-2 cell line following the rfhSP-D treatment. Growth arrest at 24 h following rfhSP-D treatment prompted the determination of cell fate at a later time point; therefore, all cell lines were analysed for likely apoptosis at 48 h.

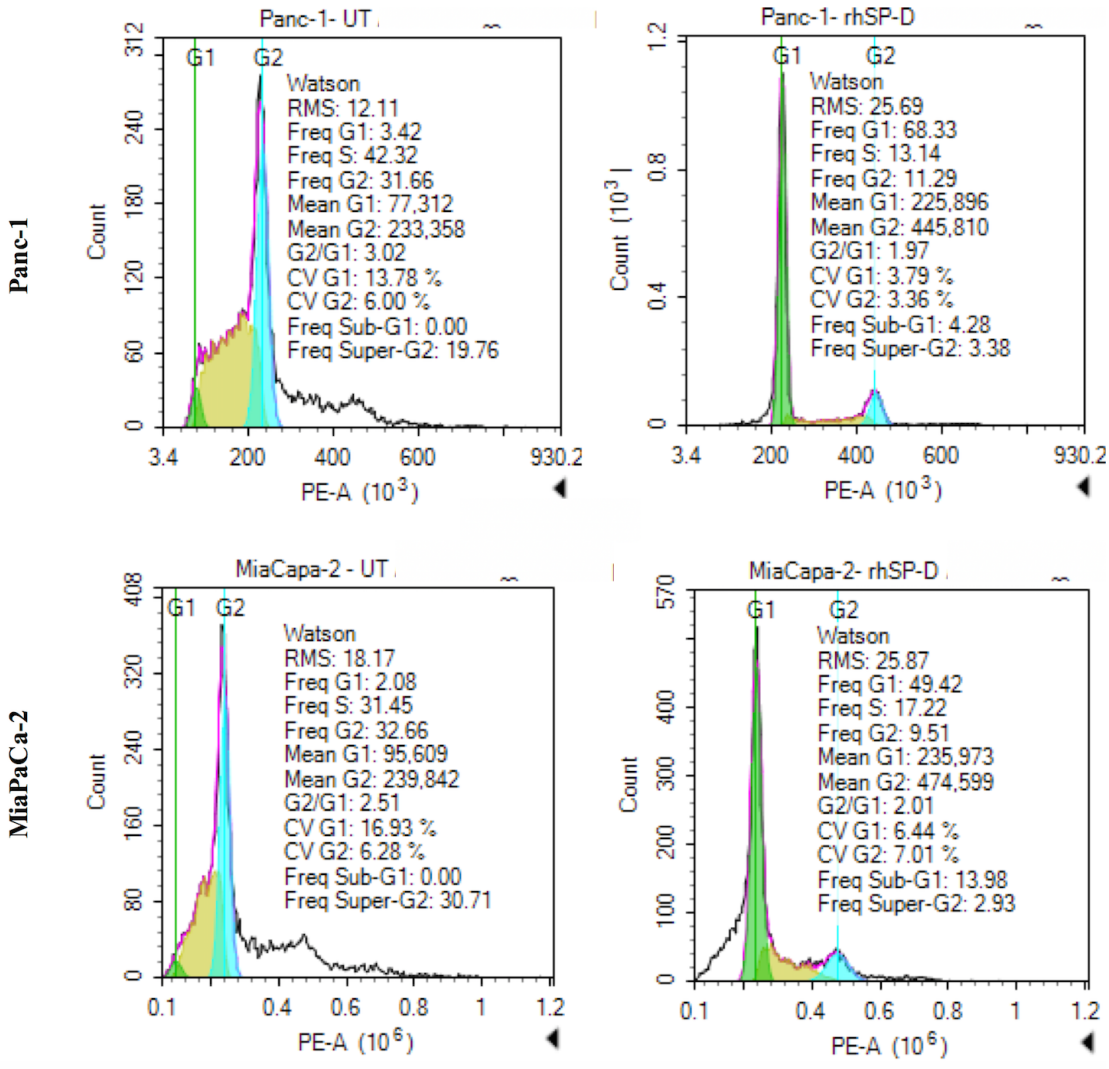

Figure 5.1 Cell cycle analysis following 24 h treatment of pancreatic cancer cell lines with rfhSP-D (20 µg/ml). Propidium iodide was used to stain the DNA in both rfhSP-D treated and untreated cells. Propidium iodide histograms were plotted using set markers within the analysis program of Novocyte Flow cytometer. The rfhSP-D treated pancreatic cancer cells show arrest in G1 phase in treated Panc-1 (68%) and MiaPaCa-2 (50%) in comparison to untreated Panc-1 (3%) and MiaPaCa-2 (2%) cells suggesting that untreated cells continued into the next cell cycle phases.

5.3.2 rfhSP-D induces apoptosis in pancreatic cancer cells by 48 h

The qualitative apoptosis analysis of Panc-1, MiaPaCa-2 and Capan-2 treated with rfhSP-D (20 μg/ml) for 48 h using fluorescence microscopy showed that the cell membrane was no longer intact and the propidium iodide bound to DNA in the treated cells compared to untreated cells, where no fluorescence was detected, indicating that cells were undergoing apoptosis at 48 h (Figure 5.2).

The flow cytometry analysis to quantify apoptosis showed significant reduction in the viable cell percentage of Panc-1 and MiaPaCa-2. The rfhSP-D induced apoptosis in ~70% of Panc-1 and MiaPaCa-2 cells and ~43% in Capan-2 at 48 h, out of which, ~25% Panc-1 cells, ~60% MiaPaCa-2 and ~28% Capan-2 were both FITC and propidium iodide positive, suggesting Annexin V/FITC binding to phosphatidylserine (PS), a cell membrane phospholipid, which is externalized during early apoptotic stage and the passage of PI, a DNA stain, through the porous cell membrane into the nucleus in order to intercalate the DNA. A significant percentage of Panc-1 cells (~43%) and not so significant for MiaPaCa-2 and Capan-2 (~12%) were positive for propidium iodide alone, suggesting that these cells were either dead or in late apoptotic stage. The percentage of viable cells, i.e. unstained, in the untreated sample was significantly higher (80%) as compared to treated (Figure 5.3). Apoptosis was further confirmed by analysing the activation of caspase to determine the pathway that may have been involved.

(a)

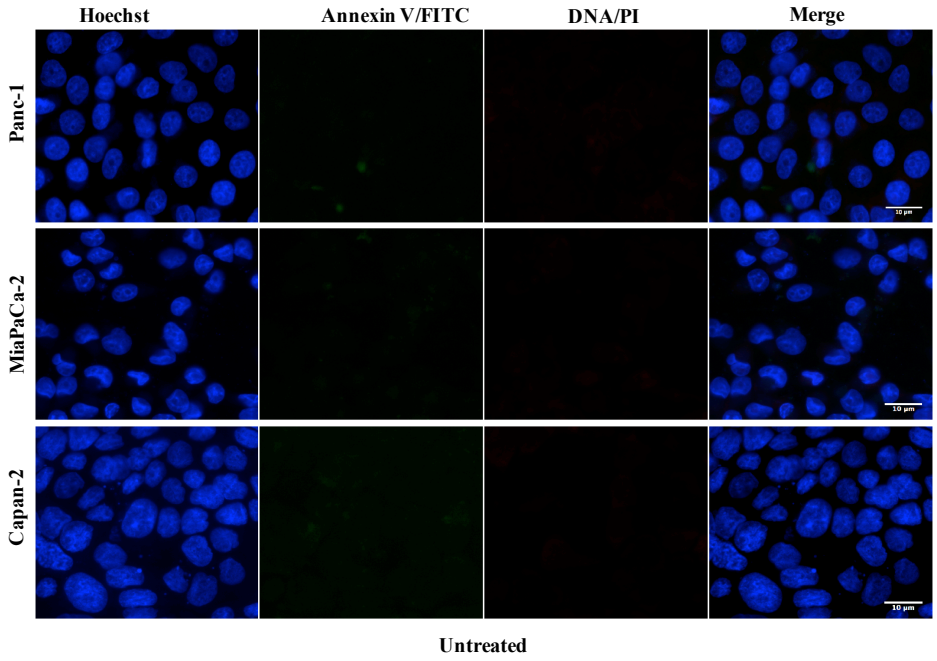

(b)

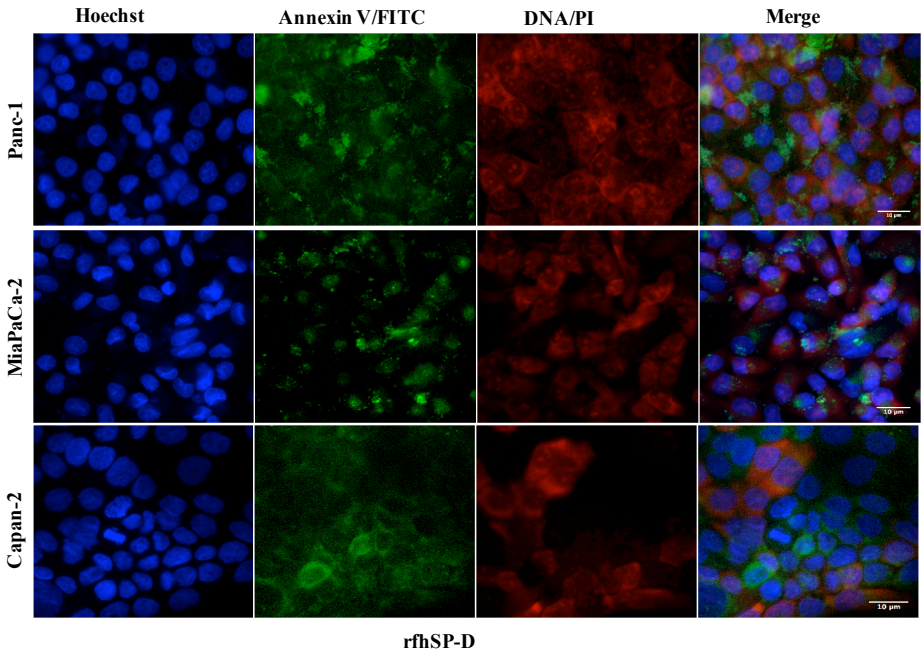

Figure 5.2 Fluorescence Microscopy analysis of apoptosis in pancreatic cancer cells following treatment with rfhSP-D (20 µg/ml) for 48h. The cell membrane was positively stained for annexin V and the DNA staining is visible in the treated cells indicating that the cells underwent apoptosis turning the membrane inside out, thus making PS available for annexin V binding and due to the porous membrane, propidium iodide was taken in which stained the DNA of apoptotic cells (Panel b). No such staining was seen in the untreated cells (Panel a). The nucleus was stained with Hoechst for both treated and untreated.

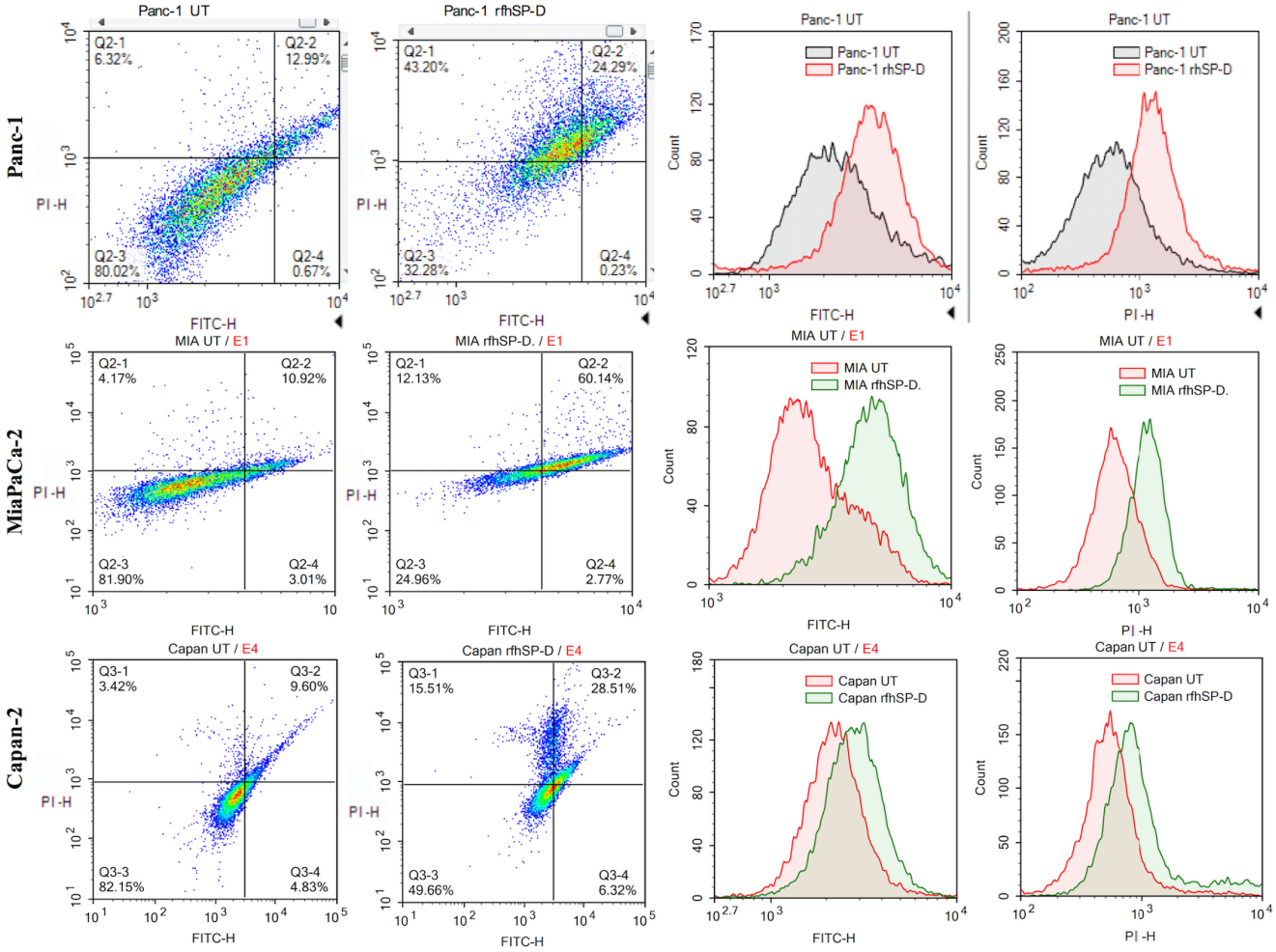

Figure 5.3 Flow Cytometry analysis of apoptosis in pancreatic cancer cell lines, Panc-1, MiaPaCa-2 and Capan-2 following treatment with rfhSP-D (20 µg/ml) for 48 h. 10,000 cells were acquired, which showed that approximately 70% of Panc-1 cells and MiaPaCa-2 and 43% Capan-2 cells underwent apoptosis as compared to untreated cells. A shift in the fluorescence intensity of both FITC and propidium iodide was also seen between treated and untreated cells.

5.3.3 rfhSP-D activates cleavage of caspase 8 and 3

Western blot analysis of caspase 3, 8 and 9 revealed that caspase 8 and 3 were cleaved in all the cell lines following treatment with rfhSP-D (20 µg/ml) for 48 h (Figure 5.4). The cleavage of caspase 3, however, was not seen in the untreated cells and faint bands appeared for Caspase 8 in the untreated cells, which further confirmed that cell death occurred via apoptosis. Interestingly, although Capan-2 cell line appeared unaffected in terms of cell cycle arrest at 24 h; yet, the cleaved bands for caspase 8 and 3 were seen in Capan-2 treated cells too, which suggested that rfhSP-D can affect the cancer cells via multiple pathways. Caspase 9 was tested as a marker for intrinsic apoptosis pathway; however, no difference was noted between treated and untreated

cells. Therefore, gene expressions were assessed for pro-apoptotic genes such as Bax, an intrinsic pathway marker, and Fas, an extrinsic pathway marker, to further determine the apoptotic pathway.

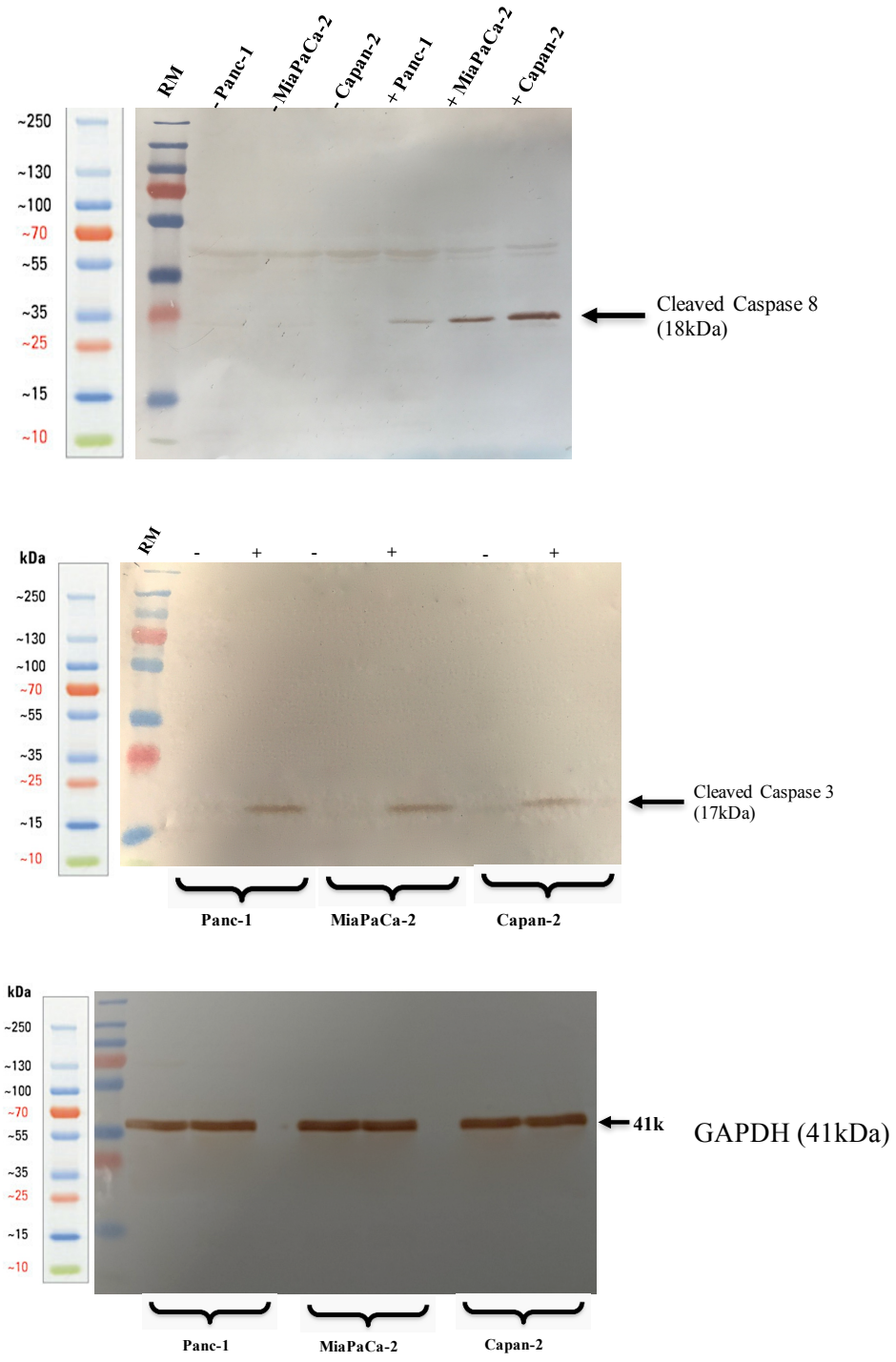

Figure 5.4 Cleavage of caspase 8 and 3 in pancreatic cancer cell lines following rfhSP-D (20 µg/ml) treatment at 48 h. The cleaved caspase 8 & 3 was detected only in the rfhSP-D treated samples (+) of all cell lines, whereas no bands appeared in the untreated cell (-) samples. Anti-GAPDH was used as a loading control. GAPDH was used a loading control. (RM: Rainbow Marker)

5.3.4 rfhSP-D upregulates the expression of pro-apoptotic marker, Fas

Human pancreatic cancer cells often escape apoptosis by downregulating apoptosis stimulators such as FasL/FasR (von Bernstorff et al., 1999), or pro-apoptotic proteins such as Bax (Friess et al., 1998). These pro-apoptotic genes, Bax and Fas, for time-points ranging from 2 h to 24 h in all the cell lines, were analysed in order to explore the apoptotic pathway. Bax was unaffected following the treatment with rfhSP-D (20 μg/ml) in all cell lines at all time-points, which, in addition to unaffected caspase 9, suggested that intrinsic pathway may not have been involved in causing the cell death. Fas expression was unaffected at earlier time-points up to 6 h (data not shown); however, it was upregulated at 12 h & 24 h in Panc-1 (log_{10} ~0.5), MiaPaCa-2 (log_{10} ~1), and Capan-2 (log_{10} ~1) cell lines, which indicated that apoptosis induction by rfhSP-D is likely to take place via the extrinsic pathway (Figure 5.5). Western blot analysis also showed upregulation of Fas at protein level in the treated cells as compared to untreated cells (Figure 5.6). Since TNF-α and NF-κB are crucial factors in the apoptotic pathway and they can regulate Fas expression (Fulda and Debatin, 2006), the effect of rfhSP-D on the gene expression of TNF-α and NF-κB as well as translocation of NF-κB from the cytoplasm to nucleus was investigated.

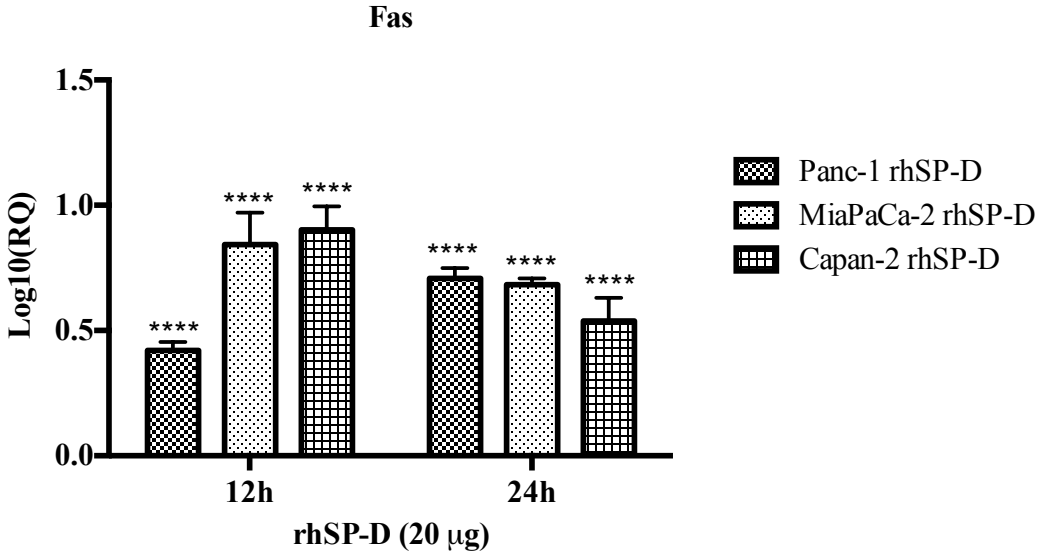

Figure 5.5 Relative quantification comparisons of Fas mRNA expression in Panc-1, MiaPaCa-2 and Capan-2 cell lines treated with rfhSP-D (20 μg/ml) for 12 and 24 h. Fas expression was upregulated in the treated samples at 12 h and 24 h for all cells compared to untreated. The gene expression of the treated was normalized using the expression of both human 18S rRNA and untreated cells. Significance was determined using the unpaired two-way ANOVA test (*$p<0.05$, *$p<0.01$ and ***$p<0.001$) (n=3).

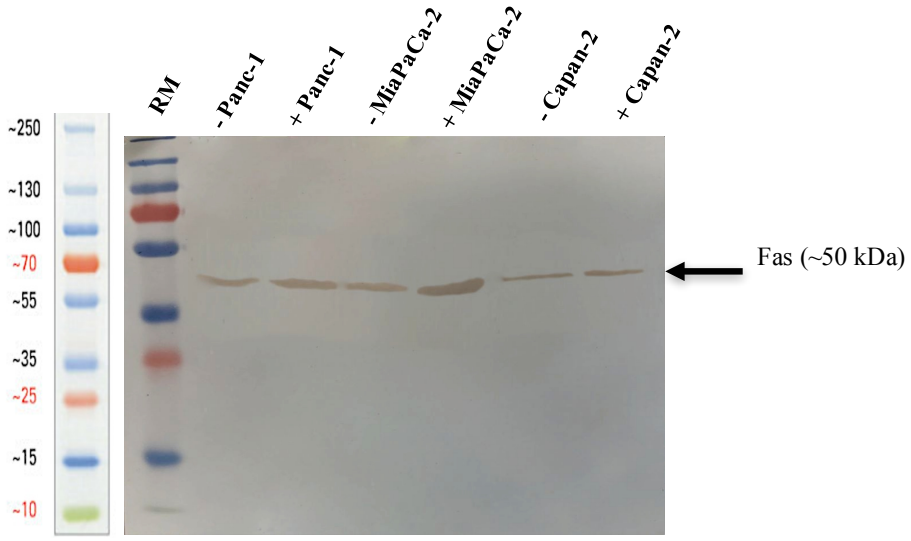

Figure 5.6 Fas expression via Western Blot analysis in Panc-1, MiaPaCa-2 and Capan-2 cell lines treated with rfhSP-D for 24 h. Fas expression was determined using rabbit anti-human Fas (1:1000) at 4°C overnight, followed by incubation with secondary anti-rabbit IgG HRP-conjugate (1:1000) for 1 h at room temperature. The membrane was washed with PBST (PBS + 0.05% Tween 20) three times, 10 min each between each step. The bands were developed using DAB substrate kit. Fas expression was upregulated in the treated samples at 24 h for all cells as compared to untreated.

5.3.5 rfhSP-D upregulated the expression of TNF-α and causes nuclear translocation of NF-κB

Following treatment with rfhSP-D (20 µg/ml), the analysis of TNF-α mRNA expression levels showed a significant up-regulation in Panc-1 ($\log_{10}$ ~0.5), MiaPaCa-2 ($\log_{10}$ ~1), and Capan-2 ($\log_{10}$ ~1) at 12 and 24 h; however, no difference was observed at earlier time-points (Figure 5.7). Similar transcriptional upregulation was noted for NF-κB for Panc-1 ($\log_{10}$ ~0.4), MiaPaCa-2 ($\log_{10}$ ~0.8), and Capan-2 ($\log_{10}$ ~0.6) at 12 and 24 h (Figure 5.7). Fluorescence microscopy of Panc-1, MiaPaCa-2 and Capan-2 cell lines showed that NF-κB was translocated to the nucleus at 24 h, which was not seen in the untreated cells (Figure 5.8). This further confirmed that NF-κB could play a key role in deciding the apoptotic fate of the cancer cells following the rfhSP-D treatment.

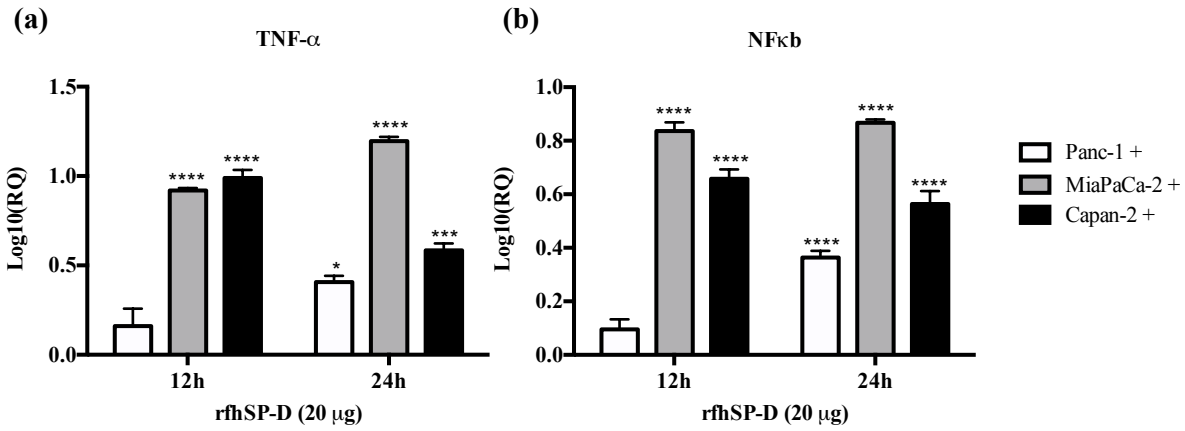

Figure 5.7 Relative quantification comparisons of TNF-α and NF-κB mRNA expression in Panc-1, MiaPaCa-2 and Capan-2 cell lines treated with rfhSP-D (20 μg/ml) for 12 and 24 h. The transcriptional expressions of both TNF-α and NF-κB were upregulated in the treated samples at 12 h and 24 h for all cells as compared to untreated. The gene expression of the treated was normalized using the expression of both human 18S rRNA and untreated cells. Significance was determined using the unpaired two-way ANOVA test (*p<0.05, *p<0.01 and ***p<0.001) (n=3).

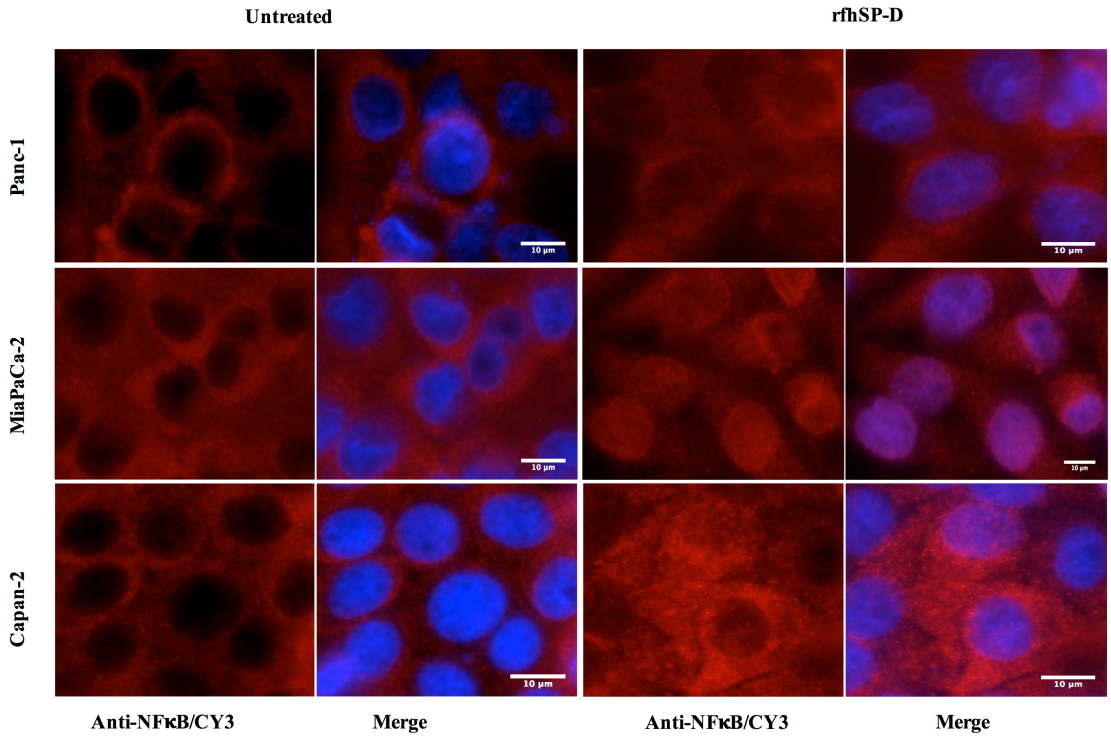

Figure 5.8 Fluorescence microscopy analysis to determine the translocation of NF-κB into nucleus following rfhSP-D treatment. After 24 h treatment, both treated and untreated cells were fixed and permeabilised using 100% cold methanol. The cells were probed with rabbit anti-human NF-κB (1:500) for 1 h followed by 1 h incubation with anti-rabbit/CY3 (1:1000) and Hoechst (1:10,000). The cells stained positively for NF-κB in the nucleus of treated cells as compared to untreated in all cell lines at 24 h.

5.3.6 rfhSP-D down-regulates the survival pathway, mTOR

The mTOR is often deregulated in pancreatic cancer (Semba et al., 2003) and its activation is associated with poor prognosis (Kennedy et al., 2011). Upon treatment with rfhSP-D (20 μg/ml), mRNA expression of mTOR was downregulated in Panc-1 and MiaPaCa-2 cell line at 12 h, however, no difference was seen in Capan-2 (Figure 5.9). In addition, fluorescence analysis revealed that in comparison to the untreated cells, a significant decrease in the cytoplasmic levels and an increased accumulation of mTOR in the nucleus was evident (Figure 5.10), where it has been shown to be present in its inactive form in previous studies (Betz et al., 2013).

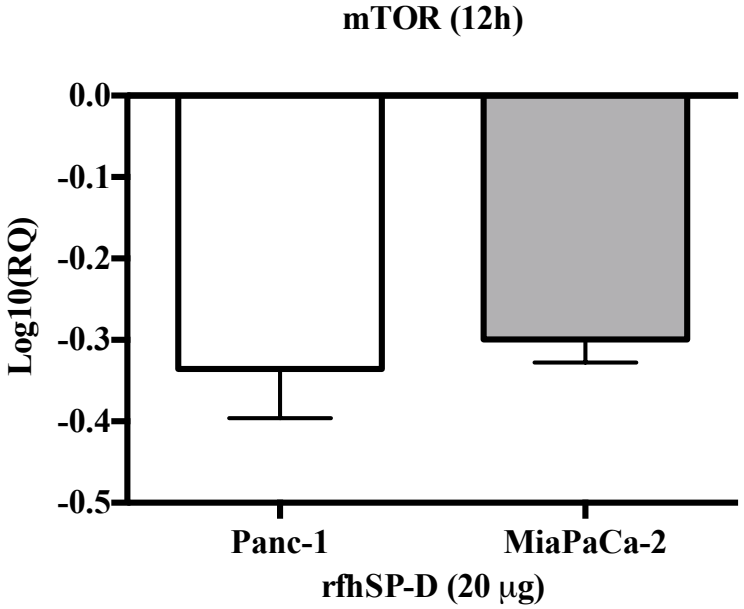

Figure 5.9 Relative quantification of mTOR expression in Panc-1 and MiaPaCa-2 cell lines treated with rfhSP-D (20 μg/ml) for 24 h. rfhSP-D treatment of Panc-1 and MiaPaCa-2 cells downregulated the mRNA expression of mTOR. The gene expression of the treated was normalized using the expression of both human 18S rRNA and untreated cells. Significance was determined using the unpaired two-way ANOVA test (*$p<0.05$, *$p<0.01$ and ***$p<0.001$) (n=3).

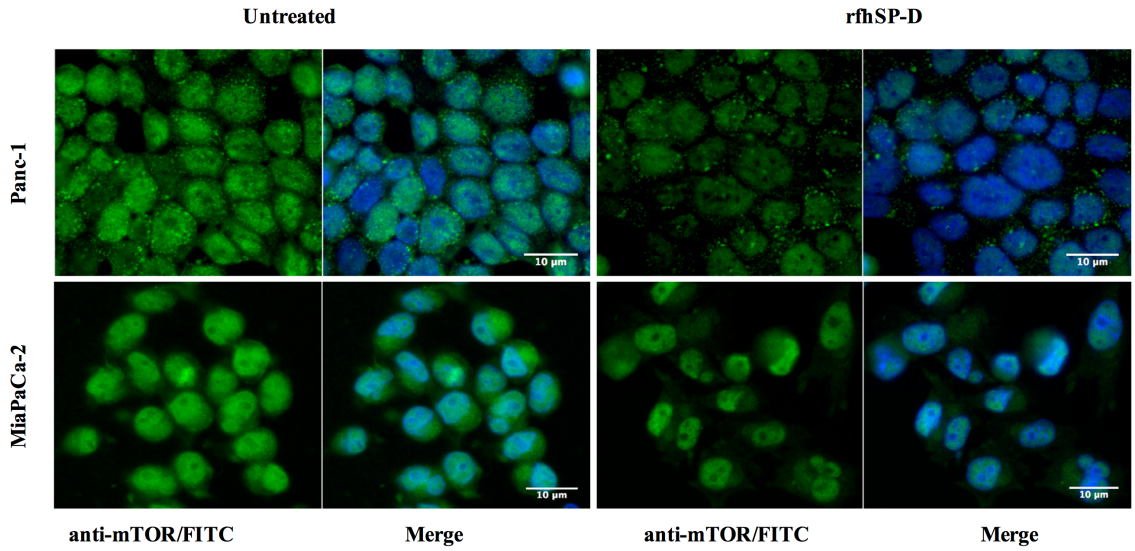

Figure 5.10 Fluorescence microscopy analysis of mTOR expression following rfhSP-D (20 µg/ml) treatment. After 15 h treatment, both treated and untreated cells were fixed and permeablised using 100% cold methanol. The cells were probed with rabbit anti-human mTOR (1:500) for 1 h followed by goat anti-rabbit Alexa 488 (1:1000) and Hoechst (1:10,000). The reduced cytoplasmic levels of mTOR were seen following the treatment compared to the untreated. Nuclear accumulation was clearly visible in the treated cells.

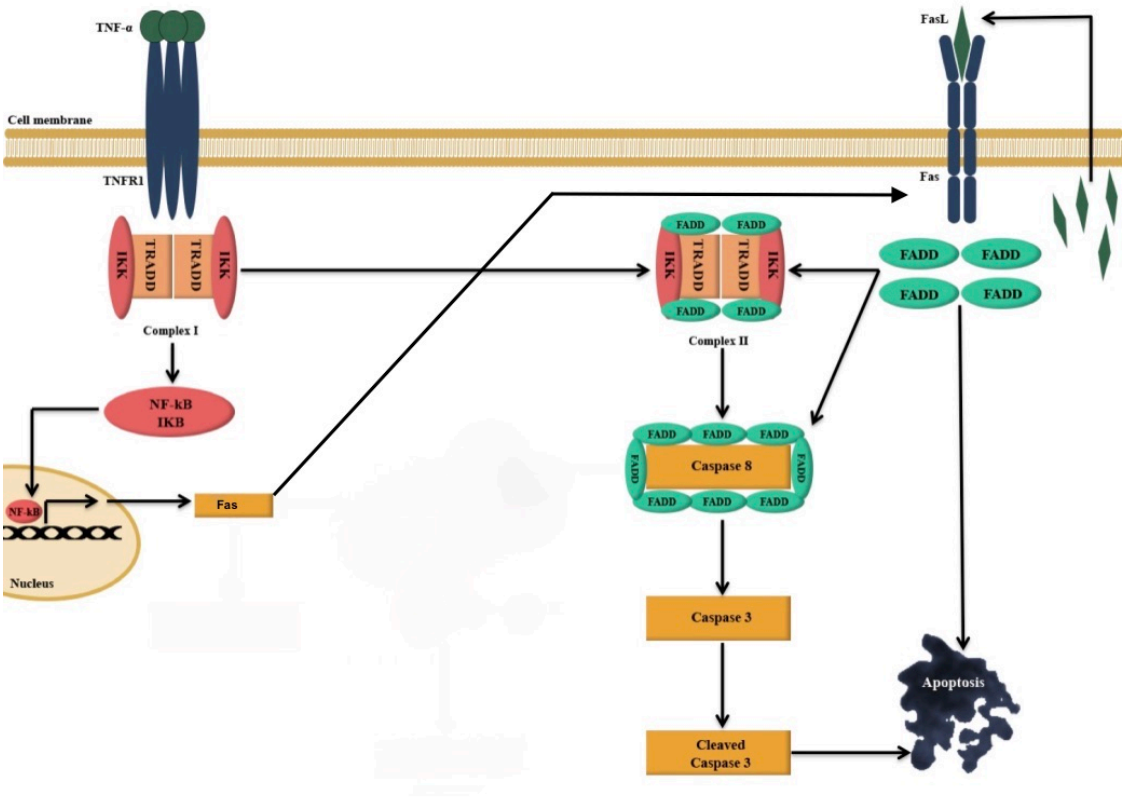

Figure 5.11 Illustration of the potential apoptotic pathway following the exogenous treatment of pancreatic cancer cells with rfhSP-D. TNF-α and Fas were upregulated. TNF-α binds to TNF type I receptor (TNFR1), which is internalized and forms a complex with TNFR1-associated DEATH domain (TRADD) (complex I), stimulating the upregulation of NF-κB. Then, a complex II is formed upon binding of complex I to Fas-Associated protein with Death Domain (FADD), which is formed when Fas is activated. NF-κB upregulation promotes Fas upregulation as it acts as a transcription factor for Fas Subsequently, Complex II activates downstream caspase cascade, which causes the cleavage of caspase 8 followed by effector caspase 3 cleavage, which brings about apoptosis. (Figure 3.17 was taken from Kaur et al, 2016 with minor modifications).

1.4 Discussion

Human SP-D is known for its important role as a first line of defense in innate immunity against invading pathogens. (Murphy, 2012; Lu et al., 1997). SP-D is a pattern recognizing soluble factor that can act as a potent opsonin for viruses, bacteria and fungi, and brings about clearance mechanisms via aggregation/agglutination, enhanced phagocytosis, production of superoxide radicals, direct microbicidal effect, and macrophage activation (Kishore et al., 2005). In most instances, SP-D binds to carbohydrate or charge patterns on the pathogen surface via its CRD region, whilst the collagen region binds to its putative receptor (calreticulin/CD91 complex being one of them) on the surface of macrophages and brings about effector functions

(Gardai et al., 2005). SP-D has also been shown to bind glycoprotein allergens derived from house dust mite, *Aspergillus fumigatus* and grass pollen allergen and interfere with specific IgE-allergen interaction and consequent histamine release from sensitized basophils (Kishore et al., 2002; Singh et al., 2017). When exogenous rfhSP-D was administered therapeutically in a murine model of pulmonary hypersensitivity induced by allergen/antigens of an opportunistic fungal pathogen, *Aspergillus fumigatus*, it lowered specific IgG and IgE levels, suppressed peripheral and pulmonary eosinophilia, and polarised Th2 to Th1 immune response in the spleen (Madan et al., 2001). These studies highlighted SP-D as a link between innate and adaptive immunity and as a modulator of inflammation. These initial studies were followed by observations that eosinophils derived from sensitized individuals were susceptible to apoptosis induction by rfhSP-D in vitro although rfhSP-D bound eosinophils derived from healthy, non-sensitised individuals equally well (Mahajan et al., 2008). Using an eosinophilic cell line, AML14.3D10 (a model cell line for leukemia), it was established, via proteomics analysis, that apoptosis induction by rfhSP-D involved upregulation of p53 (Mahajan et al., 2013; Mahajan et al., 2014). Another crucial study by Pandit et al., (2016) revealed that rfhSP-D was able to induce apoptosis in activated human PBMCs, but not in resting, non-activated PBMCs. These studies, for the first time, raised the possibility that SP-D can have a function of immune surveillance against activated self and perhaps altered self.

In this study, it was found that a recombinant form of human surfactant protein D (rfhSP-D) induces apoptosis in a range of pancreatic cancer cell lines. rfhSP-D induced apoptosis occurs regardless of p53 status using two p53 mutated, aggressive cell lines, Panc-1 (derived from head of the pancreas), MiaPaCa-2 (derived from the body and tail of the pancreas), and a p53 wild type, non-aggressive cell line, Capan-2 (derived from head of the pancreas) (Deer et al., 2010). Following the treatment with rfhSP-D, Panc-1 and MiaPaCa-2 cells were arrested in G1 phase at 24 h. In addition, upregulation of Fas, an apoptosis stimulator, and pro-apoptotic TNF-α (and associated transcription factor, NF-κB) at 24 h was consistent with the cleavage of caspase 8 and 3 at 48 h. These findings indicated that cell death is likely to occur via TNF-α/Fas-mediated apoptosis pathway (Kaur et al., 2016; Liu et al., 2012; Ashkenazi et al., 1998). The cell viability after 48 h of rfhSP-D treatment was reduced in the order of Panc-1 > MiaPaCa-2 > Capan-2, which coincided with the

approximate growth arrested percentage of Panc-1 and MiaPaCa-2 at 24 h. Although Capan-2 cells were not arrested in the cell cycle, yet they underwent apoptosis at 48 h, which may be attributed to their increased sensitivity to Fas-mediated apoptosis as compared to other two cell lines (Bernstorff et al., 1999). Fas is a type I membrane protein that belongs to TNF superfamily (Armitage et al., 1994; Schulze et al., 1998) that undergoes trimerization upon binding to its physiological ligand, FasL, to form a Fas-associated death domain protein (FADD) via its cytoplasmic domain (Boldin et al., 1995, Chinnaiyan et al., 1995). It then activates downstream caspase cascade, which subsequently causes cleavage of caspase 3 as the terminal molecular event during apoptosis (Janicke et al., 1998; Zheng et al., 1998). When the Panc-1, MiaPaCa-2, Capan-2 cell lines were treated with rfhSP-D, Fas remained unaffected up to 12 h and then upregulation of Fas transcripts as well as protein was seen at 24 h, which indicated that TNF-α (Elzey et al., 2001) and NF-κB (Lui, et al., 2012) might also be affected since they are well known to tightly regulate the Fas-mediated apoptosis pathway. TNF-α, another member of TNF superfamily, acts via TNFR2 to increase the susceptibility of the target cells to Fas-mediated death; in addition, it stimulates the downstream NF-κB signalling (Micheau and Tschopp; 2003) by recruitment and activation of inhibitor of IκB kinases (IKK), which in turn enables its translocation to the nucleus where transcription of NFκB-dependent genes such as Fas occurs (Liu et al., 2012; Oeckinghaus and Ghosh, 2009).

In this study, transcriptional levels of both NF-κB and TNF-α were upregulated at the same time-point as Fas, which was largely anticipated (Liu et, 2012). Additionally, the fluorescence microscopy revealed NF-κB translocation to nucleus at 24 h in the rfhSP-D treated cells compared to the untreated counterpart, which suggested that TNF-α induced canonical NF-κB pathway (Perkins, 2007). NF-κB can regulate both pro- as well as anti-apoptotic genes, depending upon its canonical or non-canonical signalling (Perkins, 2007 Oeckinghaus and Ghosh; 2009). Interestingly, canonical NF-κB has been shown to bind directly to the Fas promoter to facilitate cell death via Fas-mediated apoptosis pathway (Liu et al., 2012). SP-D regulation in cancer is yet unknown. NF-κB plays an important role in deciding the cell fate as its canonical activation acts a transcription factor of Fas, which upon stimulation induces apoptosis signalling (Liu et al., 2012, Kaur et al., 2016). However, SP-D has been shown to regulate steady-state NF-κB activation in alveolar

macrophages of SP-D deficient mice (Yoshida et al., 2001). Interestingly, SP-D has also been shown to trigger TNF-α production in human $CCR2^+$ inflammatory monocytes (Barrow et al., 2015). These studies present an interesting central role of SP-D, which could be important in deciding the cell viability/apoptosis. Moreover, a cleaved caspase 8 and 3 was seen at 48 h, whereas intrinsic apoptosis markers such as caspase 9 and Bax remained unaffected (Fulda and Debatin, 2006), in all rfhSP-D treated cell lines as compared to untreated cells, which further confirmed the cell death via Fas-mediated pathway alone. In addition, mTOR pathway was downregulated following the treatment with rfhSP-D, which is crucial for cell survival and proliferation, and thus, to protect the cancer cells from apoptosis (Laplante and Sabatini, 2009). These findings are also supported by studies such as targeting mTOR pathway using rapamycin (Matsubara et al., 2013), or its regulating component RICTOR knockdown (Schmidt et al., 2017), significantly reduces pancreatic cancer cell growth. Interestingly, fluorescence microscopy showed that rfhSP-D causes nuclear accumulation of mTOR in the treated cells, which may have a transcriptional role. However, the nuclear versions do not form an intact mTORC1 required for cell regulation signalling pathways (Betz and Hall, 2013).

The rfhSP-D binds to all the pancreatic cell lines tested in this study: Panc-1, MiaPaCa-2 and Capan-2 (presented in Chapter 4). However, the putative SP-D receptor or the ligand on the pancreatic cancer cell surface is not yet known. Recently, an interaction between the CRD region of human SP-D and N-glycans of EGFR has been reported which led to downregulated EGF signalling in human lung adenocarcinoma cells (Hasegawa et al., 2015). Moreover, the ability of SP-D to trigger TNF-α production in human $CCR2^+$ inflammatory monocytes via interaction with a receptor, OSCAR (Barrow et al., 2015) has been reported. In conclusion, rfhSP-D upregulates pro-apoptotic factors such as TNF-α, NF-κB and Fas to activate caspase cascade to induce apoptosis in pancreatic cancer cell lines (Figure 5.11), which needs further exploration in orthotropic murine models. The majority of conventional anti-cancer therapies only target rapidly proliferating cancer cells, therefore, new strategies involving immune molecules such as rfhSP-D that target the signalling pathways to reduce cell growth require further investigation as these would not only help eliminate the tumour but could also influence recurrence or migratory capacity of the tumour cells.

Chapter 6

General Discussion

Innate Immune surveillance comes into play during tumour development to eliminate cancer cells. This thesis, for the first time, provided evidence that complement protein C1q, which had been previously shown to promote tumour growth in the tumour microenvironment, is capable of inducing apoptosis in an ovarian cancer cell line, SKOV3, when added exogenously in a serum free medium. Thus, it defined another complement independent role of C1q. Each globular head module (ghA, ghB or ghC) of human C1q produced a similar effect to that of the full-length molecule C1q and induced apoptosis independently in ovarian cancer cells. Treatment with C1q and globular head modules for 24 h upregulated TNF-α, a pro-apoptotic cytokine and Fas, a death receptor, and activated the caspase cascade, which subsequently resulted in apoptosis induction. Moreover, the pro-survival mTOR pathway, which is usually overexpressed in ovarian cancer, was downregulated. Although the presence of C1q has been reported in ascitic fluid formed during ovarian cancer, we were unable to detect its transcripts or immunoreactivity in SKOV3. This thesis also revealed that a recombinant fragment of human SP-D (rfhSP-D) can interfere with EMT in pancreatic cancer cell lines, by downregulating the key mesenchymal markers, which contribute to the invasive phenotype of the cancer cells. Extended treatment of pancreatic cancer cells with rfhSP-D subsequently induced apoptosis. Thus, it added another layer to the many well-known protective roles of SP-D.

Ovarian and pancreatic cancers are among the most lethal of all human malignant cancers. Ovarian is the sixth most frequently diagnosed cancer among women worldwide with higher mortality rate than any other female reproductive system associated cancer. The mortality rate associated with ovarian cancers is higher due to inadequate screening test and late stage (III or IV) detection (Permuth-wey and Sellers, 2009). Pancreatic ductal adenocarcinoma (PDA) has a dismal 5-year survival rate below 7%; it is estimated to become the third leading cause of cancer-related death by end of 2030 (Siegel et al., 2016). PDA is associated with high rates of mortality due to metastasis, resistance to conventional chemotherapy, and high tumour recurrence rate after surgery (Ansari et al., 2016).

Several studies over the past few decades have shown evidences of immune surveillance activation during cancer development. However, tumour cells constantly undergo alterations to render immune surveillance ineffective by utilising various escape or avoidance mechanisms such as shedding of tumour associated antigens, elevation of immunosuppressive cytokines such as IL-10 or TGF-β, and/or

downregulating the cell death inducing factors (Garg et al., 2013). Therefore, the experimental models are crucial to further understand the biological and genetic markers, which may be altered during early stages or phenotypic characteristics that influence proliferation and aggressive nature of these cancers. This advancement in the knowledge can then be further utilised to develop rational intervention strategies to effectively detect the cancer growth at an early stage, control its growth, increase chemo-sensitivity and prevent recurrence.

Although in vitro studies in this thesis provide the first clue of anti-tumour effects of C1q and rfhSP-D against ovarian and pancreatic cancer cell lines, respectively, further validation using animal models will be the next logical step. Indeed, it was attempted to verify these in vitro results, wherever possible, using techniques such as matrigel assays, which mimic basement membrane and contains extracellular matrix proteins, in order to investigate cell invasion in the presence and absence of rfhSP-D. Similarly, C1q and globular head modules mediated apoptosis was verified using different highly sensitive techniques such as flow cytometry, fluorescence and western blot analysis.

Ovarian cancer may arise from any cell type of the ovaries such as germ cells, granulosa or stromal cells. However, 90% of the ovarian cancers develop from epithelial cells covering the surface of the ovaries. Human Ovarian Surface Epithelium (OSE) cells had been developed by Auserperg et al., in 1984 into several *in vitro* models to study ovarian epithelial carcinogenesis. These OSE cells were then transfected with various tumour inducing viruse genes to study tumorigenesis in animal models. These included subcutaneous or intraperitoneal injections of transfected OSE cells with Kirsten murine sarcoma into rat caused endometrioid tumours (Adams and Auersperg, 1981) and transfection with SV40T antigen induced immortalisation (Leung et al., 2001). The T-antigen immortalised cells were further transformed by introducing E-cadherin for epithelial differentiation (Ong et al., 2000) or human papilloma virus E6 and E7 genes to make their phenotype invasive (Gregoire et al., 2001). Thus, these models allowed the evaluation of various oncogenes that may contribute to the development of ovarian cancers. For instance, p53 deficiency combined with two oncogenes from *C-MYC, K-RAS, or AKT* were required to achieve transformation in the OSE cells (Orsulic et al., 2002). Furthermore, xenograft models, where ovarian cancer cells are injected either subcutaneously or into the peritoneal cavity, have been extensively used for

investigating novel therapies (Massazza et al., 1989). The intra-bursal space, a sac-like structure that envelops mouse ovaries, has been used for transplanting the xenografts in the ovaries, which gave a physiological advantage as the cancer cells were directly placed in the ovarian environment where the tumours generally arise. Recent studies have identified a transgenic model of epithelial ovarian cancer, which used the upstream region of Mullerian inhibitory substance type II receptor (*MISIIR*). These transgenic mouse models are ideal to investigate the pathogenic events associated with ovarian cancer as the tumour directly arises from OSE cells. These models have defined genetic lesions that could be studied at various stages as they inevitably develop ovarian cancer *in situ*. In addition, it provides understanding of oncogenes and tumour suppressor genes for their contribution to the initiation and the progression of malignancies in the mouse ovary. Finally, a number of different factors could be altered such as the genetic background of the mouse strain, the frequency of ovulation and the levels of various hormones to determine their impact on the development of tumours in the susceptible transgenic mouse line. These transgenic models could be therefore ideal to further study the effect of C1q on tumour growth *in vivo*. The complement components levels can be measured in the serum of the tumour induced transgenic mice and compared with the control as it may provide the much-needed screening strategy for an early detection.

In contrast, the murine models to better understand the molecular mechanism during the development of pancreatic cancer have remained complex and not always well-defined. Fearon and Vogelstein et al., in 1990 revealed that at least 4-5 genetic mutations were required for normal epithelium to become a carcinoma. This led to the development of several mouse models that involved activation of Kras and inactivation of p16INK4a, p53 and Smad4 tumour suppressors (Hruban and Adsay, 2001). Currently, several genetically modified mouse tumours based on Kras mutations and xenograft models (heterotopic or orthotopic) are available (Herreros-Villanueva et al., 2012). These models can therefore be utilised to evaluate the inhibitory effects of rfhSP-D on the development of pancreatic cancer *in vivo.*

Therefore, the next step towards achieving therapeutic goals of this study will be to cross-link these innate immune molecules (C1q, ghA, ghB, ghC and rfhSP-D) on carbon nanotubes (CNT) or other nano-carriers as a delivery strategy to the tumor site in the orthotropic murine models of ovarian and pancreatic cancer. rfhSP-D has been shown to opsonise the CNTs and therefore, enhanced their uptake by U937 and

THP-1 macrophages/monocytic cell lines, which was accompanied by an increased pro-inflammatory response (Pondman et al., 2017). These could be useful as these molecules will not only have a direct effect but also may bring about complement attack against the tumor cells. Moreover, the majority of conventional anti-cancer therapies only target rapidly proliferating cancer cells; therefore, new strategies involving immune molecules such as rfhSP-D, C1q and globular head modules that target the signalling pathways to reduce tumour cell growth merit further investigation as these would not only help eliminate the tumour but could also influence recurrence or migratory capacity of the tumour cells.

References

Adams, A.T. and Auersperg, N. (1981) 'Transformation of cultured rat ovarian surface epithelial cells by Kirsten murine sarcoma virus', *Cancer research,* 41(6), pp. 2063-2072.

Aguirre-Ghiso, J.A. (2007) 'Models, mechanisms and clinical evidence for cancer dormancy', *Nature reviews.Cancer,* 7(11), pp. 834-846.

Ajona, D., Hsu, Y.F., Corrales, L., Montuenga, L.M. and Pio, R. (2007) 'Down-regulation of human complement factor H sensitizes non-small cell lung cancer cells to complement attack and reduces in vivo tumor growth', *Journal of immunology (Baltimore, Md.: 1950),* 178(9), pp. 5991-5998.

Altomare, D.A., Wang, H.Q., Skele, K.L., De Rienzo, A., Klein-Szanto, A.J., Godwin, A.K. and Testa, J.R. (2004) 'AKT and mTOR phosphorylation is frequently detected in ovarian cancer and can be targeted to disrupt ovarian tumor cell growth', *Oncogene,* 23(34), pp. 5853-5857.

Ansari, D., Tingstedt, B., Andersson, B., Holmquist, F., Sturesson, C., Williamsson, C., Sasor, A., Borg, D., Bauden, M. and Andersson, R. (2016) 'Pancreatic cancer: yesterday, today and tomorrow', *Future oncology (London, England),* 12(16), pp. 1929-1946.

Armitage, R.J. (1994) 'Tumor necrosis factor receptor superfamily members and their ligands', *Current opinion in immunology,* 6(3), pp. 407-413.

Arumugam, T., Ramachandran, V., Fournier, K.F., Wang, H., Marquis, L., Abbruzzese, J.L., Gallick, G.E., Logsdon, C.D., McConkey, D.J. and Choi, W. (2009) 'Epithelial to mesenchymal transition contributes to drug resistance in pancreatic cancer', *Cancer research,* 69(14), pp. 5820-5828.

Asea, A., Rehli, M., Kabingu, E., Boch, J.A., Bare, O., Auron, P.E., Stevenson, M.A. and Calderwood, S.K. (2002) 'Novel signal transduction pathway utilized by extracellular HSP70: role of toll-like receptor (TLR) 2 and TLR4', *The Journal of biological chemistry,* 277(17), pp. 15028-15034.

Ashkenazi, A. and Dixit, V.M. (1998) 'Death receptors: signaling and modulation', *Science (New York, N.Y.),* 281(5381), pp. 1305-1308.

Auersperg, N., Siemens, C.H. and Myrdal, S.E. (1984) 'Human ovarian surface epithelium in primary culture', *In vitro,* 20(10), pp. 743-755.

Barcellos-Hoff, M.H., Lyden, D. and Wang, T.C. (2013) 'The evolution of the cancer niche during multistage carcinogenesis', *Nature reviews. Cancer,* 13(7), pp. 511-518.

Barrow, A.D., Palarasah, Y., Bugatti, M., Holehouse, A.S., Byers, D.E., Holtzman, M.J., Vermi, W., Skjodt, K., Crouch, E. and Colonna, M. (2015) 'OSCAR is a receptor for surfactant protein D that activates TNF-alpha release from human

CCR2+ inflammatory monocytes', *Journal of immunology (Baltimore, Md),* 194(7), pp. 3317-3326.

Bauer, S., Groh, V., Wu, J., Steinle, A., Phillips, J.H., Lanier, L.L. and Spies, T. (1999) 'Activation of NK cells and T cells by NKG2D, a receptor for stress-inducible MICA', *Science (New York, N.Y.),* 285(5428), pp. 727-729.

Beauchamp, R.D., Lyons, R.M., Yang, E.Y., Coffey, R.J.Jr and Moses, H.L. (1990) 'Expression of and response to growth regulatory peptides by two human pancreatic carcinoma cell lines', *Pancreas,* 5(4), pp. 369-380.

Betz, C. and Hall, M.N. (2013) 'Where is mTOR and what is it doing there?', *The Journal of cell biology,* 203(4), pp. 563-574.

Beuran, M., Negoi, I., Paun, S., Ion, A.D., Bleotu, C., Negoi, R.I. and Hostiuc, S. (2015) 'The epithelial to mesenchymal transition in pancreatic cancer: A systematic review', *Pancreatology: official journal of the International Association of Pancreatology (IAP)* 15(3), pp. 217-225.

Beutler, B. and van Huffel, C. (1994) 'Unraveling function in the TNF ligand and receptor families', *Science (New York, N.Y.),* 264(5159), pp. 667-668.

Bjorge, L., Hakulinen, J., Vintermyr, O.K., Jarva, H., Jensen, T.S., Iversen, O.E. and Meri, S. (2005) 'Ascitic complement system in ovarian cancer', *British journal of cancer,* 92(5), pp. 895-905.

Boldin, M.P., Varfolomeev, E.E., Pancer, Z., Mett, I.L., Camonis, J.H. and Wallach, D. (1995) 'A novel protein that interacts with the death domain of Fas/APO1 contains a sequence motif related to the death domain', *The Journal of biological chemistry,* 270(14), pp. 7795-7798.

Brabletz, T. (2012) 'EMT and MET in metastasis: where are the cancer stem cells?', *Cancer cell,* 22(6), pp. 699-701.

Brabletz, T., Jung, A., Spaderna, S., Hlubek, F. and Kirchner, T. (2005) 'Opinion: migrating cancer stem cells - an integrated concept of malignant tumour progression', *Nature reviews. Cancer,* 5(9), pp. 744-749.

Bu, X., Zheng, Z., Wang, C. and Yu, Y. (2007) Significance of C4d deposition in the follicular lymphoma and MALT lymphoma and their relationship with follicular dendritic cells. *Pathol Res Pract*. 2007;203(3):163-7

Bulla, R., Tripodo, C., Rami, D., Ling, G.S., Agostinis, C., Guarnotta, C., Zorzet, S., Durigutto, P., Botto, M. and Tedesco, F. (2016) 'C1q acts in the tumour microenvironment as a cancer-promoting factor independently of complement activation', *Nature communications,* 7, pp. 10338-46.

Carli, M., Bucolo, C., Pannunzio, M.T., Ongaro, G., Businaro, R. and Revoltella, R. (1979) 'Fluctuation of serum complement levels in children with neuroblastoma', *Cancer,* 43(6), pp. 2399-2404.

Champsaur, M. and Lanier, L.L. (2010) 'Effect of NKG2D ligand expression on host immune responses', *Immunological reviews,* 235(1), pp. 267-285.

Chan, F.K., Siegel, R.M. and Lenardo, M.J. (2000) 'Signaling by the TNF receptor superfamily and T cell homeostasis', *Immunity,* 13(4), pp. 419-422.

Chen, S., Caragine, T., Cheung, N.K. and Tomlinson, S. (2000) 'CD59 expressed on a tumor cell surface modulates decay-accelerating factor expression and enhances tumor growth in a rat model of human neuroblastoma', *Cancer research,* 60(11), pp. 3013-3018.

Cheng, Z.Z., Corey, M.J., Parepalo, M., Majno, S., Hellwage, J., Zipfel, P.F., Kinders, R.J., Raitanen, M., Meri, S. and Jokiranta, T.S. (2005) 'Complement factor H as a marker for detection of bladder cancer', *Clinical chemistry,* 51(5), pp. 856-863.

Chinnaiyan, A.M., O'Rourke, K., Tewari, M. and Dixit, V.M. (1995) 'FADD, a novel death domain-containing protein, interacts with the death domain of Fas and initiates apoptosis', *Cell,* 81(4), pp. 505-512.

Coral, S., Fonsatti, E., Sigalotti, L., De Nardo, C., Visintin, A., Nardi, G., Colizzi, F., Colombo, M.P., Romano, G., Altomonte, M. and Maio, M. (2000) 'Overexpression of protectin (CD59) down-modulates the susceptibility of human melanoma cells to homologous complement', *Journal of cellular physiology,* 185(3), pp. 317-323.

Corey, M.J., Kinders, R.J., Brown, L.G. and Vessella, R.L. (1997) 'A very sensitive coupled luminescent assay for cytotoxicity and complement-mediated lysis', *Journal of immunological methods,* 207(1), pp. 43-51.

Corey, M.J., Kinders, R.J., Poduje, C.M., Bruce, C.L., Rowley, H., Brown, L.G., Hass, G.M. and Vessella, R.L. (2000) 'Mechanistic studies of the effects of anti-factor H antibodies on complement-mediated lysis', *The Journal of biological chemistry,* 275(17), pp. 12917-12925.

Corrales, L., Ajona, D., Rafail, S., Lasarte, J.J., Riezu-Boj, J.I., Lambris, J.D., Rouzaut, A., Pajares, M.J., Montuenga, L.M. and Pio, R. (2012) 'Anaphylatoxin C5a creates a favorable microenvironment for lung cancer progression', *Journal of immunology (Baltimore, Md),* 189(9), pp. 4674-4683.

Crouch, E. and Wright, J.R. (2001) 'Surfactant proteins a and d and pulmonary host defense', *Annual Review of Physiology,* 63, pp. 521-554.

Cui, T., Chen, Y., Knosel, T., Yang, L., Zoller, K., Galler, K., Berndt, A., Mihlan, M., Zipfel, P.F. and Petersen, I. (2011) 'Human complement factor H is a novel diagnostic marker for lung adenocarcinoma', *International journal of oncology,* 39(1), pp. 161-168.

Deer, E.L., Gonzalez-Hernandez, J., Coursen, J.D., Shea, J.E., Ngatia, J., Scaife, C.L., Firpo, M.A. and Mulvihill, S.J. (2010) 'Phenotype and genotype of pancreatic cancer cell lines', *Pancreas,* 39(4), pp. 425-435.

Diaferia, G.R., Balestrieri, C., Prosperini, E., Nicoli, P., Spaggiari, P., Zerbi, A. and Natoli, G. (2016) 'Dissection of transcriptional and cis-regulatory control of differentiation in human pancreatic cancer', *The EMBO journal,* 35(6), pp. 595-617.

Dranoff, G. (2004) 'Cytokines in cancer pathogenesis and cancer therapy', *Nature reviews. Cancer,* 4(1), pp. 11-22.

Dunn, G.P., Bruce, A.T., Ikeda, H., Old, L.J. and Schreiber, R.D. (2002) 'Cancer immunoediting: from immunosurveillance to tumor escape', *Nature immunology,* 3(11), pp. 991-998.

Dunn, G.P., Old, L.J. and Schreiber, R.D. (2004) 'The immunobiology of cancer immunosurveillance and immunoediting', *Immunity,* 21(2), pp. 137-148.

Durrant, L.G., Chapman, M.A., Buckley, D.J., Spendlove, I., Robins, R.A. and Armitage, N.C. (2003) 'Enhanced expression of the complement regulatory protein CD55 predicts a poor prognosis in colorectal cancer patients', *Cancer immunology, immunotherapy: CII,* 52(10), pp. 638-642.

Ellenrieder, V., Hendler, S.F., Ruhland, C., Boeck, W., Adler, G. and Gress, T.M. (2001) 'TGF-beta-induced invasiveness of pancreatic cancer cells is mediated by matrix metalloproteinase-2 and the urokinase plasminogen activator system', *International journal of cancer,* 93(2), pp. 204-211.

Elzey, B.D., Griffith, T.S., Herndon, J.M., Barreiro, R., Tschopp, J. and Ferguson, T.A. (2001) 'Regulation of Fas ligand-induced apoptosis by TNF', *Journal of immunology (Baltimore, Md),* 167(6), pp. 3049-3056.

Fearon, E.R. and Vogelstein, B. (1990) 'A genetic model for colorectal tumorigenesis', *Cell,* 61(5), pp. 759-767.

Fidler, I.J. (2003) 'The pathogenesis of cancer metastasis: the 'seed and soil' hypothesis revisited', *Nature reviews. Cancer,* 3(6), pp. 453-458.

Foreman, M.G., Kong, X., DeMeo, D.L., Pillai, S.G., Hersh, C.P., Bakke, P., Gulsvik, A., Lomas, D.A., Litonjua, A.A., Shapiro, S.D., Tal-Singer, R. and Silverman, E.K. (2011) 'Polymorphisms in surfactant protein-D are associated with chronic obstructive pulmonary disease', *American journal of respiratory cell and molecular biology,* 44(3), pp. 316-322.

Friess, H., Lu, Z., Graber, H.U., Zimmermann, A., Adler, G., Korc, M., Schmid, R.M. and Buchler, M.W. (1998) 'Bax, but Not Bcl-2, Influences the Prognosis of Human Pancreatic Cancer', *Gut,* 43(3), pp. 414-421.

Friess, H., Yamanaka, Y., Buchler, M., Berger, H.G., Kobrin, M.S., Baldwin, R.L. and Korc, M. (1993) 'Enhanced expression of the type II transforming growth factor beta receptor in human pancreatic cancer cells without alteration of type III receptor expression', *Cancer research,* 53(12), pp. 2704-2707.

Fulda, S. and Debatin, K.M. (2006) 'Extrinsic versus intrinsic apoptosis pathways in anticancer chemotherapy', *Oncogene,* 25(34), pp. 4798-4811.

Fust, G., Miszlay, Z., Czink, E., Varga, L., Pálóczi, K., Szegedi, G. and Hollán, S.R. (1987) C1 and C4 abnormalities in chronic lymphocytic leukaemia and their significance. *Immunol Lett. 1987 Feb;14(3):255-9.*

Fogh, J., and Trempe, G. (1975). New Human Tumor Cell Lines. *Plenum Press* 115–159

Gao, Y., Yang, W., Pan, M., Scully, E., Girardi, M., Augenlicht, L.H., Craft, J. and Yin, Z. (2003) 'Gamma delta T cells provide an early source of interferon gamma in tumor immunity', *The Journal of experimental medicine,* 198(3), pp. 433-442.

Gardai, S.J., Bratton, D.L., Ogden, C.A. and Henson, P.M. (2006) 'Recognition ligands on apoptotic cells: a perspective', *Journal of leukocyte biology,* 79(5), pp. 896-903.

Gardai, S.J., McPhillips, K.A., Frasch, S.C., Janssen, W.J., Starefeldt, A., Murphy-Ullrich, J.E., Bratton, D.L., Oldenborg, P.A., Michalak, M. and Henson, P.M. (2005) 'Cell-surface calreticulin initiates clearance of viable or apoptotic cells through trans-activation of LRP on the phagocyte', *Cell,* 123(2), pp. 321-334.

Garg, A.D., Dudek, A.M. and Agostinis, P. (2013) 'Cancer immunogenicity, danger signals, and DAMPs: what, when, and how?', *BioFactors (Oxford, England),* 39(4), pp. 355-367.

Ghai, R., Waters, P., Roumenina, L.T., Gadjeva, M., Kojouharova, M.S., Reid, K.B., Sim, R.B. and Kishore, U. (2007) 'C1q and its growing family', *Immunobiology,* 212(4-5), pp. 253-266.

Ghebrehiwet, B., Feng, X., Kumar, R. and Peerschke, E.I. (2003) 'Complement component C1q induces endothelial cell adhesion and spreading through a docking/signaling partnership of C1q receptors and integrins', *International immunopharmacology,* 3(3), pp. 299-310.

Ghebrehiwet, B., Hosszu, K.K., Valentino, A. and Peerschke, E.I. (2012) 'The C1q family of proteins: insights into the emerging non-traditional functions', *Frontiers in immunology,* 3, pp. 52.

Girardi, M., Glusac, E., Filler, R.B., Roberts, S.J., Propperova, I., Lewis, J., Tigelaar, R.E. and Hayday, A.C. (2003) 'The distinct contributions of murine T cell receptor (TCR)gammadelta+ and TCRalphabeta+ T cells to different stages of chemically induced skin cancer', *The Journal of experimental medicine,* 198(5), pp. 747-755.

Glunde, K. and Serkova, N.J. (2006) 'Therapeutic targets and biomarkers identified in cancer choline phospholipid metabolism', *Pharmacogenomics,* 7(7), pp. 1109-1123.

Gminski, J., Mykala-Ciesla, J., Machalski, M., Drozdz, M. and Najda, J. (1992) 'Immunoglobulins and complement components levels in patients with lung cancer', *Romanian journal of internal medicine = Revue roumaine de medecine interne,* 30(1), pp. 39-44.

Gregoire, L., Rabah, R., Schmelz, E.M., Munkarah, A., Roberts, P.C. and Lancaster, W.D. (2001) 'Spontaneous malignant transformation of human ovarian surface epithelial cells in vitro', *Clinical cancer research: an official journal of the American Association for Cancer Research,* 7(12), pp. 4280-4287.

Griese, M., Steinecker, M., Schumacher, S., Braun, A., Lohse, P. and Heinrich, S. (2008) 'Children with absent surfactant protein D in bronchoalveolar lavage have more frequently pneumonia', *Pediatric allergy and immunology: official publication of the European Society of Pediatric Allergy and Immunology,* 19(7), pp. 639-647.

Griffin, J.L. and Kauppinen, R.A. (2007) 'Tumour metabolomics in animal models of human cancer', *Journal of proteome research,* 6(2), pp. 498-505.

Grivennikov, S.I., Greten, F.R. and Karin, M. (2010) 'Immunity, inflammation, and cancer', *Cell,* 140(6), pp. 883-899.

Gruss, H.J. (1996) 'Molecular, structural, and biological characteristics of the tumor necrosis factor ligand superfamily', *International journal of clinical & laboratory research,* 26(3), pp. 143-159.

Haagsman, H.P. (1998) 'Interactions of surfactant protein A with pathogens', *Biochimica et biophysica acta,* 1408(2-3), pp. 264-277.

Hakomori, S. (2002) 'Glycosylation defining cancer malignancy: new wine in an old bottle', *Proceedings of the National Academy of Sciences of the United States of America,* 99(16), pp. 10231-10233.

Hara, K., Maruki, Y., Long, X., Yoshino, K., Oshiro, N., Hidayat, S., Tokunaga, C., Avruch, J. and Yonezawa, K. (2002) 'Raptor, a binding partner of target of rapamycin (TOR), mediates TOR action', *Cell,* 110(2), pp. 177-189.

Hasegawa, Y., Takahashi, M., Ariki, S., Asakawa, D., Tajiri, M., Wada, Y., Yamaguchi, Y., Nishitani, C., Takamiya, R., Saito, A., Uehara, Y., Hashimoto, J., Kurimura, Y., Takahashi, H. and Kuroki, Y. (2015) 'Surfactant protein D suppresses lung cancer progression by downregulation of epidermal growth factor signaling', *Oncogene,* 34(32), pp. 4285-4286.

Heldin, C.H., Vanlandewijck, M. and Moustakas, A. (2012) 'Regulation of EMT by TGFbeta in cancer', *FEBS letters,* 586(14), pp. 1959-1970.

Herreros-Villanueva, M., Hijona, E., Cosme, A. and Bujanda, L. (2012) 'Mouse models of pancreatic cancer', *World journal of gastroenterology,* 18(12), pp. 1286-1294.

Hong, Q., Sze, C., Lin, S., Lee, M., He, R., Schultz, L., Chang, J., Chen, S., Boackle, R.J. and Hsu, L. (2009) 'Complement C1q activates tumor suppressor WWOX to induce apoptosis in prostate cancer cells', *PLoS One,* 4(6), pp. e5755.

Horiguchi, K., Shirakihara, T., Nakano, A., Imamura, T., Miyazono, K. and Saitoh, M. (2009) 'Role of Ras signaling in the induction of snail by transforming growth factor-beta', *The Journal of biological chemistry,* 284(1), pp. 245-253.

Hotz, B., Arndt, M., Dullat, S., Bhargava, S., Buhr, H.J. and Hotz, H.G. (2007) 'Epithelial to mesenchymal transition: expression of the regulators snail, slug, and twist in pancreatic cancer', *Clinical cancer research: an official journal of the American Association for Cancer Research,* 13(16), pp. 4769-4776.

Hruban, R.H. and Adsay, N.V. (2009) 'Molecular classification of neoplasms of the pancreas', *Human pathology,* 40(5), pp. 612-623.

Hsu, H., Shu, H.B., Pan, M.G. and Goeddel, D.V. (1996) 'TRADD-TRAF2 and TRADD-FADD interactions define two distinct TNF receptor 1 signal transduction pathways', *Cell,* 84(2), pp. 299-308.

Ikegami, M., Na, C.L., Korfhagen, T.R. and Whitsett, J.A. (2005) 'Surfactant protein D influences surfactant ultrastructure and uptake by alveolar type II cells', *American journal of physiology. Lung cellular and molecular physiology,* 288(3), pp. L552-61.

Imamichi, Y., Konig, A., Gress, T. and Menke, A. (2007) 'Collagen type I-induced Smad-interacting protein 1 expression downregulates E-cadherin in pancreatic cancer', *Oncogene,* 26(16), pp. 2381-2385.

Ishigami, S., Natsugoe, S., Tokuda, K., Nakajo, A., Che, X., Iwashige, H., Aridome, K., Hokita, S. and Aikou, T. (2000) 'Prognostic value of intratumoral natural killer cells in gastric carcinoma', *Cancer,* 88(3), pp. 577-583.

Ishii, T., Hagiwara, K., Kamio, K., Ikeda, S., Arai, T., Mieno, M.N., Kumasaka, T., Muramatsu, M., Sawabe, M., Gemma, A. and Kida, K. (2012) 'Involvement of surfactant protein D in emphysema revealed by genetic association study', *European journal of human genetics: EJHG,* 20(2), pp. 230-235.

Janicke, R.U., Sprengart, M.L., Wati, M.R. and Porter, A.G. (1998) 'Caspase-3 is required for DNA fragmentation and morphological changes associated with apoptosis', *The Journal of biological chemistry,* 273(16), pp. 9357-9360.

Jarvis, G.A., Li, J., Hakulinen, J., Brady, K.A., Nordling, S., Dahiya, R. and Meri, S. (1997) 'Expression and function of the complement membrane attack complex inhibitor protectin (CD59) in human prostate cancer', *International journal of cancer,* 71(6), pp. 1049-1055.

Junnikkala, S., Hakulinen, J., Jarva, H., Manuelian, T., Bjorge, L., Butzow, R., Zipfel, P.F. and Meri, S. (2002) 'Secretion of soluble complement inhibitors factor H and

factor H-like protein (FHL-1) by ovarian tumour cells', *British journal of cancer,* 87(10), pp. 1119-1127.

Junnikkala, S., Jokiranta, T.S., Friese, M.A., Jarva, H., Zipfel, P.F. and Meri, S. (2000) 'Exceptional resistance of human H2 glioblastoma cells to complement-mediated killing by expression and utilization of factor H and factor H-like protein 1', *Journal of immunology (Baltimore, Md.: 1950),* 164(11), pp. 6075-6081.

Jurianz, K., Ziegler, S., Garcia-Schüler, H., Kraus, S., Bohana-Kashtan, O., Fishelson, Z. and Kirschfink, M. (1999) Complement resistance of tumor cells: basal and induced mechanisms. *Mol Immunol*. 1999 Sep-Oct;36(13-14):929-39.

Kaplan, D.H., Shankaran, V., Dighe, A.S., Stockert, E., Aguet, M., Old, L.J. and Schreiber, R.D. (1998) 'Demonstration of an interferon γ-dependent tumor surveillance system in immunocompetent mice', *Proceedings of the National Academy of Sciences,* 95(13), pp. 7556-7561.

Kaufhold, S. and Bonavida, B. (2014) 'Central role of Snail1 in the regulation of EMT and resistance in cancer: a target for therapeutic intervention', *Journal of experimental & clinical cancer research: CR,* 33, pp. 62-014-0062-0.

Kaur, A., Sultan, S.H., Murugaiah, V., Pathan, A.A., Alhamlan, F.S., Karteris, E. and Kishore, U. (2016) 'Human C1q Induces Apoptosis in an Ovarian Cancer Cell Line via Tumor Necrosis Factor Pathway', *Frontiers in immunology,* 7, pp. 599.

Kawasaki, T., Etoh, R. and Yamashina, I. (1978) 'Isolation and characterization of a mannan-binding protein from rabbit liver', *Biochemical and biophysical research communications,* 81(3), pp. 1018-1024.

Kehrl, J.H., Roberts, A.B., Wakefield, L.M., Jakowlew, S., Sporn, M.B. and Fauci, A.S. (1986a) 'Transforming growth factor beta is an important immunomodulatory protein for human B lymphocytes', *Journal of immunology (Baltimore, Md),* 137(12), pp. 3855-3860.

Kehrl, J.H., Wakefield, L.M., Roberts, A.B., Jakowlew, S., Alvarez-Mon, M., Derynck, R., Sporn, M.B. and Fauci, A.S. (1986b) 'Pillars Article: production of transforming growth factor beta by human T lymphocytes and its potential role in the regulation of T cell growth. J Exp Med. 163: 1037-1050', *Journal of immunology (Baltimore, Md),* 192(7), pp. 2939-2952.

Kennedy, A.L., Morton, J.P., Manoharan, I., Nelson, D.M., Jamieson, N.B., Pawlikowski, J.S., McBryan, T., Doyle, B., McKay, C., Oien, K.A., Enders, G.H., Zhang, R., Sansom, O.J. and Adams, P.D. (2011) 'Activation of the PIK3CA/AKT pathway suppresses senescence induced by an activated RAS oncogene to promote tumorigenesis', *Molecular cell,* 42(1), pp. 36-49.

Kishore, U., Bernal, A.L., Kamran, M.F., Saxena, S., Singh, M., Sarma, P.U., Madan, T. and Chakraborty, T. (2005) 'Surfactant proteins SP-A and SP-D in human

health and disease', *Archivum Immunologiae et Therapiae Experimentalis,* 53(5), pp. 399-417.

Kishore, U., Gaboriaud, C., Waters, P., Shrive, A.K., Greenhough, T.J., Reid, K.B., Sim, R.B. and Arlaud, G.J. (2004) 'C1q and tumor necrosis factor superfamily: modularity and versatility', *Trends in immunology,* 25(10), pp. 551-561.

Kishore, U., Greenhough, T.J., Waters, P., Shrive, A.K., Ghai, R., Kamran, M.F., Bernal, A.L., Reid, K.B., Madan, T. and Chakraborty, T. (2006) 'Surfactant proteins SP-A and SP-D: structure, function and receptors', *Molecular immunology,* 43(9), pp. 1293-1315.

Kishore, U., Gupta, S.K., Perdikoulis, M.V., Kojouharova, M.S., Urban, B.C. and Reid, K.B. (2003) 'Modular organization of the carboxyl-terminal, globular head region of human C1q A, B, and C chains', *Journal of immunology (Baltimore, Md),* 171(2), pp. 812-820.

Kishore, U. and Reid, K.B. (2000) 'C1q: structure, function, and receptors', *Immunopharmacology,* 49(1-2), pp. 159-170.

Kishore, U., Thielens, N.M. and Gaboriaud, C. (2016) 'Editorial: State-of-the-Art Research on C1q and the Classical Complement Pathway', *Frontiers in immunology,* 7, pp. 398.

Kouser, L., Madhukaran, S.P., Shastri, A., Saraon, A., Ferluga, J., Al-Mozaini, M. and Kishore, U. (2015) 'Emerging and novel functions of complement protein C1q', *Frontiers in immunology,* 6 (317).

Kraut, E.H. and Sagone, A.L.,Jr (1981) 'Alternative pathway of complement in multiple myeloma', *American Journal of Hematology,* 11(4), pp. 335-345.

Kyriazis AA, Kyriazis AP, Sternberg CN (1986). Morphological, biological, biochemical, and karyotypic characteristics of human pancreatic ductal adenocarcinoma Capan-2 in tissue culture and the nude mouse. Cancer Res.; 46:5810–5815.

Laplante, M. and Sabatini, D.M. (2009) 'mTOR signaling at a glance', *Journal of cell science,* 122(Pt 20), pp. 3589-3594.

Lee, S.H., Meng, X.W., Flatten, K.S., Loegering, D.A. and Kaufmann, S.H. (2013) 'Phosphatidylserine exposure during apoptosis reflects bidirectional trafficking between plasma membrane and cytoplasm', *Cell death and differentiation,* 20(1), pp. 64-76.

Leung, E.H., Leung, P.C. and Auersperg, N. (2001) 'Differentiation and growth potential of human ovarian surface epithelial cells expressing temperature-sensitive SV40 T antigen', *In vitro cellular & developmental biology. Animal,* 37(8), pp. 515-521.

Lieber M, Mazzetta J, Nelson-Rees W (1975) Establishment of a continuous tumor-cell line (panc-1) from a human carcinoma of the exocrine pancreas. *Int J Cancer.*;15:741–747.

Lingappa, J.R., Dumitrescu, L., Zimmer, S.M., Lynfield, R., McNicholl, J.M., Messonnier, N.E., Whitney, C.G. and Crawford, D.C. (2011) 'Identifying host genetic risk factors in the context of public health surveillance for invasive pneumococcal disease', *PloS one,* 6(8), pp. e23413.

Liu, F., Bardhan, K., Yang, D., Thangaraju, M., Ganapathy, V., Waller, J.L., Liles, G.B., Lee, J.R. and Liu, K. (2012) 'NF-kappaB directly regulates Fas transcription to modulate Fas-mediated apoptosis and tumor suppression', *The Journal of biological chemistry,* 287(30), pp. 25530-25540.

Liu, J., Miwa, T., Hilliard, B., Chen, Y., Lambris, J.D., Wells, A.D. and Song, W.C. (2005) 'The complement inhibitory protein DAF (CD55) suppresses T cell immunity in vivo', *The Journal of experimental medicine,* 201(4), pp. 567-577.

Liu, Y. and Zeng, G. (2012) 'Cancer and innate immune system interactions: translational potentials for cancer immunotherapy', *Journal of immunotherapy (Hagerstown, Md* 35(4), pp. 299-308.

Loberg, R.D., Wojno, K.J., Day, L.L. and Pienta, K.J. (2005) 'Analysis of membrane-bound complement regulatory proteins in prostate cancer', *Urology,* 66(6), pp. 1321-1326.

Lu, J. (1997) 'Collectins: collectors of microorganisms for the innate immune system', *BioEssays: news and reviews in molecular, cellular and developmental biology,* 19(6), pp. 509-518.

Lu, J. and Kishore, U. (2017) 'C1 Complex: An Adaptable Proteolytic Module for Complement and Non-Complement Functions', *Frontiers in immunology,* 8, pp. 592.

Lu, J., Teh, C., Kishore, U. and Reid, K.B. (2002) 'Collectins and ficolins: sugar pattern recognition molecules of the mammalian innate immune system', *Biochimica et biophysica acta,* 1572(2-3), pp. 387-400.

Lucas, S.D., Karlsson-Parra, A., Nilsson, B., Grimelius, L., Akerstrom, G., Rastad, J. and Juhlin, C. (1996) 'Tumor-specific deposition of immunoglobulin G and complement in papillary thyroid carcinoma', *Human pathology,* 27(12), pp. 1329-1335.

Madan, T., Kishore, U., Shah, A., Eggleton, P., Strong, P., Wang, J.Y., Aggrawal, S.S., Sarma, P.U. and Reid, K.B. (1997) 'Lung surfactant proteins A and D can inhibit specific IgE binding to the allergens of Aspergillus fumigatus and block allergen-induced histamine release from human basophils', *Clinical and experimental immunology,* 110(2), pp. 241-249.

Madan, T., Kishore, U., Singh, M., Strong, P., Clark, H., Hussain, E.M., Reid, K.B. and Sarma, P.U. (2001a) 'Surfactant proteins A and D protect mice against pulmonary hypersensitivity induced by Aspergillus fumigatus antigens and allergens', *The Journal of clinical investigation,* 107(4), pp. 467-475.

Madan, T., Kishore, U., Singh, M., Strong, P., Hussain, E.M., Reid, K.B. and Sarma, P.U. (2001b) 'Protective role of lung surfactant protein D in a murine model of invasive pulmonary aspergillosis', *Infection and immunity,* 69(4), pp. 2728-2731.

Madsen, J., Kliem, A., Tornoe, I., Skjodt, K., Koch, C. and Holmskov, U. (2000) 'Localization of lung surfactant protein D on mucosal surfaces in human tissues', *Journal of immunology (Baltimore, Md),* 164(11), pp. 5866-5870.

Mahajan, L., Gautam, P., Dodagatta-Marri, E., Madan, T. and Kishore, U. (2014) 'Surfactant protein SP-D modulates activity of immune cells: proteomic profiling of its interaction with eosinophilic cells', *Expert review of proteomics,* 11(3), pp. 355-369.

Mahajan, L., Madan, T., Kamal, N., Singh, V.K., Sim, R.B., Telang, S.D., Ramchand, C.N., Waters, P., Kishore, U. and Sarma, P.U. (2008) 'Recombinant surfactant protein-D selectively increases apoptosis in eosinophils of allergic asthmatics and enhances uptake of apoptotic eosinophils by macrophages', *International immunology,* 20(8), pp. 993-1007.

Mahajan, L., Pandit, H., Madan, T., Gautam, P., Yadav, A.K., Warke, H., Sundaram, C.S., Sirdeshmukh, R., Sarma, P.U., Kishore, U. and Surolia, A. (2013) 'Human surfactant protein D alters oxidative stress and HMGA1 expression to induce p53 apoptotic pathway in eosinophil leukemic cell line', *PloS one,* 8(12), pp. e85046.

Maier, H.J., Wirth, T. and Beug, H. (2010) 'Epithelial-mesenchymal transition in pancreatic carcinoma', *Cancers,* 2(4), pp. 2058-2083.

Malvezzi, M., Bertuccio, P., Rosso, T., Rota, M., Levi, F., La Vecchia, C. and Negri, E. (2015) 'European cancer mortality predictions for the year 2015: does lung cancer have the highest death rate in EU women?', *Annals of oncology: official journal of the European Society for Medical Oncology,* 26(4), pp. 779-786.

Maness, P.F. and Orengo, A. (1977) 'Serum complement levels in patients with digestive tract carcinomas and other neoplastic diseases', *Oncology,* 34(2), pp. 87-89.

Massague, J. (2000) 'How cells read TGF-beta signals', *Nature reviews.Molecular cell biology,* 1(3), pp. 169-178.

Massague, J. and Wotton, D. (2000) 'Transcriptional control by the TGF-beta/Smad signaling system', *The EMBO journal,* 19(8), pp. 1745-1754.

Massazza, G., Tomasoni, A., Lucchini, V., Allavena, P., Erba, E., Colombo, N., Mantovani, A., D'Incalci, M., Mangioni, C. and Giavazzi, R. (1989) 'Intraperitoneal and subcutaneous xenografts of human ovarian carcinoma in

nude mice and their potential in experimental therapy', *International journal of cancer,* 44(3), pp. 494-500.

Matsubara, S., Ding, Q., Miyazaki, Y., Kuwahata, T., Tsukasa, K. and Takao, S. (2013) 'mTOR plays critical roles in pancreatic cancer stem cells through specific and stemness-related functions', *Scientific reports,* 3, pp. 3230.

Matsutani, M., Suzuki, T., Hori, T., Terao, H., Takakura, K. and Nishioka, K. (1984) 'Cellular immunity and complement levels in hosts with brain tumours', *Neurosurgical review,* 7(1), pp. 29-35.

McConnell, I., Klein, G., Lint, T.F. and Lachmann, P.J. (1978) 'Activation of the alternative complement pathway by human B cell lymphoma lines is associated with Epstein-Barr virus transformation of the cells', *European journal of immunology,* 8(7), pp. 453-458.

Merle, N.S., Noe, R., Halbwachs-Mecarelli, L., Fremeaux-Bacchi, V. and Roumenina, L.T. (2015) 'Complement System Part II: Role in Immunity', *Frontiers in immunology,* 6, pp. 257.

Micheau, O. and Tschopp, J. (2003) 'Induction of TNF receptor I-mediated apoptosis via two sequential signaling complexes', *Cell,* 114(2), pp. 181-190.

Morgan, B.P. (1992) 'Effects of the membrane attack complex of complement on nucleated cells', *Current topics in microbiology and immunology,* 178, pp. 115-140.

Moskovich, O. and Fishelson, Z. (2007) 'Live cell imaging of outward and inward vesiculation induced by the complement c5b-9 complex', *The Journal of biological chemistry,* 282(41), pp. 29977-29986.

Murphy, K. (2012) ***Innate Immunity: The First Lines of Defense, Janeway's Immunobiology***. 8th edn. Garland Science, Chapter 2..

Mustafa, T., Klonisch, T., Hombach-Klonisch, S., Kehlen, A., Schmutzler, C., Koehrle, J., Gimm, O., Dralle, H. and Hoang-Vu, C. (2004) 'Expression of CD97 and CD55 in human medullary thyroid carcinomas', *International journal of oncology,* 24(2), pp. 285-294.

Nagata, S. (1997) 'Apoptosis by death factor', *Cell,* 88(3), pp. 355-365.

Nayak, A., Dodagatta-Marri, E., Tsolaki, A.G. and Kishore, U. (2012) 'An Insight into the Diverse Roles of Surfactant Proteins, SP-A and SP-D in Innate and Adaptive Immunity', *Frontiers in immunology,* 3, pp. 131.

Niehans, G.A., Cherwitz, D.L., Staley, N.A., Knapp, D.J. and Dalmasso, A.P. (1996) 'Human carcinomas variably express the complement inhibitory proteins CD46 (membrane cofactor protein), CD55 (decay-accelerating factor), and CD59 (protectin)', *The American journal of pathology,* 149(1), pp. 129-142.

Nishioka, K., Kawamura, K., Hirayama, T., Kawashima, T. and Shimada, K. (1976) 'The complement system in tumor immunity: significance of elevated levels of complement in tumor bearing hosts', *Annals of the New York Academy of Sciences,* 276, pp. 303-315.

Nishioka, R., Itoh, S., Gui, T., Gai, Z., Oikawa, K., Kawai, M., Tani, M., Yamaue, H. and Muragaki, Y. (2010) 'SNAIL induces epithelial-to-mesenchymal transition in a human pancreatic cancer cell line (BxPC3) and promotes distant metastasis and invasiveness in vivo', *Experimental and molecular pathology,* 89(2), pp. 149-157.

Noll, E.M., Eisen, C., Stenzinger, A., Espinet, E., Muckenhuber, A., Klein, C., Vogel, V., Klaus, B., Nadler, W., Rosli, C., Lutz, C., Kulke, M., Engelhardt, J., Zickgraf, F.M., Espinosa, O., Schlesner, M., Jiang, X., Kopp-Schneider, A., Neuhaus, P., Bahra, M., Sinn, B.V., Eils, R., Giese, N.A., Hackert, T., Strobel, O., Werner, J., Buchler, M.W., Weichert, W., Trumpp, A. and Sprick, M.R. (2016) 'CYP3A5 mediates basal and acquired therapy resistance in different subtypes of pancreatic ductal adenocarcinoma', *Nature medicine,* 22(3), pp. 278-287.

Oeckinghaus, A. and Ghosh, S. (2009) 'The NF-kappaB family of transcription factors and its regulation', *Cold Spring Harbor perspectives in biology,* 1(4), pp. a000034.

Ohashi, K., Burkart, V., Flohe, S. and Kolb, H. (2000) 'Cutting edge: heat shock protein 60 is a putative endogenous ligand of the toll-like receptor-4 complex', *Journal of immunology (Baltimore, Md),* 164(2), pp. 558-561.

Ohtani, K., Suzuki, Y., Eda, S., Kawai, T., Kase, T., Yamazaki, H., Shimada, T., Keshi, H., Sakai, Y., Fukuoh, A., Sakamoto, T. and Wakamiya, N. (1999) 'Molecular cloning of a novel human collectin from liver (CL-L1)', *The Journal of biological chemistry,* 274(19), pp. 13681-13689.

Okroj, M., Hsu, Y.F., Ajona, D., Pio, R. and Blom, A.M. (2008) 'Non-small cell lung cancer cells produce a functional set of complement factor I and its soluble cofactors', *Molecular immunology,* 45(1), pp. 169-179.

Ollert, M.W., David, K., Bredehorst, R. and Vogel, C.W. (1995) 'Classical complement pathway activation on nucleated cells. Role of factor H in the control of deposited C3b', *Journal of immunology (Baltimore, Md),* 155(10), pp. 4955-4962.

Ollert, M.W., Frade, R., Fiandino, A., Panneerselvam, M., Petrella, E.C., Barel, M., Pangburn, M.K., Bredehorst, R. and Vogel, C.W. (1990) 'C3-cleaving membrane proteinase. A new complement regulatory protein of human melanoma cells', *Journal of immunology (Baltimore, Md.: 1950),* 144(10), pp. 3862-3867.

Ong, A., Maines-Bandiera, S.L., Roskelley, C.D. and Auersperg, N. (2000) 'An ovarian adenocarcinoma line derived from SV40/E-cadherin-transfected normal

human ovarian surface epithelium', *International journal of cancer,* 85(3), pp. 430-437.

Orsulic, S., Li, Y., Soslow, R.A., Vitale-Cross, L.A., Gutkind, J.S. and Varmus, H.E. (2002) 'Induction of ovarian cancer by defined multiple genetic changes in a mouse model system', *Cancer cell,* 1(1), pp. 53-62.

Oshimori, N., Oristian, D. and Fuchs, E. (2015) 'TGF-beta promotes heterogeneity and drug resistance in squamous cell carcinoma', *Cell,* 160(5), pp. 963-976.

Ostrand-Rosenberg, S. (2008) 'Immune surveillance: a balance between protumor and antitumor immunity', *Current opinion in genetics & development,* 18(1), pp. 11-18.

Pandit, H., Thakur, G., Koippallil Gopalakrishnan, A.R., Dodagatta-Marri, E., Patil, A., Kishore, U. and Madan, T. (2016) 'Surfactant protein D induces immune quiescence and apoptosis of mitogen-activated peripheral blood mononuclear cells', *Immunobiology,* 221(2), pp. 310-322.

Pandya, P.H., Murray, M.E., Pollok, K.E. and Renbarger, J.L. (2016) 'The Immune System in Cancer Pathogenesis: Potential Therapeutic Approaches', *Journal of immunology research,* 2016, pp. 4273943.

Pangburn, M.K. and Rawal, N. (2002) 'Structure and function of complement C5 convertase enzymes', *Biochemical Society transactions,* 30(Pt 6), pp. 1006-1010.

Park, Y.C., Ye, H., Hsia, C., Segal, D., Rich, R.L., Liou, H., Myszka, D.G. and Wu, H. (2000) 'A novel mechanism of TRAF signaling revealed by structural and functional analyses of the TRADD–TRAF2 interaction', *Cell,* 101(7), pp. 777-787.

Peinado, H., Quintanilla, M. and Cano, A. (2003) 'Transforming growth factor beta-1 induces snail transcription factor in epithelial cell lines: mechanisms for epithelial mesenchymal transitions', *The Journal of biological chemistry,* 278(23), pp. 21113-21123.

Peng, D., Wang, J., Zhou, J. and Wu, G.S. (2010) 'Role of the Akt/mTOR survival pathway in cisplatin resistance in ovarian cancer cells', *Biochemical and biophysical research communications,* 394(3), pp. 600-605.

Peres Lde, P., da Luz, F.A., Pultz Bdos, A., Brigido, P.C., de Araujo, R.A., Goulart, L.R. and Silva, M.J. (2015) 'Peptide vaccines in breast cancer: The immunological basis for clinical response', *Biotechnology Advances,* 33(8), pp. 1868-1877.

Perkins, N.D. (2007) 'Integrating cell-signalling pathways with NF-kappaB and IKK function', *Nature reviews. Molecular cell biology,* 8(1), pp. 49-62.

Permuth-Wey, J. and Sellers, T.A. (2009) 'Epidemiology of ovarian cancer', *Methods in molecular biology (Clifton, N.J.),* 472, pp 413-437.

Pondman K, Paudyal B, Sim R, Kaur A, Kouser L, Tsolaki A, Jones LA, Salvador-Morales C, Khan HA, ten HB, Stenbeck G, Kishore U. Pulmonary surfactant protein SP-D opsonises carbon nanotubes and augments their phagocytosis and subsequent pro-inflammatory immune response. *Nanoscale.* 2017;9(3):1097-1109

Persson, A., Rust, K., Chang, D., Moxley, M., Longmore, W. and Crouch, E. (1988) 'CP4: a pneumocyte-derived collagenous surfactant-associated protein. Evidence for heterogeneity of collagenous surfactant proteins', *Biochemistry,* 27(23), pp. 8576-8584.

Pio, R., Corrales, L. and Lambris, J.D. (2014) 'The role of complement in tumor growth', *Advances in Experimental Medicine and Biology,* 772, pp. 229-262.

Ramsland, P.A., Hutchinson, A.T. and Carter, P.J. (2015) 'Therapeutic antibodies: Discovery, design and deployment', *Molecular immunology,* 67(2 Pt A), pp. 1-3.

Reid, K.B. (1998) 'Interactions of surfactant protein D with pathogens, allergens and phagocytes', *Biochimica et biophysica acta,* 1408(2-3), pp. 290-295.

Reid, K.B. (1986) 'Activation and control of the complement system', *Essays in biochemistry,* 22, pp. 27-68.

Reiss, M. (1999) 'TGF-beta and cancer', *Microbes and Infection,* 1(15), pp. 1327-1347.

Rhim, A.D., Mirek, E.T., Aiello, N.M., Maitra, A., Bailey, J.M., McAllister, F., Reichert, M., Beatty, G.L., Rustgi, A.K., Vonderheide, R.H., Leach, S.D. and Stanger, B.Z. (2012) 'EMT and dissemination precede pancreatic tumor formation', *Cell,* 148(1-2), pp. 349-361.

Ricklin, D., Hajishengallis, G., Yang, K. and Lambris, J.D. (2010) 'Complement: a key system for immune surveillance and homeostasis', *Nature immunology,* 11(9), pp. 785-797.

Rook, A.H., Kehrl, J.H., Wakefield, L.M., Roberts, A.B., Sporn, M.B., Burlington, D.B., Lane, H.C. and Fauci, A.S. (1986) 'Effects of transforming growth factor beta on the functions of natural killer cells: depressed cytolytic activity and blunting of interferon responsiveness', *Journal of immunology (Baltimore, Md),* 136(10), pp. 3916-3920.

Roshani, R., McCarthy, F. and Hagemann, T. (2014) 'Inflammatory cytokines in human pancreatic cancer', *Cancer letters,* 345(2), pp. 157-163.

Saelens, X., Festjens, N., Walle, L.V., Van Gurp, M., van Loo, G. and Vandenabeele, P. (2004) 'Toxic proteins released from mitochondria in cell death', *Oncogene,* 23(16), pp. 2861-2874.

Salih, H.R., Antropius, H., Gieseke, F., Lutz, S.Z., Kanz, L., Rammensee, H.G. and Steinle, A. (2003) 'Functional expression and release of ligands for the activating immunoreceptor NKG2D in leukemia', *Blood,* 102(4), pp. 1389-1396.

Sarbassov, D.D., Ali, S.M., Kim, D., Guertin, D.A., Latek, R.R., Erdjument-Bromage, H., Tempst, P. and Sabatini, D.M. (2004) 'Rictor, a novel binding partner of mTOR, defines a rapamycin-insensitive and raptor-independent pathway that regulates the cytoskeleton', *Current biology,* 14(14), pp. 1296-1302.

Schaub, B., Westlake, R.M., He, H., Arestides, R., Haley, K.J., Campo, M., Velasco, G., Bellou, A., Hawgood, S., Poulain, F.R., Perkins, D.L. and Finn, P.W. (2004) 'Surfactant protein D deficiency influences allergic immune responses', *Clinical and experimental allergy: journal of the British Society for Allergy and Clinical Immunology,* 34(12), pp. 1819-1826.

Schlesinger, M., Broman, I. and Lugassy, G. (1996) 'The complement system is defective in chronic lymphatic leukemia patients and in their healthy relatives', *Leukemia,* 10(9), pp. 1509-1513.

Schmidt, K.M., Hellerbrand, C., Ruemmele, P., Michalski, C.W., Kong, B., Kroemer, A., Hackl, C., Schlitt, H.J., Geissler, E.K. and Lang, S.A. (2017) 'Inhibition of mTORC2 component RICTOR impairs tumor growth in pancreatic cancer models', *Oncotarget,* 8(15), pp. 24491-24505.

Schoenborn, J.R. and Wilson, C.B. (2007) 'Regulation of interferon-gamma during innate and adaptive immune responses', *Advances in Immunology,* 96, pp. 41-101.

Schreiber, R.D., Old, L.J. and Smyth, M.J. (2011) 'Cancer immunoediting: integrating immunity's roles in cancer suppression and promotion', *Science (New York, N.Y.),* 331(6024), pp. 1565-1570.

Schulze-Osthoff, K., Ferrari, D., Los, M., Wesselborg, S. and Peter, M.E. (1998) 'Apoptosis signaling by death receptors', *European journal of biochemistry,* 254(3), pp. 439-459.

Scott, A.M., Wolchok, J.D. and Old, L.J. (2012) 'Antibody therapy of cancer', *Nature Reviews Cancer,* 12(4), pp. 278-287.

Semba, S., Moriya, T., Kimura, W. and Yamakawa, M. (2003) 'Phosphorylated Akt/PKB controls cell growth and apoptosis in intraductal papillary-mucinous tumor and invasive ductal adenocarcinoma of the pancreas', *Pancreas,* 26(3), pp. 250-257.

Shankaran, V., Ikeda, H., Bruce, A.T., White, J.M., Swanson, P.E., Old, L.J. and Schreiber, R.D. (2001) 'IFNgamma and lymphocytes prevent primary tumour development and shape tumour immunogenicity', *Nature,* 410(6832), pp. 1107-1111.

Shapiro, L. and Scherer, P.E. (1998) 'The crystal structure of a complement-1q family protein suggests an evolutionary link to tumor necrosis factor', *Current biology: CB,* 8(6), pp. 335-338.

Shinkai, Y., Rathbun, G., Lam, K.P., Oltz, E.M., Stewart, V., Mendelsohn, M., Charron, J., Datta, M., Young, F. and Stall, A.M. (1992) 'RAG-2-deficient mice lack mature lymphocytes owing to inability to initiate V(D)J rearrangement', *Cell,* 68(5), pp. 855-867.

Siegel, R.L., Miller, K.D. and Jemal, A. (2016) 'Cancer statistics, 2016', *CA: a cancer journal for clinicians,* 66(1), pp. 7-30.

Silveyra, P. and Floros, J. (2012) 'Genetic variant associations of human SP-A and SP-D with acute and chronic lung injury', *Frontiers in bioscience (Landmark edition),* 17, pp. 407-429.

Singh, M., Madan, T., Waters, P., Parida, S.K., Sarma, P.U. and Kishore, U. (2003) 'Protective effects of a recombinant fragment of human surfactant protein D in a murine model of pulmonary hypersensitivity induced by dust mite allergens', *Immunology letters,* 86(3), pp. 299-307.

Singh, S.K., Chen, N.M., Hessmann, E., Siveke, J., Lahmann, M., Singh, G., Voelker, N., Vogt, S., Esposito, I., Schmidt, A., Brendel, C., Stiewe, T., Gaedcke, J., Mernberger, M., Crawford, H.C., Bamlet, W.R., Zhang, J.S., Li, X.K., Smyrk, T.C., Billadeau, D.D., Hebrok, M., Neesse, A., Koenig, A. and Ellenrieder, V. (2015) 'Antithetical NFATc1-Sox2 and p53-miR200 signaling networks govern pancreatic cancer cell plasticity', *The EMBO journal,* 34(4), pp. 517-530.

Singh, S.K., Fiorelli, R., Kupp, R., Rajan, S., Szeto, E., Lo Cascio, C., Maire, C.L., Sun, Y., Alberta, J.A., Eschbacher, J.M., Ligon, K.L., Berens, M.E., Sanai, N. and Mehta, S. (2017) 'Post-translational Modifications of OLIG2 Regulate Glioma Invasion through the TGF-beta Pathway', *Cell reports,* 19(11), pp. 2410-2412.

Smyth, M.J., Crowe, N.Y. and Godfrey, D.I. (2001) 'NK cells and NKT cells collaborate in host protection from methylcholanthrene-induced fibrosarcoma', *International immunology,* 13(4), pp. 459-463.

Srivastava, P. (2002) 'Interaction of heat shock proteins with peptides and antigen presenting cells: chaperoning of the innate and adaptive immune responses', *Annual Review of Immunology,* 20, pp. 395-425.

Stevens, B., Allen, N.J., Vazquez, L.E., Howell, G.R., Christopherson, K.S., Nouri, N., Micheva, K.D., Mehalow, A.K., Huberman, A.D. and Stafford, B. (2007) 'The classical complement cascade mediates CNS synapse elimination', *Cell,* 131(6), pp. 1164-1178.

Subramanian, G., Schwarz, R.E., Higgins, L., McEnroe, G., Chakravarty, S., Dugar, S. and Reiss, M. (2004) 'Targeting endogenous transforming growth factor beta

receptor signaling in SMAD4-deficient human pancreatic carcinoma cells inhibits their invasive phenotype1', *Cancer research,* 64(15), pp. 5200-5211.

Sun, L., Wu, G., Willson, J.K., Zborowska, E., Yang, J., Rajkarunanayake, I., Wang, J., Gentry, L.E., Wang, X.F. and Brattain, M.G. (1994) 'Expression of transforming growth factor beta type II receptor leads to reduced malignancy in human breast cancer MCF-7 cells', *The Journal of biological chemistry,* 269(42), pp. 26449-26455.

Takeda, K., Smyth, M.J., Cretney, E., Hayakawa, Y., Kayagaki, N., Yagita, H. and Okumura, K. (2002) 'Critical role for tumor necrosis factor-related apoptosis-inducing ligand in immune surveillance against tumor development', *The Journal of experimental medicine,* 195(2), pp. 161-169.

Tan, L. A., Yu, B., Sim, F. C. J., Kishore, U., & Sim, R. B. (2010). Complement activation by phospholipids: the interplay of factor H and C1q. Protein & Cell, 1(11), 1033–1049. http://doi.org/10.1007/s13238-010-0125-8

Tanaka, M., Arimura, Y., Goto, A., Hosokawa, M., Nagaishi, K., Yamashita, K., Yamamoto, H., Sonoda, T., Nomura, M., Motoya, S., Imai, K. and Shinomura, Y. (2009) 'Genetic variants in surfactant, pulmonary-associated protein D (SFTPD) and Japanese susceptibility to ulcerative colitis', *Inflammatory bowel diseases,* 15(6), pp. 918-925.

Teng, M.W., Swann, J.B., Koebel, C.M., Schreiber, R.D. and Smyth, M.J. (2008) 'Immune-mediated dormancy: an equilibrium with cancer', *Journal of leukocyte biology,* 84(4), pp. 988-993.

Teraoka, H., Sawada, T., Yamashita, Y., Nakata, B., Ohira, M., Ishikawa, T., Nishino, H. and Hirakawa, K. (2001) 'TGF-beta1 promotes liver metastasis of pancreatic cancer by modulating the capacity of cellular invasion', *International journal of oncology,* 19(4), pp. 709-715.

van den Broek, M.E., Kagi, D., Ossendorp, F., Toes, R., Vamvakas, S., Lutz, W.K., Melief, C.J., Zinkernagel, R.M. and Hengartner, H. (1996) 'Decreased tumor surveillance in perforin-deficient mice', *The Journal of experimental medicine,* 184(5), pp. 1781-1790.

van Kooten, C., Fiore, N., Trouw, L.A., Csomor, E., Xu, W., Castellano, G., Daha, M.R. and Gelderman, K.A. (2008) 'Complement production and regulation by dendritic cells: molecular switches between tolerance and immunity', *Molecular immunology,* 45(16), pp. 4064-4072.

Varga, L., Czink, E., Miszlai, Z., Paloczi, K., Banyai, A., Szegedi, G. and Fust, G. (1995) 'Low activity of the classical complement pathway predicts short survival of patients with chronic lymphocytic leukaemia', *Clinical and experimental immunology,* 99(1), pp. 112-116.

Vasta, G.R. (2009) 'Roles of galectins in infection', Nature reviews.Microbiology, 7(6), pp. 424-438.

Vetter, C.S., Groh, V., Straten, P.t., Spies, T., Bröcker, E. and Becker, J.C. (2002) Expression of Stress-induced MHC Class I Related Chain Molecules on Human Melanoma. *J Invest Dermatol*. 2002 Apr;118(4):600-5.

von Bernstorff, W., Spanjaard, R.A., Chan, A.K., Lockhart, D.C., Sadanaga, N., Wood, I., Peiper, M., Goedegebuure, P.S. and Eberlein, T.J. (1999) 'Pancreatic cancer cells can evade immune surveillance via nonfunctional Fas (APO-1/CD95) receptors and aberrant expression of functional Fas ligand', *Surgery,* 125(1), pp. 73-84.

Wahl, S.M., McCartney-Francis, N. and Mergenhagen, S.E. (1989) 'Inflammatory and immunomodulatory roles of TGF-beta', *Immunology today,* 10(8), pp. 258-261.

Walport, M.J. (2001) 'Complement. First of two parts', *The New England journal of medicine,* 344(14), pp. 1058-1066.

Wang, J.Y., Kishore, U., Lim, B.L., Strong, P. and Reid, K.B. (1996) 'Interaction of human lung surfactant proteins A and D with mite (Dermatophagoides pteronyssinus) allergens', *Clinical and experimental immunology,* 106(2), pp. 367-373.

Wang, J.Y., Shieh, C.C., You, P.F., Lei, H.Y. and Reid, K.B. (1998) 'Inhibitory effect of pulmonary surfactant proteins A and D on allergen-induced lymphocyte proliferation and histamine release in children with asthma', *American journal of respiratory and critical care medicine,* 158(2), pp. 510-518.

Welch, H.G. and Black, W.C. (2010) 'Overdiagnosis in cancer', *Journal of the National Cancer Institute,* 102(9), pp. 605-613.

Wellner, U., Schubert, J., Burk, U.C., Schmalhofer, O., Zhu, F., Sonntag, A., Waldvogel, B., Vannier, C., Darling, D., zur Hausen, A., Brunton, V.G., Morton, J., Sansom, O., Schuler, J., Stemmler, M.P., Herzberger, C., Hopt, U., Keck, T., Brabletz, S. and Brabletz, T. (2009) 'The EMT-activator ZEB1 promotes tumorigenicity by repressing stemness-inhibiting microRNAs', *Nature cell biology,* 11(12), pp. 1487-1495.

Wert, S.E., Yoshida, M., LeVine, A.M., Ikegami, M., Jones, T., Ross, G.F., Fisher, J.H., Korfhagen, T.R. and Whitsett, J.A. (2000) 'Increased metalloproteinase activity, oxidant production, and emphysema in surfactant protein D gene-inactivated mice', *Proceedings of the National Academy of Sciences of the United States of America,* 97(11), pp. 5972-5977.

White, R.T., Damm, D., Miller, J., Spratt, K., Schilling, J., Hawgood, S., Benson, B. and Cordell, B. (1985) 'Isolation and characterization of the human pulmonary surfactant apoprotein gene', *Nature,* 317(6035), pp. 361-363.

Wolfgang, C.L., Herman, J.M., Laheru, D.A., Klein, A.P., Erdek, M.A., Fishman, E.K. and Hruban, R.H. (2013) 'Recent progress in pancreatic cancer', *CA: a cancer journal for clinicians,* 63(5), pp. 318-348.

Wurstle, M.L., Laussmann, M.A. and Rehm, M. (2012) 'The central role of initiator caspase-9 in apoptosis signal transduction and the regulation of its activation and activity on the apoptosome', *Experimental cell research,* 318(11), pp. 1213-1220.

Yoshida, M., Korfhagen, T.R. and Whitsett, J.A. (2001) 'Surfactant protein D regulates NF-kappa B and matrix metalloproteinase production in alveolar macrophages via oxidant-sensitive pathways', *Journal of immunology (Baltimore, Md),* 166(12), pp. 7514-7519.

Yunis AA, Arimura GK, Russin DJ. Human pancreatic carcinoma (MIA PaCa-2) in continuous culture: sensitivity to asparaginase. *Int J Cancer*. 1977;19:218–235.

Ytting, H., Christensen, I.J., Thiel, S., Jensenius, J.C. and Nielsen, H.J. (2005) 'Serum mannan-binding lectin-associated serine protease 2 levels in colorectal cancer: relation to recurrence and mortality', *Clinical cancer research: an official journal of the American Association for Cancer Research,* 11(4), pp. 1441-1446.

Ytting, H., Jensenius, J.C., Christensen, I.J., Thiel, S. and Nielsen, H.J. (2004) 'Increased activity of the mannan-binding lectin complement activation pathway in patients with colorectal cancer', *Scandinavian Journal of Gastroenterology,* 39(7), pp. 674-679.

Yuan, S., Yu, X., Asara, J.M., Heuser, J.E., Ludtke, S.J. and Akey, C.W. (2011) 'The holo-apoptosome: activation of procaspase-9 and interactions with caspase-3', *Structure (London, England : 1993),* 19(8), pp. 1084-1096.

Zhang, S.Q., Kovalenko, A., Cantarella, G. and Wallach, D. (2000) 'Recruitment of the IKK signalosome to the p55 TNF receptor: RIP and A20 bind to NEMO (IKKγ) upon receptor stimulation', *Immunity,* 12(3), pp. 301-311.

Zhang, K., Jiao, X., Liu, X., Zhang, B., Wang, J., Wang, Q., Tao, Y. and Zhang, D. (2010) 'Knockdown of snail sensitizes pancreatic cancer cells to chemotherapeutic agents and irradiation', *International journal of molecular sciences,* 11(12), pp. 4891-4892.

Zheng, T.S., Schlosser, S.F., Dao, T., Hingorani, R., Crispe, I.N., Boyer, J.L. and Flavell, R.A. (1998) 'Caspase-3 controls both cytoplasmic and nuclear events associated with Fas-mediated apoptosis in vivo', *Proceedings of the National Academy of Sciences of the United States of America,* 95(23), pp. 13618-13623.